University of São Paulo
"Luiz de Queiroz" College of Agriculture

Aetiology and epidemiology of grapevine anthracnose

Ricardo Feliciano dos Santos

Thesis presented to obtain the degree of Doctor in Science. Area: Plant Pathology

Piracicaba
2017

Ricardo Feliciano dos Santos
Agronomist

Aetiology and epidemiology of grapevine anthracnose

Advisor:
Prof. Dr. **MARCEL BELLATO SPÓSITO**

Thesis presented to obtain the degree of Doctor in Science. Area: Plant Pathology

Piracicaba
2017

Dados Internacionais de Catalogação na Publicação
DIVISÃO DE BIBLIOTECA – DIBD/ESALQ/USP

Santos, Ricardo Feliciano dos

Aetiology and epidemiology of grapevine anthracnose / Ricardo Feliciano dos Santos. - - Piracicaba, 2017.

119 p.

Tese (Doutorado) - - USP / Escola Superior de Agricultura “Luiz de Queiroz”.

1. *Vitis* spp. 2. *Elsinoë ampelina* 3. Diversidade genética 4. Produção de conídios 5. Patometria 6. Progresso temporal e espacial I. Título

I dedicate with love to

my parents Vicente and Kátia,

my grandparents Diogo (in memoriam) and Adelina,

my brother Rodrigo

and my fiancée Amanda.

ACKNOWLEDGEMENTS

I wish to express my sincere thanks to the following:

God for guiding my steps.

The “Luiz de Queiroz” College of Agriculture - University of São Paulo (ESALQ-USP) and the Graduate Program in Plant Pathology for my education during my doctoral study.

The Brazilian National Council for Scientific and Technological Development (CNPq) for providing the scholarship from March 2014 to February 2015 (grant number: 140710/2014-0).

The São Paulo Research Foundation for providing the scholarship in Brazil from March 2015 to October 2017 (grant number: 2014/24472-1) and in Australia from August 2016 to March 2017 (Research Internship Abroad – BEPE, grant number: 2016/01508-6).

My advisor Dr. Marcel Bellato Spósito for his generosity, guidance, support, friendship and knowledge, which were essential during my doctoral study.

The professor Dr. Lilian Amorim for her help and constructive suggestions.

My supervisor Dr. Mark Sosnowski for his help, guidance, patience and encouragement during my stay at South Australian Research and Development Institute, Australia.

The professor Dr. Nelson Sidnei Massola Júnior and Dr. Maisa Ciampi-Guillardi for their advice and support on molecular biology procedures.

The professors and staff of the Department of Plant Pathology and Nematology for their support and extensive knowledge provided.

The staff of the University of Adelaide and the South Australian Research and Development Institute for their valuable support. Thanks especially to Matthew Ayres for his friendship, help and interesting conversations about the Aussie life.

The Australian and Brazilian grape growers for providing anthracnose samples.

My colleagues from the Graduate Program in Plant Pathology at ESALQ.

My colleagues and friends from the Epidemiology Laboratory for all their support, talks, friendship and scientific discussions.

All my friends for their presence throughout this study.

All my family. Thanks especially to my parents, Vicente and Kátia, my brother Rodrigo and my grandmother Adelina for their continuous love, help and support.

My fiancée Amanda for her unconditional support, patience, encouragement and love.

Lastly, everyone who supported me throughout the course of this journey.

Thank you all!

"A person who never made a mistake never tried anything new."

Albert Einstein

CONTENTS

RESUMO 10
ABSTRACT 11
1 GENERAL INTRODUCTION 13
References 14
2 AETIOLOGY OF ANTHRACNOSE ON GRAPEVINE SHOOTS IN BRAZIL 17
Abstract 17
2.1 Introduction 17
2.2 Materials and methods 19
2.2.1 Fungal isolates 19
2.2.2 Molecular characterization 20
2.2.3 Morphological characterization 22
2.2.4 Pathogenicity 23
2.3 Results 24
2.3.1 Molecular characterization 24
2.3.2 Morphological characterization 33
2.3.3 Pathogenicity 35
2.4 Discussion 37
References 41
Supporting information 47
3 PHYLOGENY, MORPHOLOGY AND PATHOGENICITY OF *ELSINOË AMPELINA*, THE CAUSAL AGENT OF GRAPEVINE ANTHRACNOSE IN BRAZIL AND AUSTRALIA 49
Abstract 49
3.1 Introduction 49
3.2 Materials and methods 51
3.2.1 Sampling and fungal isolation 51
3.2.2 DNA isolation, PCR amplification and sequencing 53
3.2.3 Phylogenetic analyses 54
3.2.4 Intraspecific diversity 54
3.2.5 Morphological characterization 54
3.2.6 Pathogenicity tests 55

3.3 Results 57
3.3.1 Phylogenetic analyses 57
3.3.2 Intraspecific diversity 61
3.3.3 Morphological characterization 61
3.3.4 Pathogenicity 62
3.4 Discussion 64
References 67
Supporting information 72
4 *IN VITRO* PRODUCTION OF CONIDIA OF *ELSINOË AMPELINA*, THE CAUSAL FUNGUS OF GRAPEVINE ANTHRACNOSE 73
Abstract 73
4.1 Introduction 73
4.2 Materials and methods 74
4.2.1 Fungal isolates 74
4.2.2 *In vitro* production of conidia 75
4.2.3 Conidia quantification and germination 76
4.2.4 Infectivity of conidia produced *in vitro* 77
4.2.5 Statistical analyses 78
4.3 Results 78
4.4 Discussion 81
References 82
5 DEVELOPMENT AND VALIDATION OF A STANDARD AREA DIAGRAM SET FOR ASSESSMENT OF ANTHRACNOSE SEVERITY ON GRAPEVINE LEAVES 87
Abstract 87
5.1 Introduction 87
5.2 Materials and methods 89
5.2.1 Development of the SADs 89
5.2.2 Validation of the SADs 89
5.2.3 Data analyses 90
5.3 Results 91
5.4 Discussion 96
References 98

6 TEMPORAL AND SPATIAL DYNAMICS OF ANTHRACNOSE IN A BRAZILIAN VINEYARD 103
Abstract 103
6.1 Introduction 103
6.2 Materials and methods 105
6.2.1 Experimental area 105
6.2.2 Disease assessment 105
6.2.3 Temporal analysis 106
6.2.4 Spatial analysis 107
6.3 Results 108
6.3.1 Temporal analysis 108
6.3.2 Spatial analysis 110
6.4 Discussion 113
References 116

RESUMO

Etiologia e epidemiologia da antracnose da videira

Antracnose da videira é uma importante doença, responsável por severas perdas de produtividade em regiões húmidas em diversos locais do planeta. Este estudo objetivou: *i*: identificar o agente causal da antracnose da videira no Brasil; *ii*: caracterizar isolados de *Elsinoë ampelina* do Brasil e Austrália através de análises filogenéticas, morfologia e testes de patogenicidade; *iii*: desenvolver um método eficiente para produção de conídios de *E. ampelina*; *iv*: desenvolver e validar uma escala diagramática para avaliar a severidade de antracnose em folhas; e *v*: estudar o progresso temporal e espacial da antracnose em um vinhedo brasileiro. Para identificar os agentes causais da doença, folhas, ramos e bagas com sintomas de antracnose foram coletados em 38 vinhedos das regiões sul e sudeste do Brasil e 39 isolados de *E. ampelina* e 13 isolados de *Colletotrichum* spp. foram obtidos. Para isolados de *E. ampelina*, sequências de espaçador interno transcrito (ITS), histona H3 (HIS3) e fator de elongação 1-α (TEF) foram analisadas. HIS3 foi a região mais informativa com 55 sítios polimórficos. Foram identificadas sete espécies de *Colletotrichum*: *C. siamense*, *C. gloeosporioides*, *C. fructicola*, *C. viniferum*, *C. nymphaeae*, *C. truncatum* e *C. cliviae*. Nos testes de patogenicidade, somente isolados de *E. ampelina* causaram sintomas de antracnose em *Vitis vinifera* 'Moscato Giallo' e *Vitis labrusca* 'Niagara Rosada'. Para a caracterização de *E. ampelina* do Brasil e Austrália, 35 isolados foram analisados. Sequências de ITS e TEF de todos os isolados foram monomórficas. A rede de haplótipos gerada a partir de sequências de HIS3 resultou na formação de quatro haplótipos. Alta diversidade genética foi observada em dois isolados brasileiros, haplótipo EA4, sugerindo a perda do intron durante a evolução da espécie. Colônias apresentaram coloração variável, textura enrugada, ausência de esporos e lento crescimento. Isolados brasileiros apresentaram conídios maiores que conídios de isolados australianos. Para induzir a esporulação, fragmentos de micélio foram agitados e incubados em água da chuva e água destilada durante 7 dias. Isolados produziram diferentes concentrações de conídios e a germinação foi superior a 88,5%. Nos testes de infectividade, os conídios causaram sintomas de antracnose em folhas. A escala diagramática desenvolvida compreende seis diagramas em cores reais com severidade variando de 1,1 a 27,4%. O uso da escala diagramática melhorou a acurácia, precisão, concordância e reprodutibilidade das estimativas conduzidas por 12 avaliadores. A dinâmica temporal e espacial da antracnose foi conduzida em vinhedo de 'Niagara Rosada' em 2014 e 2015. A incidência de videiras com folhas, ramos e bagas sintomáticos e a severidade em folhas foram registradas. Os sintomas de antracnose ocorreram rapidamente após a brotação sendo observada resistência ontogênica em todos os órgãos avaliados. O modelo monomolecular mostrou o melhor ajuste para o progresso da incidência. As análises temporais sugerem que o progresso da incidência e severidade durante o tempo é influenciado principalmente pelo inóculo inicial devido à resistência ontogênica dos órgãos. As análises espaciais mostraram um padrão espacial predominantemente aleatório de videiras sintomáticas. Em conclusão, esta tese apresenta uma compreensão mais aprofundada da etiologia e epidemiologia de uma importante doença da videira.

Palavras-chave: *Vitis* spp.; *Elsinoë ampelina*; Diversidade genética; Produção de conídios; Patometria; Progresso temporal e espacial

ABSTRACT

Aetiology and epidemiology of grapevine anthracnose

Grapevine anthracnose is an important disease, responsible for severe yield losses in humid regions around the world. This study aimed to: *i*: identify the causal agents of grapevine anthracnose in Brazil; *ii*: characterize *Elsinoë ampelina* isolates from Brazil and Australia by means of phylogenetic analyses, morphological features and pathogenicity tests; *iii*: develop an efficient method for conidial production of *E. ampelina*; *iv*: develop and validate a standard area diagram set (SADs) for assessing anthracnose severity on grapevine leaves; and *v*: study the temporal and spatial progression of anthracnose in a Brazilian vineyard. To identify the causal agents of the disease, leaves, stems and berries with anthracnose symptoms were collected from 38 vineyards in southern and southeastern Brazil and 39 *E. ampelina* and 13 *Colletotrichum* spp. isolates were obtained. For *E. ampelina* isolates, the internal transcribed spacer (ITS), histone H3 (HIS3) and elongation factor 1-α (TEF) sequences were analysed. HIS3 was the most informative region with 55 polymorphic sites. Seven *Colletotrichum* species were identified: *C. siamense*, *C. gloeosporioides*, *C. fructicola*, *C. viniferum*, *C. nymphaeae*, *C. truncatum* and *C. cliviae*. In pathogenicity tests, only *E. ampelina* isolates caused anthracnose symptoms on *Vitis vinifera* 'Moscato Giallo' and *Vitis labrusca* 'Niagara Rosada'. To characterize *E. ampelina* from Brazil and Australia, 35 isolates were analysed. ITS and TEF sequences of all isolates were monomorphic. The haplotype network generated from HIS3 dataset showed four distinct haplotypes. High genetic variability was observed in two Brazilian isolates, haplotype EA4, which may have lost the intron region during species evolution. Colonies showed variable coloration, wrinkled texture, absence of spores and slow growth. Brazilian isolates produced conidia larger than conidia from Australian isolates. To induce the conidial production, mycelial fragments were shake-incubated in rainwater and distilled water for 7 days. Isolates produced different concentrations of conidia and the conidial germination was more than 88.5%. In infectivity tests, conidia caused typical anthracnose symptoms on leaves. The SADs developed comprises six true colour diagrams with severity ranging from 1.1 to 27.4%. The use of the SADs improved the accuracy, precision, agreement and inter-rater reliability of the estimates conducted by 12 raters. The temporal and spatial dynamics of anthracnose was carried out in a 'Niagara Rosada' vineyard in 2014 and 2015. The incidence of vines with diseased leaves, stems and berries and the severity disease on leaves were recorded. Anthracnose symptoms occurred rapidly after bud break and ontogenic resistance was observed for all organs assessed. The monomolecular model showed the best fit to the incidence progress. Temporal analyses suggest that the progress of anthracnose incidence and severity over time is governed mainly by the primary inoculum due to age-related resistance of the vine organs. Spatial analyses showed a predominantly random spatial pattern of diseased vines. In conclusion, this thesis presents a more in-depth understanding of the aetiology and epidemiology of an important grapevine disease.

Keywords: *Vitis* spp.; *Elsinoë ampelina*; Genetic diversity; Production of conidia; Pathometry; Temporal and spatial progress

1 GENERAL INTRODUCTION

The cultivation of grapevines plays a major social and economic role worldwide. In 2016, vineyards occupied around 7.5 million ha globally, producing 75.8 million tons of grapes (OIV, 2017). In Brazil and Australia, vineyards are spread over 81,518 and 148,489 ha, respectively (FAO, 2014). In both countries, the grape production is used as fresh fruit and for wine, sparkling, juice and raisin production. However, serious crop losses have been associated with pests and pathogens that include insects, nematodes, viruses, bacteria, fungi and oomycetes. In this context, the occurrence of fungal diseases is one of the most important problems faced by grape growers around the world, which have a profound influence on the quality and quantity of grapes produced (Wilcox *et al.*, 2015).

The warm and humid environment in some Brazilian and Australian grape-growing regions is conducive to the occurrence of anthracnose. Anthracnose symptoms appear from bud break until the end of the crop cycle, infecting aerial and succulent parts of the vine. Symptomatic leaves, petioles, stems, tendrils, rachises and berries show numerous circular or angular, dark brown to dark grey lesions (Thind, 2015). In south and southeast Brazil, anthracnose is one of the main diseases during rainy years (Bardin *et al.*, 2010; Barros *et al.*, 2015). In Australia, the disease has occurred in Victoria, New South Wales and South Australia in years of high rainfall (Magarey *et al.*, 1993). In Australia and Japan, it has been observed that table grape cultivars are more susceptible to anthracnose than wine grape cultivars (Hart *et al.*, 1993; Kono *et al.*, 2013).

Grapevine anthracnose, also known as grapevine black spot and bird's-eye rot, is a disease apparently originated in Europe from where it spread around the world (Agrios, 2005). Historically, the disease has been associated with the fungus *Elsinoë ampelina* Shear (anamorph *Sphaceloma ampelinum* de Bary) in several countries (de Castella & Brittlebank, 1917; Brook, 1973; Schilder *et al.*, 2005; Poolsawat *et al.*, 2010; Carisse & Lefebvre, 2011). Since the 90's, *Colletotrichum* species have also been reported as causal agents of the disease in Asia (Kumar *et al.*, 1994; Sawant *et al.*, 2012a,b; Liu *et al.*, 2016). However, in Brazil, *Colletotrichum* species have never been reported as causal agents of grapevine anthracnose. Little is known about the genetic variability of fungal isolates involved in this pathosystem worldwide. Besides that, *E. ampelina* colonies grow slowly and rarely produce conidia on artificial media, thus making it difficult to perform experiments that require a large quantity of inoculum (Kono *et al.*, 2009).

Despite the importance of grapevine anthracnose in humid areas, there are few studies on its epidemiology in the literature (Brook, 1973, 1992; Carisse & Lefebvre, 2011; Carisse & Morissete-Tomas, 2013). The importance of the primary and secondary inoculum and the temporal and spatial dynamics of anthracnose are unknown in Brazil. In epidemiological and control studies, the estimation of plant disease severity is an essential variable to compare different disease management strategies. In this context, the development and validation of a standard area diagram set (SADs) to assess the anthracnose severity would facilitate studies involving this important disease of grapevines. SADs is a simple, accurate, precise and fast tool widely used to aid the estimation of disease severity in several crops (Del Ponte *et al.*, 2017).

In order to investigate the aetiology and epidemiology of grapevine anthracnose, this study aimed to:

- identify the causal agents of grapevine anthracnose in Brazil through multilocus phylogeny, morphological characterization and pathogenicity tests (**Chapter 2**);
- characterize *E. ampelina* isolates from Brazil and Australia by means of phylogenetic analyses, morphological features and pathogenicity tests (**Chapter 3**);
- develop an efficient method for production of conidia of *E. ampelina* (**Chapter 4)**;
- develop and validate a standard area diagram set for assessing anthracnose severity on grapevine leaves (**Chapter 5**);
- study the temporal and spatial progression of anthracnose in a Brazilian vineyard to better understand the disease epidemiology (**Chapter 6**).

References

Agrios GN, 2005. *Plant Pathology*. Burlington, MA, USA: Elsevier Academic Press.

Bardin L, Pedro Júnior MJ, Moraes JFL, 2010. Risco climático de ocorrência de doenças fúngicas na videira 'Niagara Rosada' na região do polo turístico do circuito das frutas do estado de São Paulo. *Bragantia* **69**, 1019–26.

Barros LB, Biasi LA, Carisse O, May De Mio LL, 2015. Incidence of grape anthracnose on different *Vitis labrusca* and hybrid cultivars and rootstocks combination under humid subtropical climate. *Australasian Plant Pathology* **44**, 397–403.

Brook PJ, 1973. Epidemiology of grapevine anthracnose, caused by *Elsinoe ampelina*. *New Zealand Journal of Agricultural Research* **16**, 333–42.

Brook PJ, 1992. Epidemiology of grapevine anthracnose and downy mildew in an Auckland, New Zealand vineyard. *New Zealand Journal of Crop and Horticultural Science* **20**, 37–49.

Carisse O, Lefebvre A, 2011. A model to estimate the amount of primary inoculum of *Elsinoë ampelina*. *Plant Disease* **95**, 1167–71.

Carisse O, Morissete-Tomas V, 2013. Epidemiology of grape anthracnose: factors associated with defoliation of grape leaves infected by *Elsinoë ampelina*. *Plant Disease* **97**, 222–30.

de Castella F, Brittlebank C, 1917. Anthracnose or black spot of the vine. *The Journal of the Department of Agriculture of Victoria*, 1–19.

Del Ponte EM, Pethybridge SJ, Bock CH, Michereff SJ, Machado FJ, Spolti P, 2017. Standard area diagrams for aiding severity estimation : scientometrics, pathosystems and methodological trends in the last 25 years. *Phytopathology*, in press.

FAO - Food and Agriculture Organization of the United Nations, 2014. FAOSTAT. [http://www.fao.org/faostat/en/#data]. Accessed 26 July 2017.

Hart KH, Magarey RD, Emmett RW, Magarey PA, 1993. Susceptibility of grapevine selections to black spot (anthracnose) *Elsinoe ampelina*. *Australian Grapegrower & Winemaker* **352**, 85–7.

Kono A, Nakaune R, Yamada M, Nakano M, Mitani N, Ueno T, 2009. Effect of culture conditions on conidia formation by *Elsinoë ampelina*, the causal organism of grapevine anthracnose. *Plant Disease* **93**, 481–4.

Kono A, Sato A, Ban Y, Mitani N, 2013. Resistance of *Vitis* germplasm to *Elsinoë ampelina* (de Bary) Shear evaluated by lesion number and diameter. *HortScience* **48**, 1433–9.

Kumar S, Third TS, Mohan C, 1994. Occurrence of *Gloeosporium ampelophagum* and *Colletotrichum gloeosporioides*, the incitants of grape anthracnose, during different months in Punjab. *Plant Disease Research* **9**, 222–4.

Liu M, Zhang W, Zhou Y *et al.*, 2016. First report of twig anthracnose on grapevine caused by *Colletotrichum nymphaeae* in China. *Plant disease* **100**, 2530.

Magarey RD, Emmett RW, Magarey PA, Franz PR, 1993. Evaluation of control of grapevine anthracnose caused by *Elsinoe ampelina* by pre-infection fungicides. *Australasian Plant Pathology* **22**, 48–52.

OIV - International Organisation of Vine and Wine, 2017. 2017 World viticulture situation: OIV statistical report on world vitiviniculture. [http://www.oiv.int/public/medias/5479/oiv-en-bilan-2017.pdf]. Accessed 12 September 2017.

Poolsawat O, Tharapreuksapong A, Wongkaew S, Reisch B, Tantasawat P, 2010. Genetic diversity and pathogenicity analysis of *Sphaceloma ampelinum* causing grape anthracnose in Thailand. *Journal of Phytopathology* **158**, 837–40.

Sawant IS, Narkar SP, Shetty DS, Upadhyay A, Sawant SD, 2012a. Emergence of *Colletotrichum gloeosporioides sensu lato* as the dominant pathogen of anthracnose disease of grapes in India as evidenced by cultural, morphological and molecular data. *Australasian Plant Pathology* **41**, 493–504.

Sawant IS, Narkar SP, Shetty DS, Upadhyay A, Sawant SD, 2012b. First report of *Colletotrichum capsici* causing anthracnose on grapes in Maharashtra, India. *New Disease Reports* **25**, 2.

Schilder AMC, Smokevitch SM, Catal M, Mann WK, 2005. First report of anthracnose caused by *Elsinoë ampelina* on grapes in Michigan. *Plant Disease* **89**, 1011.

Thind TS, 2015. Anthracnose. In: Wilcox W, Gubler W, Uyemoto J, eds. *Compendium of grape diseases, disorders, and pests*. St Paul, MN, USA: APS Press, 17–9.

Wilcox W, Gubler W, Uyemoto J, 2015. *Compendium of grape diseases, disorders, and pests*. St Paul, MN, USA: APS Press.

2 AETIOLOGY OF ANTHRACNOSE ON GRAPEVINE SHOOTS IN BRAZIL

Abstract

Anthracnose is an important disease in vineyards in South and Southeast Brazil, the main grape-producing regions in the country. This study aimed to identify the causal agents of grapevine anthracnose in Brazil through multilocus phylogenetic analyses, morphological characterization and pathogenicity tests. Thirty-nine *Elsinoë ampelina* and 13 *Colletotrichum* spp. isolates were obtained from leaves, stems and berries with anthracnose symptoms collected in 38 vineyards in southern and southeastern Brazil. For *E. ampelina* isolates, the internal transcribed spacer (ITS), histone H3 (HIS3) and elongation factor 1-α (TEF) sequences were analysed. HIS3 was the most informative region with 55 polymorphic sites including deletions and substitutions of bases, enabling the grouping of isolates into five haplotypes. Colonies of *E. ampelina* showed slow growth, variable colouration and a wrinkled texture on potato dextrose agar. Conidia were cylindrical to oblong with rounded ends, hyaline, aseptate, (3.57-) 5.64 (-6.95) µm long and (2.03-) 2.65 (-3.40) µm wide. Seven species of *Colletotrichum* were identified: *C. siamense*, *C. gloeosporioides*, *C. fructicola*, *C. viniferum*, *C. nymphaeae*, *C. truncatum* and *C. cliviae*, with a wide variation in colony and conidium morphology. Only *E. ampelina* caused anthracnose symptoms on leaves, tendrils and stems of *Vitis vinifera* and *V. labrusca*. High disease severity and a negative correlation between disease severity and shoot dry weight were observed only when relative humidity was above 95%. In this study, only *E. ampelina* caused anthracnose symptoms on grapevine shoots in Brazil.

Keywords: Black spot; *Colletotrichum* spp.; *Elsinoë ampelina*; Genetic diversity; Pathogenicity; *Vitis* species

2.1 Introduction

Grapevine is cultivated in Brazil between parallels 9° and 30°S, with higher density in the southeastern and southern regions between latitudes 20° and 30°S. These regions contain 78%, representing 68,779 ha, of Brazilian grapevine production (IBGE, 2016). The American species *Vitis labrusca*, including the Niagara Rosada, Niagara Branca, Concord and Isabel cultivars, is used for juice, wine and fresh market production. *Vitis labrusca* is responsible for 49% of grape production in São Paulo State, the largest producer of the Southeast region, and 80% of the production in Rio Grande do Sul State, the largest grape producer of the southern region (Oliveira *et al.*, 2008; Protas & Camargo, 2011). The annual growth cycle of Brazilian grapevines in both regions begins with bud break in September and lasts until harvest in December and January. This period is characterized by temperatures between 25 and 30 °C and by frequent rain. The warm and humid environment in these grape-growing areas is conducive to the occurrence of diseases on shoots, especially downy mildew and anthracnose (Amorim *et al.*, 2016). Overall, wine grapes are highly resistant to anthracnose, whereas table

grapes belonging to the species *V. labrusca* and *V. vinifera* are susceptible (Hart *et al.*, 1993; Schilder *et al.*, 2005; Kono *et al.*, 2013). Anthracnose represents a constraint to production of susceptible cultivars in humid regions in Asia, where the disease is well established (Thind, 2015). Major outbreaks, which may cause yield losses as high as 50%, occur when there is synchronism between rain and the presence of susceptible host tissues (Anderson, 1956; Prakongkha *et al.*, 2013).

Infection occurs mostly in young tissues, including stems, leaves, petioles, tendrils, rachises and berries. The first symptoms are numerous slightly depressed circular or angular spots, dark brown in colour, on all aerial parts of the plants (Thind, 2015). As the disease develops, lesions may coalesce and form cankers or blight on stems, causing early defoliation and delaying the ripening of berries. The symptoms on the berries compromise fruit quality for the fresh market (Amorim *et al*., 2016).

The causal agent of anthracnose is *Elsinoë ampelina* Shear (Brook, 1973; Kumar *et al.*, 1994; Pedro Júnior *et al.*, 1999; Schilder *et al.*, 2005; Poolsawat *et al.*, 2010; Carisse & Lefebvre, 2011). However, *Colletotrichum gloeosporioides* species complex (Chowdappa *et al.*, 2009; Sawant *et al.*, 2012a), *Colletotrichum acutatum* species complex (Chowdappa *et al.*, 2009; Baroncelli *et al.*, 2014; Liu *et al.*, 2016) and *Colletotrichum capsici* (Sawant *et al.*, 2012a,b) have also been reported as causal agents of the disease. In most cases, identification of the causal agent of anthracnose was based on cultural and morphological characteristics and sometimes, for *Colletotrichum*, species-specific primers were also used. Consequently, few DNA sequences of *E. ampelina* have been deposited in the GenBank database and those that have, obtained from isolates from Michigan (USA), only represent the internal transcribed spacer (ITS) region (Schilder *et al.*, 2005); which hinders reliable pathogen identification and knowledge of its genetic variability. For the genus *Colletotrichum*, several genes of isolates in various pathosystems have been sequenced and deposited in GenBank. The main regions sequenced are ITS, β-tubulin, and glyceraldehyde-3-phosphate dehydrogenase (GAPDH), which allow differentiation of the species within the *C. acutatum* and *C. gloeosporioides* complexes (Baroncelli *et al.*, 2015; Velho *et al.*, 2015).

Most cultivars of *V. vinifera* and *V. labrusca* from Brazilian vineyards are susceptible to anthracnose (Giovaninni, 2001; Barros *et al.*, 2015). However, there have been no studies on the aetiology of the disease in the country. This study aimed to identify the causal agents of grapevine anthracnose in Brazil through multilocus phylogeny, morphological characterization and pathogenicity tests.

2.2 Materials and methods

2.2.1 Fungal isolates

Leaves, stems, and berries of grapevines with anthracnose symptoms were collected from 38 vineyards in southern and southeastern Brazil (Fig. 1). Small fragments of typical anthracnose lesions were disinfected in 70% alcohol (1 min) and 2.5% sodium hypochlorite (3 min), followed by three rinses with sterile distilled water. Subsequently, the fragments were dried on sterilized filter paper, deposited on water agar (WA; Difco Laboratories) and incubated for 7 days at 25 °C with a photoperiod of 12 h. Putative colonies of *E. ampelina* (Fig. S1) and *Colletotrichum* spp. were then transferred to potato dextrose agar (PDA; Difco Laboratories) amended with streptomycin sulphate (0.5 g L^{-1}). To obtain pure cultures of *E. ampelina*, mycelia were dislodged from the colony, sterile distilled water was added and they were mixed using a Drigalski spatula. Then, 150 µL of this mycelial suspension were spread over a Petri dish containing WA. After 14 h, the dishes were observed under an optical microscope, and the isolates were purified by removing a hyphal tip to a plate containing PDA. For the purification of *Colletotrichum* isolates, 150 µL of a conidial suspension were plated on WA. After 8 h, a single germinating conidium was transferred to PDA. The purified isolates were grown at 25°C for 10 days on plates of PDA medium with fragments of 1 cm^2 sterilized filter paper on the surface. After fungal growth, the pieces of filter paper were removed from the culture medium, stored in 2 mL microtubes containing silica gel and kept at 4 °C in the Department of Plant Pathology and Nematology, ESALQ, University of São Paulo.

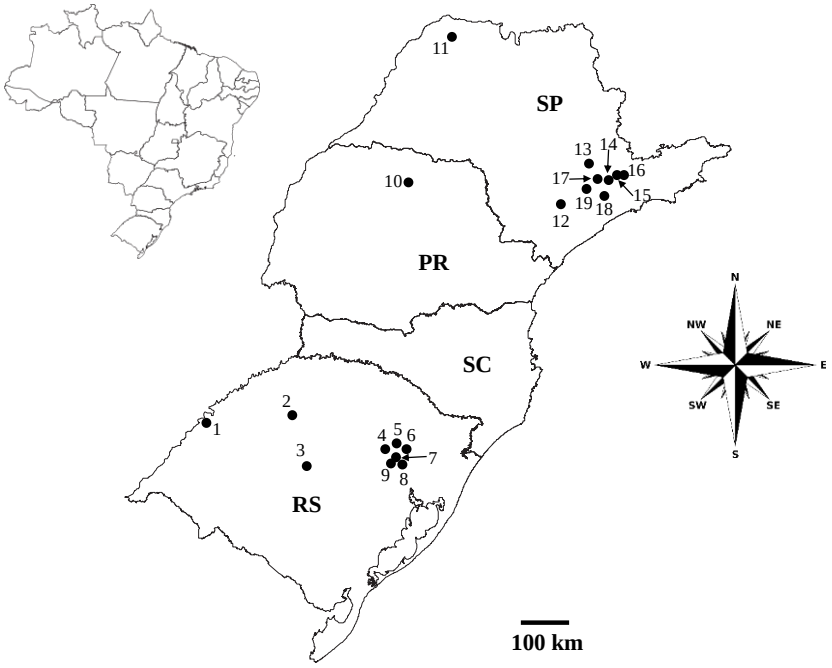

Figure 1 Collection sites of isolates of *Elsinoë ampelina* and *Colletotrichum* spp. associated with grapevine anthracnose symptoms in southern and southeastern Brazil. Municipalities where samples were collected are indicated on the map by numbers: 1-São Borja (*v* = 1; *n* = 1); 2-Augusto Pestana (*v* = 4; *n* = 4); 3-Santa Maria (*v* = 4; *n* = 4); 4-Cotiporã (*v* = 2; *n* = 2); 5-Nova Roma do Sul (*v* = 1; *n* = 2); 6-Flores da Cunha (*v* = 2; *n* = 2); 7-Bento Gonçalves (*v* = 3; *n* = 4); 8-Farroupilha (*v* = 2; *n* = 2); 9-Garibaldi (*v* = 1; *n* = 1); 10-Londrina (*v* = 1; *n* = 1); 11-Jales (*v* = 1; *n* = 1); 12-São Miguel Arcanjo (*v* = 1; *n* = 1); 13-Piracicaba (*v* = 1; *n* = 3); 14-Jundiaí (*v* = 3; *n* = 6); 15-Jarinu (*v* = 1; *n* = 2); 16-Atibaia (*v* = 2; *n* = 4); 17-Indaiatuba (*v* = 2; *n* = 3); 18-São Roque (*v* = 4; *n* = 5); and 19-Porto Feliz (*v* = 2; *n* = 4). *v* is the number of vineyards sampled and *n* is the number of isolates analysed in each municipality. PR - Paraná State; RS - Rio Grande do Sul State; SC - Santa Catarina State; SP - São Paulo State.

2.2.2 Molecular characterization

For each *E. ampelina* and *Colletotrichum* spp. isolate, a small amount of mycelium was collected from pure cultures grown on PDA at 25 °C with a 12 h photoperiod for 2 weeks. DNA was extracted and purified using the Wizard Genomic DNA Purification Kit (Promega), following the manufacturer's instructions. For *E. ampelina* isolates, PCR-based techniques were used for the amplification of the internal transcribed spacer region (ITS; spanning ITS1, ITS2, and the 5.8S ribosomal RNA gene), a partial sequence of the histone H3 gene (HIS3), and a partial sequence of the translation elongation factor 1-α gene (TEF) using, respectively, the primers pairs ITS1 and ITS4 (White *et al.*, 1990), CYLH3F and CYLH3R (Crous *et al.*, 2004) and elongation-1-F and elongation-1-R (Hyun *et al.*, 2009). For *Colletotrichum* isolates, the ITS region, a partial sequence of the β-tubulin gene (TUB2), and

a partial sequence of the glyceraldehyde-3-phosphate dehydrogenase gene (GAPDH) were amplified with the primers pairs ITS1 and ITS4 (White *et al.*, 1990), Bt2a and Bt2b (Glass & Donaldson, 1995) and GDF1 and GDR1 (Guerber *et al.*, 2003), respectively.

Each PCR contained 2 µL DNA (25 ng μL^{-1}), 8.5 µL nuclease-free water, 1 µL of each primer (10 µM) and 12.5 µL GoTaq Colorless Master Mix 2x (Promega) in a total volume of 25 µL. The amplification programme for the ITS and TUB2 loci consisted of initial denaturation at 94 °C for 2 min, followed by 35 cycles of denaturation at 94 °C for 1 min, annealing at 55 °C for 1 min and extension at 72 °C for 1 min, and a final extension at 72 °C for 10 min. For GAPDH, the same conditions were used except the annealing step was 60 °C for 45 sec. For TEF, initial denaturation at 94 °C for 2 min was followed by 40 cycles of amplification (94 °C for 30 sec, 55 °C for 1 min and 72 °C for 1 min) and a final extension at 72 °C for 5 min. For HIS3, initial denaturation at 95 °C for 3 min was followed by 34 cycles of amplification (95 °C for 1 min, 56.9 °C for 1 min and 72 °C for 1 min) and a final extension at 72°C for 4 min. PCR was carried out in a TC-512 thermal cycler (Techne).

The PCR-amplified products were analysed by electrophoresis in a 2% agarose gel stained with SYBR Safe (Invitrogen), in 0.5× Tris borate EDTA (TBE) buffer and viewed under UV light. PCR products were purified using the Wizard SV Gel and PCR Clean-Up System kit (Promega), following the manufacturer's instructions. Sequencing of PCR products was performed using a 3130xl Genetic Analyzer (Applied Biosystems).

The forward and reverse sequences were edited using Sequencher 5.4.1 (Gene Codes Corporation, 2016) to obtain consensus sequences. Consensus sequences were compared with sequences deposited in GenBank using the Basic Local Alignment Sequence Tool (BLAST; Boratyn *et al.*, 2013). The GenBank sequences with the highest similarity scores were selected and aligned with the sequences obtained from this study using the ClustalW algorithm in BioEdit (Hall, 1999). Mesquite software was used to concatenate the multiple alignments (Maddison & Maddison, 2011).

Three phylogenetic analyses were carried out with the amplicons generated. The first phylogenetic tree was built using ITS sequences of *Elsinoë/Sphaceloma* species, the second tree was built using multilocus alignment (ITS and HIS3) of *E. ampelina*, and finally a third tree was built using multilocus alignment (ITS, TUB2 and GAPDH) of *Colletotrichum* spp. Nucleotide substitution models for each gene were determined and included for each locus based on the Akaike information criterion (AIC) using MrModeltest v.2.3 (Nylander, 2004). Bayesian inference was used to rebuild the phylogenies using a Markov Chain Monte Carlo

(MCMC) algorithm to generate phylogenetic trees with Bayesian posterior probabilities. Four MCMC chains were executed simultaneously for random trees with 10^7 generations. Trees were randomly sampled every 1000 generations and 25% of generations were discarded as burn-in. For each phylogenetic analysis, the Bayesian inference was conducted twice in MrBayers v.3.1.1 (Ronquist & Huelsenbeck, 2003). Trees were edited in TreeView (Page, 1996). All sequences generated in this study were deposited in GenBank.

2.2.3 Morphological characterization

To assess characteristics of *E. ampelina* and *Colletotrichum* spp. colonies, mycelial plugs, 6.5 mm in diameter, were excised from the edges of actively growing colonies on PDA, deposited at the centres of Petri dishes containing PDA medium and incubated at 25 °C with a 12 h photoperiod. Colony texture, density, colour and diameter, and absence/presence of staining spore mass were used for characterization of the isolates. For *Colletotrichum* spp. isolates, the colony diameter was assessed at 5 days and the other cultural features at 7 days, and for *E. ampelina* all assessments were performed at 30 days. Colour was described using the mycological colour chart of Rayner (1970). Colony diameter (mm) was measured using a digital calliper in two perpendicular directions, and a mean colony diameter was obtained. The experimental design was completely randomized with three replicates per isolate. The experiment was performed twice.

As *E. ampelina* did not sporulate *in vitro*, mycelia from colonies grown on PDA for 30 days were fragmented and 10 mL of liquid Fries' medium were added in Petri dishes (Whiteside, 1975). The dishes were incubated at room temperature in the dark for 48 h. The suspension of microcolonies and rare conidia formed in Fries' medium was sprayed on young leaves of cv. Niagara Rosada. The plants were covered with plastic bags and kept at 25 °C in the dark for 48 h. After removal from the moist chamber, the plants were kept at 25 °C with a 12 h photoperiod for 7 days. Leaves with sporulating lesions were detached and transferred to Petri dishes. A 50 µL drop of sterile distilled water was placed on top of each lesion. After 4 h, the drop was removed and the conidia were measured with an optical microscope. *Colletotrichum* spp. isolates were grown on synthetic nutrient-poor agar (SNA; Nirenberg, 1976) with two 1 cm^2 pieces of filter paper at 20 °C with a 12 h photoperiod for 10 days.

For each *E. ampelina* and *Colletotrichum* spp. isolate, the lengths and widths of 30 conidia were measured. The conidial shapes were also observed. Measurements were taken at

× 1000 magnification using an Axio Lab.A1 microscope (Carl Zeiss). Images were captured using an Axiocam 503 colour digital video camera (Carl Zeiss).

2.2.4 Pathogenicity

One-year-old plants of *V. vinifera* cv. Moscato Giallo (wine grape) grafted on 'SO4' rootstock and *V. labrusca* cv. Niagara Rosada (table grape) grafted on 'IAC-766' rootstock were inoculated with 17 isolates representative of the subclades identified in the phylogenetic analyses. *Elsinoë ampelina* isolates were grown for 30 days on PDA at 25 °C with a 12 h photoperiod, and the colonies were fragmented in sterile distilled water using scalpel and pestle. The mycelial suspension was calibrated with a Neubauer chamber at 2×10^5 CFU mL^{-1} for each isolate. Conidial suspensions of *Colletotrichum* spp. isolates were obtained from colonies grown on PDA for 7 days at 25 °C with a 12 h photoperiod and adjusted to 2×10^5 conidia mL^{-1}. The suspensions were sprayed to the point of runoff on plants at growth stage 14 (four unfolded leaves; Lorenz *et al.*, 1995). The plants were covered with plastic bags and incubated in a growth room at 25 °C in the dark for 48 h. Plants sprayed with water only were used as a control. After the initial incubation period, for each cultivar, plants were placed either in the greenhouse with average relative humidity between 60 and 70% (environment 1) or in a growth room containing a humidifier (Britânia) to maintain the relative humidity higher than 95% (environment 2). In both environments, plants were kept at 25 °C for 10 days, with leaves and stems assessed daily for symptoms.

Five days after inoculation, the number of lesions was quantified visually in 4 cm^2 of the top two leaves using a scale from 0 to 5 (adapted from Poolsawat *et al.*,2012): 0 = no lesions, 1 = 1-6 lesions, 2 = 7-25, 3 = 26-50, 4 = 51-100 and 5 = > 100 lesions. Images of the top two leaves of each plant were captured 12 days after inoculation, and disease severity was quantified based on the percentage of leaf area covered by lesions using ImageJ (Rasband, 1997). The value of 100% disease severity was assigned for leaves that wilted or dropped. The shoot dry weight was determined by drying shoots in a forced-air oven at 60 °C until a constant weight was reached. For re-isolation of the pathogen, fragments from leaves, tendrils and stems with symptoms were disinfected, as described previously, and transferred to Petri dishes containing PDA. The colonies were incubated for 21 days and the morphological characteristics of the isolates were analysed. The experimental design was completely randomized. For each experiment, four replicates per isolate were used; each replicate

consisted of one plant. The variables of number of lesions, disease severity and shoot dry weight were transformed using $(x + 1)^{1/2}$. Transformed data were subjected to analysis of variance (ANOVA) and the means were compared using the Scott-Knott test ($P < 0.05$). The relationship between the variables evaluated was verified using the Pearson correlation coefficient ($P < 0.05$). Comparisons between the experiments (environments and cultivars) were performed by *F* test ($P < 0.05$). All statistical analyses were performed using 'R' v. 3.3.0 (R Core Team, 2016).

2.3 Results

2.3.1 Molecular characterization

The amplicons of *Elsinoë ampelina* generated by PCR were 412, 351-400 and 602 bp in length for the TEF, HIS3 and ITS regions, respectively (Table 1). The phylogenetic analysis using ITS sequences was carried out to enable comparison with the only three sequences of *E. ampelina* deposited in GenBank. Even for other species of the genus *Elsinoë/Sphaceloma*, only ITS sequences were available. Bayesian phylogenetic analysis used the evolutionary model GTR+I+G based on the AIC criterion. *Elsinoë ampelina* isolates were grouped into three clades, two with two isolates each and a third clade with 35 isolates (Fig. 2). The alignment and analysis of 39 TEF sequences showed a lack of nucleotide variation at this locus, thus they were not used in the multilocus phylogenetic analysis. For the multilocus analysis, including *C. nymphaeae* (CBS 173.51) as a outgroup, the substitution models selected were HKY+I for ITS and GTR for HIS3. Isolates AV34, AV85, AV95 and AV111 from different locations and plant organs remained in a separate clade with high posterior probability value (Fig. 3). For *E. ampelina*, HIS3 was the most informative locus, with 55 polymorphic sites, including deletions and substitutions of bases, enabling the grouping of isolates into five haplotypes.

Table 1 Species, isolate code, host and tissue of isolation, location of origin and GenBank accession numbers for *Elsinoë* spp. (anamorph: *Sphaceloma* spp.) isolates used in this study in Brazil, 2014

Species	Isolate code	Host	Tissue	Location[a]	GenBank accession numbers[b]		
					ITS	HIS3	TEF
Elsinoë ampelina	AV20	*Vitis riparia* × (*V. rupestris* × *V. cordifolia*) cv. Riparia do Traviú[c]	Leaf	Piracicaba, SP, Brazil	**KX786349**	**KX786466**	**KX786388**
	AV25	*V. labrusca* cv. Niagara Rosada	Leaf	Jundiaí, SP, Brazil	**KX786350**	**KX786467**	**KX786389**
	AV34	*V. labrusca* cv. Niagara Rosada	Leaf	Jundiaí, SP, Brazil	**KX786351**	**KX786468**	**KX786390**
	AV37	*V. labrusca* cv. Niagara Rosada	Leaf	Jundiaí, SP, Brazil	**KX786352**	**KX786469**	**KX786391**
	AV39	*V. labrusca* cv. Bordô	Berry	Santa Maria, RS, Brazil	**KX786353**	**KX786470**	**KX786392**
	AV40	*V. vinifera* cv. Moscato Bailey	Leaf	Santa Maria, RS Brazil	**KX786354**	**KX786471**	**KX786393**
	AV44	*V. labrusca* cv. Tardia de Caxias	Leaf	Santa Maria, RS, Brazil	**KX786355**	**KX786472**	**KX786394**
	AV47	*V. vinifera* cv. Moscato Branco	Leaf	Augusto Pestana, RS, Brazil	**KX786356**	**KX786473**	**KX786395**
	AV48	*V. labrusca* cv. Niagara Rosada	Berry	Jundiaí, SP, Brazil	**KX786357**	**KX786474**	**KX786396**
	AV49	*V. riparia* cv. Gloria de Montpellier[c]	Leaf	Porto Feliz, SP, Brazil	**KX786358**	**KX786475**	**KX786397**
	AV51	*V. labrusca* cv. Niagara Rosada	Berry	Porto Feliz, SP, Brazil	**KX786359**	**KX786476**	**KX786398**
	AV52	*V. riparia* cv. Gloria de Montpellier[c]	Leaf	Porto Feliz, SP, Brazil	**KX786360**	**KX786477**	**KX786399**
	AV53	*V. labrusca* cv. Niagara Rosada	Berry	Porto Feliz, SP, Brazil	**KX786361**	**KX786478**	**KX786400**
	AV55	*V. labrusca* cv. Niagara Rosada	Berry	Jarinu, SP, Brazil	**KX786362**	**KX786479**	**KX786401**
	AV56	*V. labrusca* cv. Niagara Rosada	Berry	Jarinu, SP, Brazil	**KX786363**	**KX786480**	**KX786402**
	AV60	*V. labrusca* cv. Niagara Branca	Leaf	Atibaia, SP, Brazil	**KX786364**	**KX786481**	**KX786403**
	AV62	*V. labrusca* cv. Niagara Rosada	Leaf	Atibaia, SP, Brazil	**KX786365**	**KX786482**	**KX786404**
	AV63	*V. labrusca* cv. Niagara Rosada	Berry	Atibaia, SP, Brazil	**KX786366**	**KX786483**	**KX786405**
	AV64	*V. labrusca* cv. Niagara Rosada	Stem	Atibaia, SP, Brazil	**KX786367**	**KX786484**	**KX786406**
	AV67	*V. labrusca* cv. Niagara Rosada	Berry	Indaiatuba, SP, Brazil	**KX786368**	**KX786485**	**KX786407**
	AV71	*V. vinifera* cv. Moscato Branco	Leaf	Indaiatuba, SP, Brazil	**KX786369**	**KX786486**	**KX786408**
	AV72	*V. labrusca* cv. Niagara Rosada	Leaf	Indaiatuba, SP, Brazil	**KX786370**	**KX786487**	**KX786409**
	AV82	*Vitis* spp. - hybrid cv. BRS Violeta	Stem	São Roque, SP, Brazil	**KX786371**	**KX786488**	**KX786410**
	AV84	Riparia do Traviú × *V. caribaea* cv. IAC-766[c]	Leaf	São Roque, SP, Brazil	**KX786372**	**KX786489**	**KX786411**
	AV85	*V. vinifera* × (*Vitis vinifera* ×*Vitis rupestris* ×*Vitis lincecumii*) cv. BRS Lorena	Leaf	São Roque, SP, Brazil	**KX786373**	**KX786490**	**KX786412**
	AV86	*V. labrusca* cv. Niagara Rosada	Leaf	São Roque, SP, Brazil	**KX786374**	**KX786491**	**KX786413**
	AV93	*V. vinifera* × (*V. rupestris* × *V. lincecumii*) cv. Seibel 2	Berry	Garibaldi, RS, Brazil	**KX786375**	**KX786492**	**KX786414**
	AV95	*V. labrusca* cv. Niagara Branca	Berry	Nova Roma do Sul, RS, Brazil	**KX786376**	**KX786493**	**KX786415**

(continued)

Table 1 (continued)

Species	Isolate code	Host	Tissue	Location[a]	GenBank accession numbers[b]		
					ITS	HIS3	TEF
	AV97	*V. vinifera* cv. Zante Currant	Berry	Augusto Pestana, RS, Brazil	**KX786377**	**KX786494**	**KX786416**
	AV99	*V. labrusca* cv. Bordô	Leaf	Flores da Cunha, RS, Brazil	**KX786378**	**KX786495**	**KX786417**
	AV102	*V. labrusca* cv. Niagara Rosada	Berry	Augusto Pestana, RS, Brazil	**KX786379**	**KX786496**	**KX786418**
	AV103	*V. labrusca* cv. Isabel Precoce	Berry	Farroupilha, RS, Brazil	**KX786380**	**KX786497**	**KX786419**
	AV104	*Vitis* spp. - hybrid BRS Carmen	Berry	Farroupilha, RS, Brazil	**KX786381**	**KX786498**	**KX786420**
	AV107	*V. vinifera* - hybrid cv. BRS Morena	Leaf	Cotiporã, RS, Brazil	**KX786382**	**KX786499**	**KX786421**
	AV111	*V. labrusca* cv. Concord	Berry	Bento Gonçalves, RS, Brazil	**KX786383**	**KX786500**	**KX786422**
	AV113	*V. vinifera* cv. Moscato Giallo	Berry	Bento Gonçalves, RS, Brazil	**KX786384**	**KX786501**	**KX786423**
	AV114	*V. labrusca* cv. Isabel	Berry	Bento Gonçalves, RS, Brazil	**KX786385**	**KX786502**	**KX786424**
	AV115	*V. vinifera*- hybrid cv. BRS Clara	Berry	Cotiporã, RS, Brazil	**KX786386**	**KX786503**	**KX786425**
	AV117	*V. labrusca* cv. Niagara Rosada	Berry	São Borja, RS, Brazil	**KX786387**	**KX786504**	**KX786426**
	EAMI-1	*Vitis* spp. cv. Marquis	-	USA	AY826762	-	-
	EAMI-2	*Vitis* spp. cv. Marquis	-	USA	AY826763	-	-
	EAMI-3	*Vitis* spp. cv. Marquis	-	USA	AY826764	-	-
E. australis	70212	*Citrus unshiu* cv. Satsuma mandarin	-	Argentina	FJ010291	-	-
E. banksiae	STE-U 2678	*Banksia serrata*	-	Australia	AF227197	-	-
E. fawcettii	Jin-6	*Citrus*	-	South Korea	FJ010323	-	-
E. eucalypticola	CBS 124765	*Eucalyptus* sp.	-	Australia	GQ303275	-	-
E. eucalyptorum	CBS 120084	*Eucalyptus propinqua*	-	Australia	DQ923530	-	-
Sphaceloma asclepiadis	CPC 18583	-	-	Brazil	JN943494	-	-
S. erythrinae	CPC 18542	-	-	Brazil	JN943487	-	-
S. freyliniae	CBS 128204	*Freylinia lanceolata*	-	South Africa	HQ599577	-	-
S. krugii	CPC 18585	-	-	Brazil	JN943490	-	-
S. manihoticola		*Manihot esculenta*	-	Brazil	AY739018	-	-
S. perseae	CBS 28864	*Perseae americana*	-	Brazil	HM191255	-	-
S. tectificae	CBS 124777	*Eucalyptus tectifica*	-	Australia	GQ303294	-	-

[a]RS - Rio Grande do Sul State; SP - São Paulo State.
[b]Sequence numbers in bold were obtained in the present study.
[c]Rootstock.

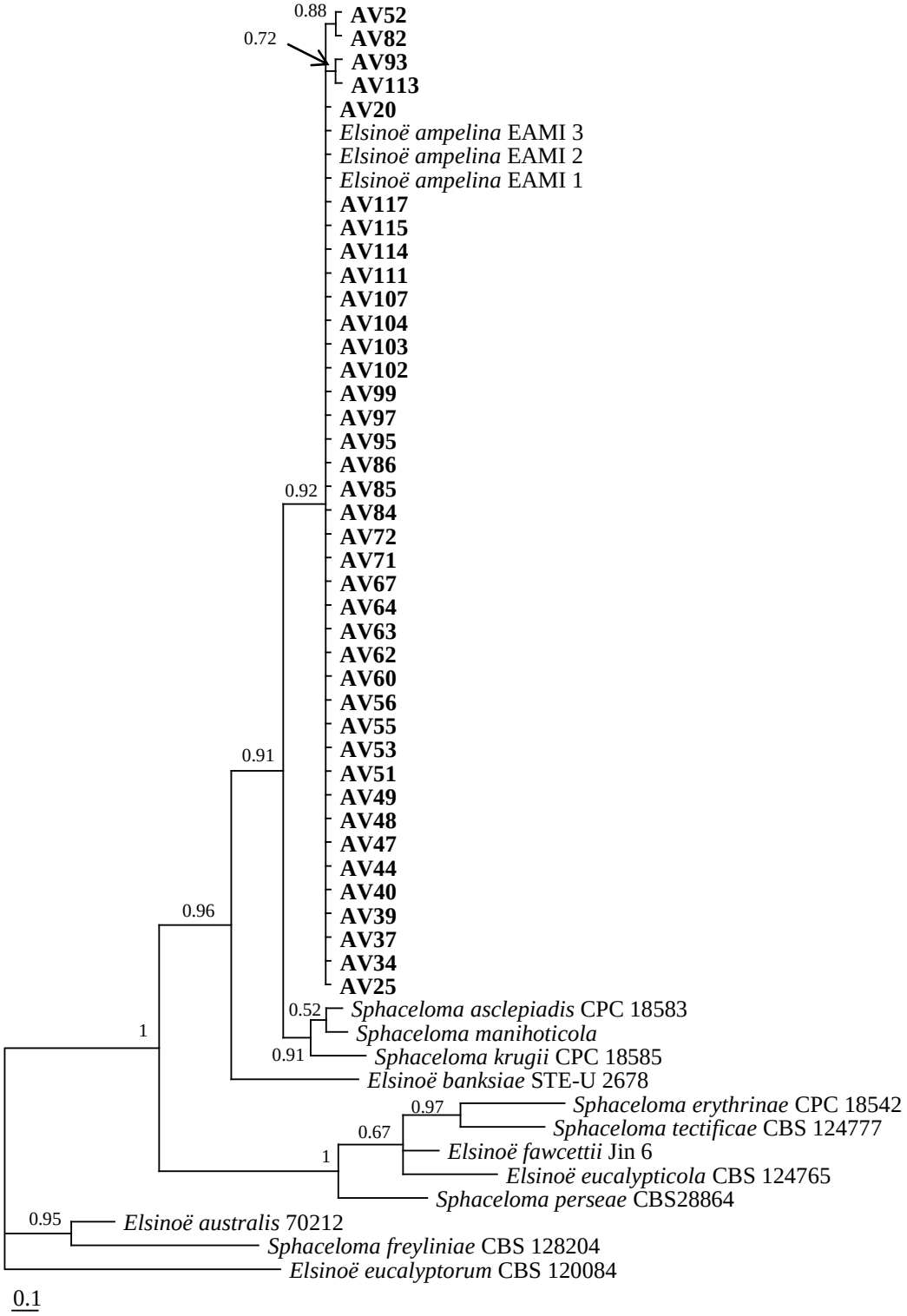

Figure 2 Phylogenetic tree derived from a Bayesian analysis of an alignment based on ITS sequences of *Elsinoë/Sphaceloma* isolates, run for 10^7 generations using the GTR+I+G model of nucleotide substitution. GenBank accession numbers of all isolates used in the phylogeny are listed in detail in Table 1. The numbers on the nodes are Bayesian posterior probability values. Isolates in bold were obtained in the present study in Brazil, 2014.

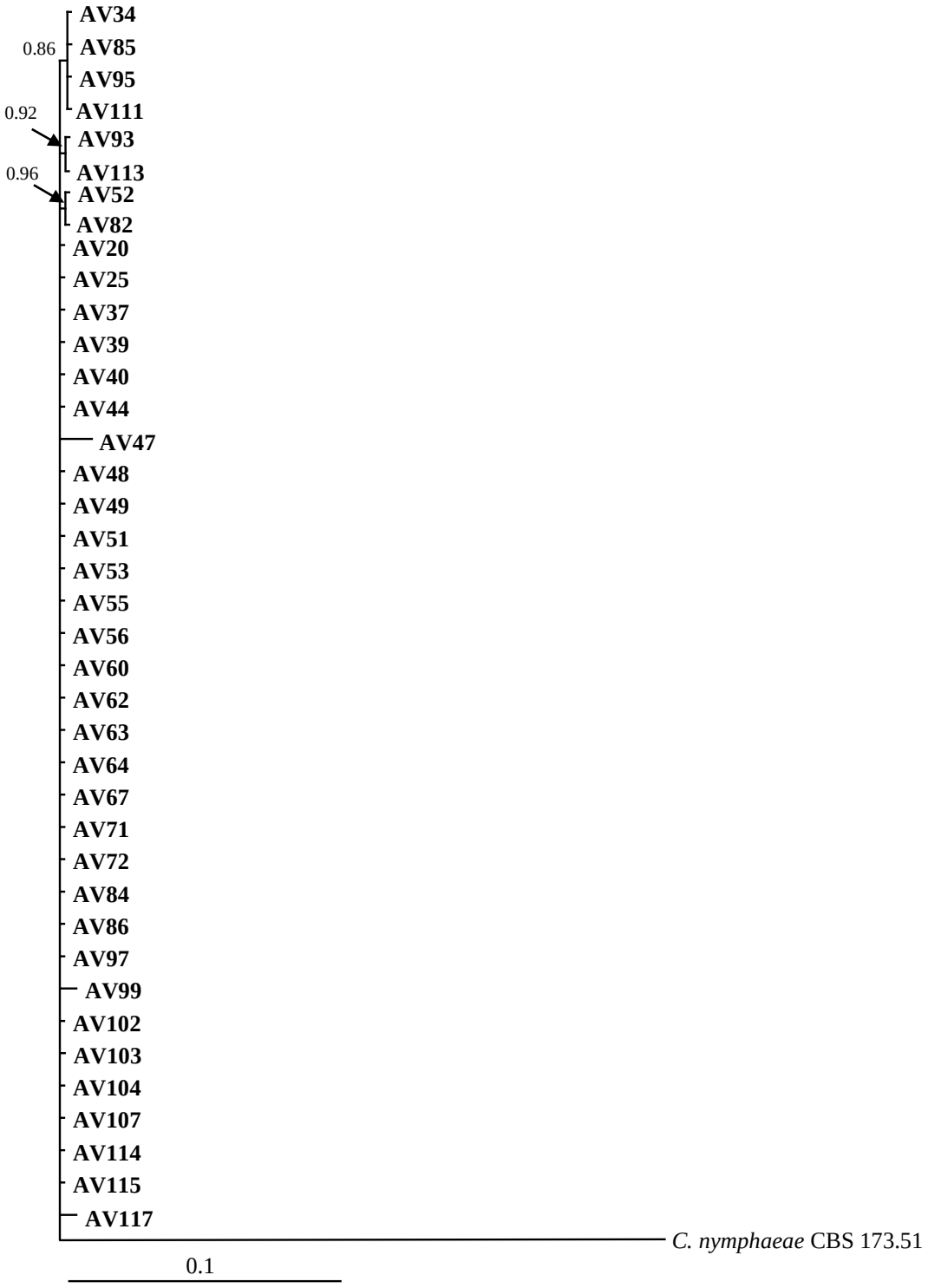

Figure 3 Phylogenetic tree derived from a Bayesian analysis of a combined ITS and HIS3 sequence alignment of *Elsinoë ampelina* isolates, run for 10^7 generations using the HKY+I and GTR models of nucleotide substitution for ITS and HIS3, respectively. GenBank accession numbers of all isolates used in the phylogeny are listed in detail in Table 1. The numbers on the nodes are Bayesian posterior probability values. Isolates in bold were obtained in the present study in Brazil, 2014. *Colletotrichum nymphaeae* was used as the outgroup.

The multilocus analysis for 50 *Colletotrichum* isolates, including *C. orbiculare* (CBS 57097) as an outgroup, was carried out using a sequence alignment of 1229 characters. The sequences obtained were 555-565, 252-291 and 489-497 bp in length for ITS, GAPDH, and TUB2, respectively (Table 2). The substitution models used were GTR+G for ITS, HKY+I+G for GAPDH and GTR+I+G for TUB2. The isolates were separated into four major clades: *C. gloeosporioides* and *C. acutatum* species complexes, as well as *C. truncatum* and *C. cliviae*, with Bayesian posterior probability values between 0.99 and 1. Therefore, the 13 isolates analysed in this study were identified as *C. siamense*, *C. gloeosporioides*, *C. fructicola*, *C. viniferum*, *C. nymphaeae*, *C. cliviae* and *C. truncatum* (Fig. 4).

Table 2 Species, isolate code, host and tissue of isolation, location of origin and GenBank accession numbers for *Colletotrichum* spp. isolates used in this study in Brazil, 2014

Species	Isolate code	Host	Tissue	Location[a]	GenBank accession numbers[b]		
					ITS	GAPDH	TUB2
Colletotrichum	CBS 127598	*Olea europaea*	-	South Africa	JQ948363	JQ948694	JQ950014
acutatum	CBS 112996	*Carica papaya*	-	Australia	JQ005776	JQ948677	JQ005860
C. aenigma	ICMP 18608	*Persea americana*	-	Israel	JX010244	JX010044	JX010389
C. alienum	ICMP 12071	*Malus domestica*	-	New Zealand	JX010251	JX010028	JX010411
C. aotearoa	ICMP 18537	*Coprosma* sp.	-	New Zealand	JX010205	JX010005	JX010420
C. asianum	ICMP 18580	*Coffea arabica*	-	Thailand	FJ972612	JX010053	JX010406
C. brisbanense	CBS 292.67	*Capsicum annuum*	-	Australia	JQ948291	JQ948621	JQ949942
C. chrysanthemi	CBS 126519	*Chrysanthemum coronarium*	Vascular tissue	Netherlands	JQ948272	JQ948602	JQ949923
C. cliviae	LC3546	*Camellia sinensis*	-	China	KJ955215	KJ954916	KJ955361
	CBS 125375	*Clivia miniata*	-	China	JX519223	JX546611	JX519249
	AV1	*V. riparia* × *V. labrusca* cv. Baco Blanc	Leaf	Augusto Pestana, RS, Brazil	**KX786427**	**KX786440**	**KX786453**
C. cosmi	CBS 853.73	*Cosmos* sp.	Seed	Netherlands	JQ948274	JQ948604	JQ949925
C. costaricense	CBS 330.75	*Coffea arabica* cv. Typica	Fruit	Costa Rica	JQ948180	JQ948510	JQ949831
C. cuscutae	IMI 304802	*Cuscuta* sp.	-	Dominica	JQ948195	JQ948525	JQ949846
C. fioriniae	CBS 125396	*Malus domestica*	Fruit	EUA	JQ948299	JQ948629	JQ949950
C. fructicola	CBS 238.49	*Ficus edulis*	-	Germany	JX010181	JX009923	JX010400
	ICMP 18581	*Coffea arabica*	-	Thailand	JX010165	JX010033	JX010405
	AV24	*V. labrusca* cv. Niagara Rosada	Leaf	Jundiaí, SP, Brazil	**KX786433**	**KX786446**	**KX786459**
C. gloeosporioides	ICMP 18695	*Citrus* sp.	-	USA	JX010153	JX009979	-
	IMI 356878	*Citrus sinensis*	-	Italy	JX010152	JX010056	JX010445
	AV4	*V. labrusca* cv. Niagara Rosada	Leaf	Londrina, PR, Brazil	**KX786428**	**KX786441**	**KX786454**
	AV31	*V. labrusca* cv. Niagara Rosada	Leaf	Jundiaí, SP, Brazil	**KX786434**	**KX786447**	**KX786460**
C. horii	NBRC 7478	*Diospyros kaki*	-	Japan	GQ329690	GQ329681	JX010450
C. kahawae subsp. *ciggaro*	CBS 237.49	*Hypericum perforatum*	-	Germany	JX010146	JX010050	HQ596280
C. lupini	CBS 109222	*Lupinus albus*	-	Germany	JQ948170	JQ948500	JQ949821
C. melonis	CBS 159.84	*Cucumis melo*	Fruit	Brazil	JQ948194	JQ948524	JQ949845
C. musae	CBS 116870	*Musa* sp.	-	USA	JX010146	JX010050	HQ596280
C. nymphaeae	CSL 1441	*Fragaria* x *ananassa*	-	United Kingdom	KM246574	KM252179	KM251929

(continued)

Table 2 (continued)

Species	Isolate code	Host	Tissue	Location[a]	GenBank accession numbers[b]		
					ITS	**GAPDH**	**TUB2**
	CBS 173.51	*Mahonia aquifolium*	Leaf	Italy	JQ948200	JQ948530	JQ949851
	AV59	*V. labrusca* cv. Isabel Precoce	Berry	Santa Maria, RS, Brazil	**KX786435**	**KX786448**	**KX786461**
	AV78	*V. labrusca* cv. Niagara Rosada	Leaf	São Roque, SP, Brazil	**KX786437**	**KX786450**	**KX786463**
	AV87	*V. labrusca* cv. Isabel	Berry	Flores da Cunha, RS, Brazil	**KX786438**	**KX786451**	**KX786464**
	AV90	*V. labrusca* cv. Niagara Branca	Berry	Nova Roma do Sul, RS, Brazil	**KX786439**	**KX786452**	**KX786465**
C. orbiculare	CBS 570.97	*Cucumis sativus*	-	Europe	KF178466	KF178490	KF178587
C. siamense	ICMP 17795	*Malus domestica*	-	USA	JX010162	JX010051	JX010393
	ICMP 12567	*Persea americana*	-	Australia	JX010250	JX009940	JX010387
	AV11	Riparia do Traviú × *V. caribaea* cv. IAC-766[c]	Leaf	Piracicaba, SP, Brazil	**KX786431**	**KX786444**	**KX786457**
	AV19	*V. riparia* × *(V. rupestris* × *V. cordifolia)* cv. Riparia do Traviú[c]	Leaf	Piracicaba, SP, Brazil	**KX786432**	**KX786445**	**KX786458**
C. simmondsii	CBS 122122	*Carica papaya*	Fruit	Australia	JQ948276	JQ948606	JQ949927
C. tamarilloi	CBS 129814	*Solanum betaceum*	Fruit	Colombia	JQ948184	JQ948514	JQ949835
C. theobromicola	CBS 124945	*Theobroma cacao*	-	Panama	JX010294	JX010006	JX010447
C. tropicale	CBS 124949	*Theobroma cacao*	-	Panama	JX010264	JX010007	JX010407
C. truncatum	CTM12	*Phaseolus lunatus*	-	Malaysia	JX971135	KC109590	KC109470
	CBS 710.70	*Phaseolus vulgaris*	-	Brazil	GU227864	GU228256	GU228158
	AV5	*V. labrusca* cv. Niagara Rosada	Leaf	Jales, SP, Brazil	**KX786429**	**KX786442**	**KX786455**
	AV6	*V. labrusca* cv. Niagara Rosada	Leaf	São Miguel Arcanjo, SP, Brazil	**KX786430**	**KX786443**	**KX786456**
C. viniferum	GZAAS5.08601	*V. vinifera* cv. Shuijing	Berry	China	JN412804	JN412798	JN412813
	JZB330015	*V.vinifera* cv. Syrah	Berry	China	KF156852	KF377483	KF288971
	GZAAS5.08622	*V. vinifera* cv. Shuijing	Berry	China	JN412806	JN412796	JN412812
	AV76	*V. labrusca* cv. Concord	Leaf	Bento Gonçalves, RS, Brazil	**KX786436**	**KX786449**	**KX786462**

[a]PR - Paraná State; RS - Rio Grande do Sul State; SP - São Paulo State.
[b]Sequence numbers in bold were obtained in the present study.
[c]Rootstock.

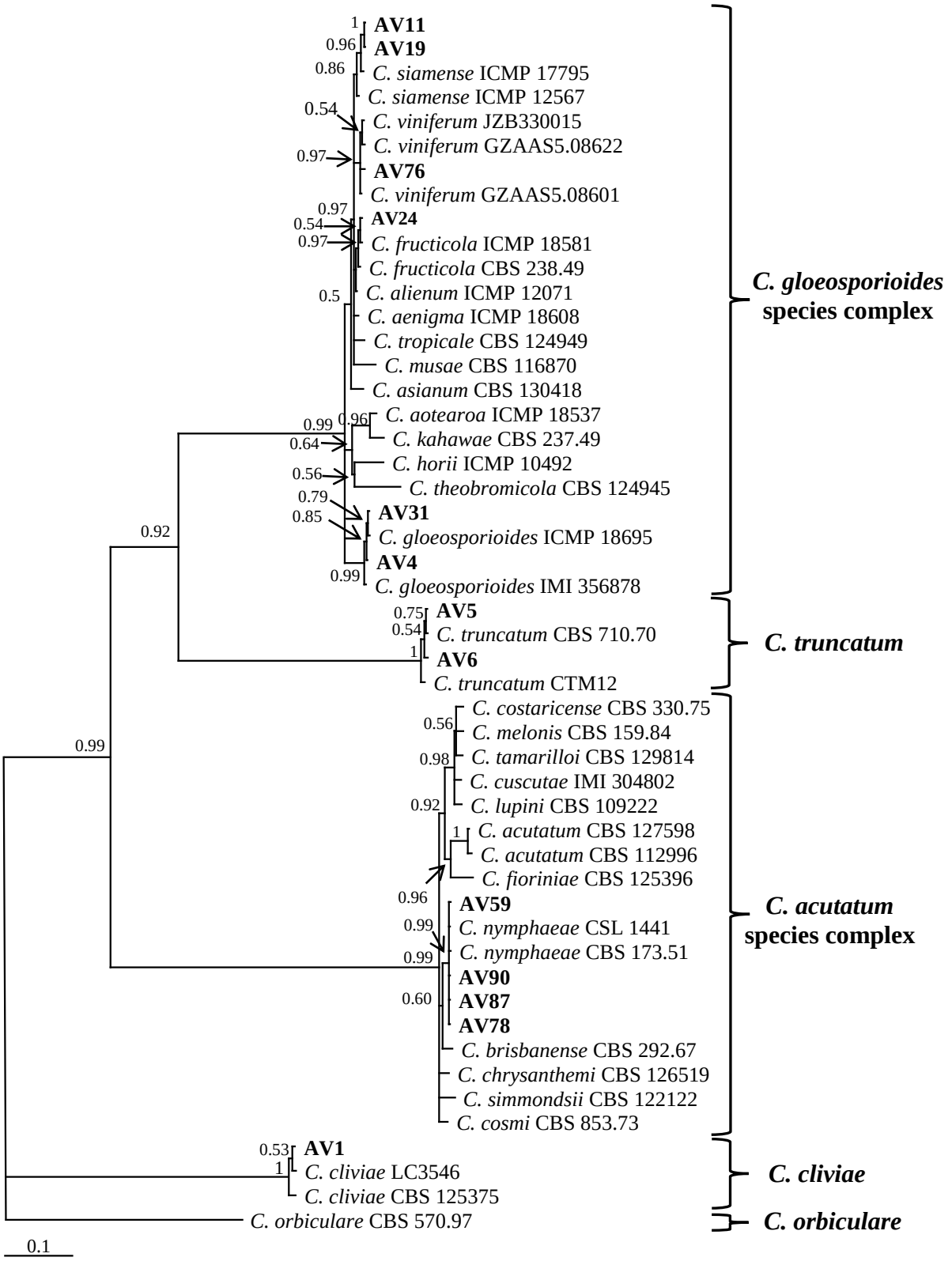

Figure 4 Phylogenetic tree derived from a Bayesian analysis of a combined ITS, GAPDH and TUB2 sequence alignment of *Colletotrichum* spp. isolates, run for 10^7 generations using the GTR+G, HKY+I+G and GTR+I+G models of nucleotide substitution for ITS, GAPDH and TUB2, respectively. GenBank accession numbers of all isolates used in the phylogeny are listed in detail in Table 2. The numbers on the nodes are Bayesian posterior probability values. Isolates in bold were obtained in the present study in Brazil, 2014.

2.3.2 Morphological characterization

Elsinoë ampelina was the most abundant species (75% of all isolates analysed), with great diversity of colony colour ranging from white to dark vinaceous, wrinkled texture, absence of spore masses, sparse to absent aerial mycelia and slow growth on PDA, measuring 22.5 to 28.1 mm in diameter after 30 days (Table 3). None of the *E. ampelina* isolates produced diffusible pigment on PDA. *Elsinoë ampelina* isolates did not produce any conidia on PDA, oatmeal agar, corn agar, Sabourad's agar, yeast extract agar, Richard's agar or Czapek's agar media incubated at 25 °C with 0, 12 and 24 h photoperiods for 30 days (data not shown). On Fries' medium, the presence of conidia was rare (Fig. 5). The lesions in the inoculated leaves also presented low sporulation. *Elsinoë ampelina* isolates produced conidia that were cylindrical to oblong, hyaline, aseptate, with both ends rounded, (3.57-) 5.64 (-6.95) µm long and (2.03-) 2.65 (-3.40) µm wide.

Isolates of *Colletotrichum* showed high variation in colony colour ranging from white to mouse grey, cottony to felty aerial mycelia and fast growth ranging from 48.8 to 76.4 mm in diameter on PDA after 5 days of incubation. Only *C. nymphaeae*, belonging to the *C. acutatum* species complex, showed abundant sporulation, forming orange concentric zones (Table 3). Conidia of *Colletotrichum* spp. isolates showed a wide variation in size and shape. *Colletotrichum truncatum* had falcate conidia, which had acute ends and measured (23.32-) 26.75 (-31.21) × (3.32-) 3.92 (-4.87) µm. Meanwhile, the remaining species of *Colletotrichum* analysed showed cylindrical conidia. *Colletotrichum fructicola*, *C. siamense* and *C. viniferum* belonging to the *C. gloeosporioides* species complex and also *C. cliviae* showed conidia with rounded ends that measured (8.45-) 12.63 (-15.33) × (3.33-) 4.10 (-4.83), (9.79-) 14.36 (-17.66) × (3.73-) 4.54 (-5.58), (10.91-) 13.51 (-15.74) × (4.42-) 5.23 (-5.85) and (8.94-) 15.64 (-20.07) × (4.35-) 5.50 (-6.89) µm, respectively. *Colletotrichum gloeosporioides* isolates showed conidia with rounded and sometimes acute ends, measuring (12.35-) 15.62 (-18.56) × (4.22-) 5.04 (-5.96) µm. For *C. nymphaeae*, conidia showed acute and sometimes rounded ends, measuring (9.57-) 14.69 (-17.31) × (3.83-) 4.46 (-5.62) µm.

Table 3 Frequency of isolates in the population analysed and cultural characteristics including colony diameter, texture and colour of *Elsinoë ampelina* and *Colletotrichum* spp. in Brazil, 2014

Species	Frequency (%)	Cultural characteristics		
		Diameter (mm)[a]	Texture	Colour[b]
Elsinoë ampelina	1.92	23.2	Wrinkled	Violet slate with white edge
	9.62	24.5	Wrinkled	Sepia with dark brick edge
	11.54	26.6	Wrinkled	Dark vinaceous with isabelline edge
	28.88	23.9	Wrinkled	Peach with scarlet edge
	21.15	28,1	Wrinkled	Peach to white with peach edge
	1.92	22.5	Wrinkled	White with ochreous sectors
Colletotrichum cliviae	1.92	76.4	Cottony	Pale mouse gray with white to pale mouse gray edge
C. fructicola	1.92	60.6	Cottony	White to pale mouse grey
C. gloeosporioides	3.84	63.0	Cottony	White with mouse gray centre and orange masses of spores
C. nymphaeae	7.69	48.8	Felty-cottony	White to saffron with concentric rings of orange sporulation
C. siamense	3.84	70.5	Cottony	White to pale mouse grey
C. truncatum	3.84	51.3	Felty	Mouse grey to olivaceous grey
C. viniferum	1.92	58.8	Cottony	White to pale mouse grey

[a]Diameter of colony on potato dextrose agar after 30 days for *E. ampelina* and after 5 days for *Colletotrichum* spp.
[b]Colony colour was described using the mycological colour chart of Rayner (1970).

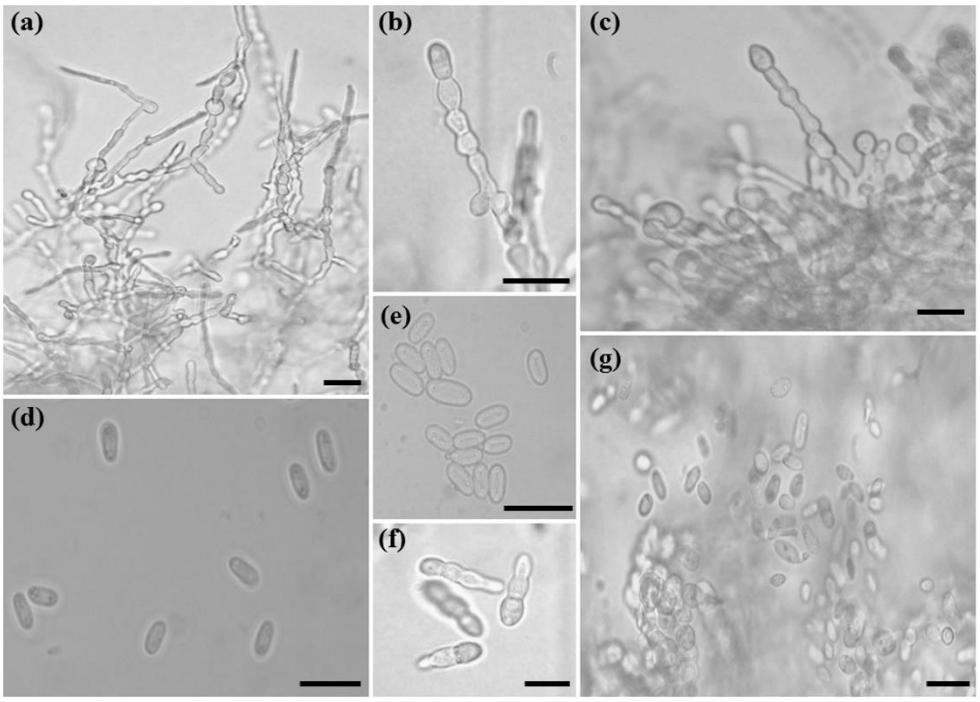

Figure 5 *Elsinoë ampelina* (isolate AV25): (a) monilioid hyphae developed on potato dextrose agar; (b, c) monilioid hyphae developed on microcolony in Fries' medium; (d, e) conidia obtained from leaf lesions; (f) germination of hyaline conidia in Fries' medium showing development of septa at 24 h; and (g) conidia produced in Fries' medium. Scale bars: 10 µm.

2.3.3 Pathogenicity

All *E. ampelina* isolates inoculated on *V. vinifera* 'Moscato Giallo' and *V. labrusca* 'Niagara Rosada' caused anthracnose symptoms on leaves, stems and tendrils (Fig. 6). The disease severity was greater in the two youngest leaves than in the other leaves. *Colletotrichum* spp. isolates did not cause any symptoms, with the exception of *C. viniferum* (isolate AV76), which caused small necrotic lesions on leaves of 'Moscato Giallo' 2 days after inoculation. These lesions were similar to a hypersensitive reaction, did not show sporulation and became less apparent 5-6 days after inoculation. The control plants did not show any anthracnose symptoms. In both cultivars, kept in the greenhouse or the growth room, the first anthracnose symptoms on leaves occurred 2-3 days and on stems between 3 to 7 days after inoculation.

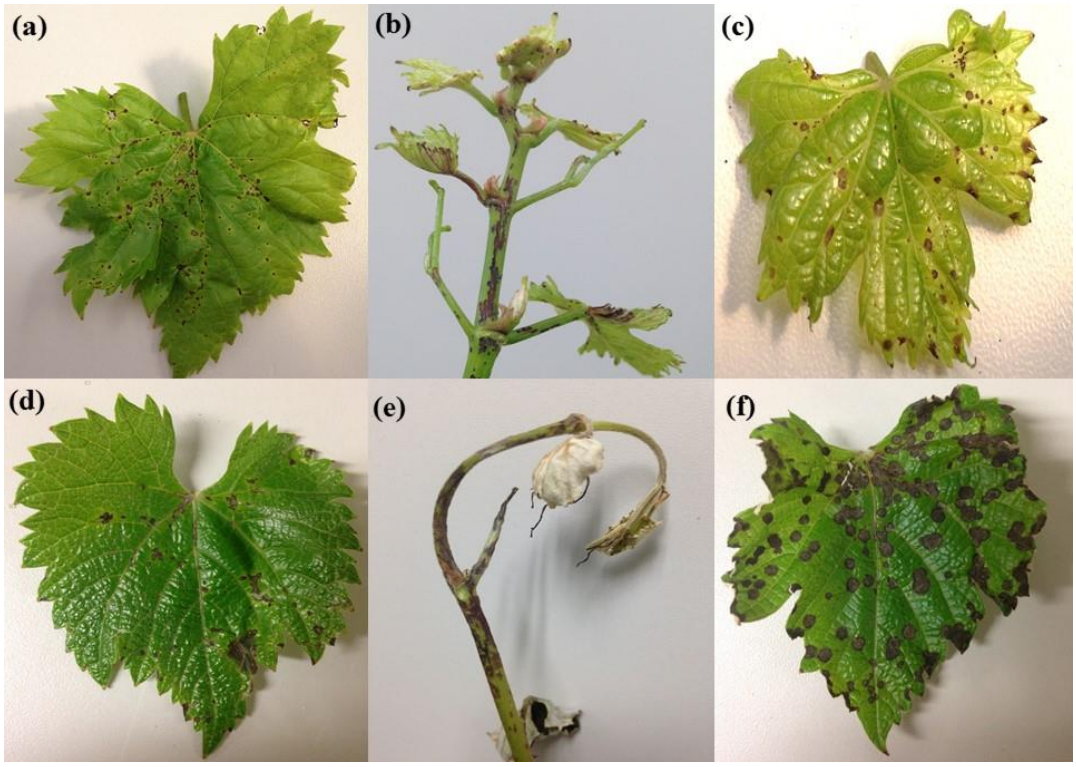

Figure 6 Anthracnose symptoms on grapevine 12 days after inoculation with *Elsinoë ampelina* (isolate AV47) in Brazil, 2015: (a-c) *Vitis vinifera* 'Moscato Giallo'; (a) leaf – environment 1 (relative humidity between 60 and 70%); (b) stem and leaves – environment 2 (relative humidity > 95%); (c) leaf – environment 2. (d-f) *Vitis labrusca* 'Niagara Rosada': (d) leaf – environment 1; (e) stem and leaves – environment 2; and (f) leaf – environment 2.

Elsinoë ampelina isolates showed different levels of disease severity in both cultivars assessed (Tables 4 & 5). Regardless of disease severity, plants inoculated with *E. ampelina*

showed a significant decrease in shoot dry weight, which was due to shoot necrosis; this was not observed in plants inoculated with *Colletotrichum* spp. In both cultivars, *E. ampelina* isolates caused higher disease severity and higher shoot dry weight reduction ($P < 0.05$) when plants were kept at a relative humidity higher >95% than at 60-70%. At 95% relative humidity, there was a negative correlation between disease severity and shoot dry weight in 'Niagara Rosada' (r = -0.33) and 'Moscato Giallo' (r = -0.59). For 'Niagara Rosada', the humid environment increased the number of lesions. However, for 'Moscato Giallo', the numbers of lesions were not significantly different in the two environments ($P < 0.05$). Comparing the two cultivars, the greatest number of lesions and the highest disease severity were observed in 'Niagara Rosada' in both environments ($P < 0.05$). All *E. ampelina* isolates were re-isolated from the plants with symptoms on leaves, stems and tendrils.

Table 4 Number of lesions per leaf, leaf disease severity and shoot dry weight for different isolates of *Elsinoë ampelina* and *Colletotrichum* spp. inoculated on *Vitis vinifera* 'Moscato Giallo' in Brazil, 2015

Species	Isolate	Environment 1[a]			Environment 2[b]		
		No of lesions[c]	Leaf disease severity[d] (%)	Shoot dry weight (g)	No of lesions	Leaf disease severity (%)	Shoot dry weight (g)
	Control	0 e	0 d	1.11 a	0 c	0 d	1.20 a
Elsinoë ampelina	AV20	0.75 d	0.40 c	0.67 b	1.63 b	2.06 c	0.99 b
	AV25	1.25 c	0.47 c	0.94 a	1.75 b	1.92 c	1.08 b
	AV34	1.50 c	0.53 c	0.49 b	1.88 b	2.51 c	0.62 d
	AV37	2.50 b	0.93 c	0.57 b	2.38 a	3.36 c	0.74 c
	AV47	2.00 b	2.13 a	0.79 a	2.00 b	3.20 c	0.80 c
	AV52	2.25 b	0.78 c	0.84 a	2.13 a	5.30 b	0.84 c
	AV53	1.25 c	0.64 c	0.63 b	1.63 b	4.92 b	0.82 c
	AV97	2.38 b	1.14 b	0.58 b	2.25 a	2.94 c	0.80 c
	AV113	1.50 c	2.36 a	0.86 a	1.75 b	7.11 a	0.72 c
	AV115	3.63 a	2.43 a	0.55 b	2.63 a	7.70 a	0.61 d
Colletotrichum cliviae	AV1	0 e	0 d	0.93 a	0 c	0 d	1.05 b
C. fructicola	AV24	0 e	0 d	0.78 a	0 c	0 d	0.99 b
C. gloeosporioides	AV4	0 e	0 d	0.80 a	0 c	0 d	1.08 b
C. nymphaeae	AV78	0 e	0 d	1.01 a	0 c	0 d	1.25 a
C. siamense	AV19	0 e	0 d	0.76 a	0 c	0 d	0.96 b
C. truncatum	AV6	0 e	0 d	0.97 a	0 c	0 d	1.18 a
C. viniferum	AV76	0 e	0 d	0.87 a	0 c	0 d	0.95 b

Means within column followed by different letters differ significantly ($P < 0.05$) according to Scott-Knott test.
[a]Environment 1: greenhouse with relative humidity 60-70%.
[b]Environment 2: growth room with relative humidity > 95%.
[c]Number of lesions in 4 cm^2 leaf area were rated using the following scale: 0 = no lesions, 1 = 1-6 lesions, 2 = 7-25, 3 = 26-50; 4 = 51-100 and 5 = > 100 lesions [Adapted from Poolsawat *et al.* (2012)].
[d]Leaf disease severity was quantified based on the percentage of leaf area covered by lesions.

Table 5 Number of lesions per leaf, leaf disease severity and shoot dry weight for different isolates of *Elsinoë ampelina* and *Colletotrichum* spp. inoculated on *Vitis labrusca* 'Niagara Rosada' in Brazil, 2015

Species	Isolate	Environment 1[a]			Environment 2[b]		
		No of lesions[c]	Leaf disease severity[d] (%)	Shoot dry weight (g)	No of lesions	Leaf disease severity (%)	Shoot dry weight (g)
	Control	0 d	0 c	0.95 a	0 f	0 d	0.84 a
Elsinoë ampelina	AV20	2.13 c	1.32 b	0.77 a	1.75 e	14.29 c	0.40 b
	AV25	2.88 a	1.92 b	0.81 a	3.63 a	58.91 a	0.52 b
	AV34	2.50 c	3.64 a	0.61 b	2.75 c	26.39 b	0.36 b
	AV37	2.63 b	2.52 b	0.65 b	2.88 c	37.77 b	0.41 b
	AV47	3.00 a	3.44 a	0.72 b	3.25 b	72.16 a	0.21 c
	AV52	2.25 c	3.04 a	0.54 b	2.38 d	10.51 c	0.45 b
	AV53	3.13 a	3.78 a	0.64 b	3.75 a	60.20 a	0.17 c
	AV97	2.63 b	2.45 b	0.68 b	2.05 d	56.16 a	0.35 b
	AV113	3.00 a	1.89 b	0.85 a	3.75 a	62.11 a	0.55 b
	AV115	2.75 b	3.96 a	0.64 b	3.00 b	22.11 b	0.46 b
Colletotrichum cliviae	AV1	0 d	0 c	0.84 a	0 f	0 d	0.80 a
C. fructicola	AV24	0 d	0 c	0.92 a	0 f	0 d	0.87 a
C. gloeosporioides	AV4	0 d	0 c	0.84 a	0 f	0 d	0.81 a
C. nymphaeae	AV78	0 d	0 c	0.98 a	0 f	0 d	0.84 a
C. siamense	AV19	0 d	0 c	0.92 a	0 f	0 d	0.79 a
C. truncatum	AV6	0 d	0 c	1.00 a	0 f	0 d	0.81 a
C. viniferum	AV76	0 d	0 c	0.95 a	0 f	0 d	0.77 a

Means within column followed by different letters differ significantly ($P < 0.05$) according to Scott-Knott test.
[a]Environment 1: greenhouse with relative humidity 60-70%.
[b]Environment 2: growth room with relative humidity > 95%.
[c]Number of lesions in 4 cm^2 leaf area were rated using the following scale: 0 = no lesions, 1 = 1-6 lesions, 2 = 7-25, 3 = 26-50; 4 = 51-100 and 5 = > 100 lesions [Adapted from Poolsawat *et al.* (2012)].
[d]Leaf disease severity was quantified based on the percentage of leaf area covered by lesions.

2.4 Discussion

Elsinoë ampelina was the only causal agent of grapevine anthracnose identified in populations of isolates collected in *Vitis* spp. in Brazil. Although isolates of *Colletotrichum* spp. were isolated from anthracnose lesions, none were pathogenic to the cultivars used in this study. Multilocus DNA analysis was used for the first time for the identification of *E. ampelina* in grapevine. Sequence analysis of the ITS region has been widely used for the molecular identification of *Elsinoë/Sphaceloma* in several pathosystems (Hyun *et al.*, 2009; Everett *et al.*, 2011; Miles *et al.*, 2015; Minutolo *et al.*, 2016) and the ITS region used together with the TEF gene (Hyun *et al.*, 2009; Miles *et al.*, 2015). Hyun *et al.* (2009) reported that *E. australis* and *E. fawcettii* isolates associated with citrus scab in Argentina, Brazil, New Zealand and the United States showed 88 polymorphic sites within the ITS

region and 34 within the TEF gene; thus, these isolates can be easily differentiated by analysis of ITS and TEF sequences.

The 39 ITS sequences of *E. ampelina* obtained in this study, together with three other *E. ampelina* sequences from the United States (Schilder *et al.*, 2005), were grouped in a main clade with a Bayesian posterior probability of 0.92, markedly distinct from other *Elsinoë/Sphaceloma* spp. sequences obtained from GenBank. Isolates of *E. ampelina* from the United States did not show any polymorphic sites within the ITS locus (Schilder *et al.*, 2005), being identical to 35 Brazilian isolates obtained in this study. Nucleotide substitutions were observed in only two isolates at position 192 and in two other isolates at position 234 within the 602 bp sequenced, which suggests low genetic variability within the ITS region. Additionally, the 39 TEF sequences obtained did not contain any polymorphic sites in the 412 bp analysed and was, therefore, a monomorphic locus. The low genetic variability of the ITS region and the absence of variability within the TEF gene indicates high conservation of these genomic regions in this fungal species. The low variability may also be related to the absence of sexual reproduction in this species in Brazil (Amorim *et al.*, 2016).

In this study, the third locus used for molecular characterization was the HIS3 gene, which has never been used for the genus *Elsinoë/Sphaceloma*. In contrast to the low variability of the ITS and TEF sequences, HIS3 sequences showed the highest degree of polymorphism (55 polymorphic sites within 351-400 bp), including deletions and substitutions of nucleotides. This result suggests that the HIS3 region may be used for studies of genetic diversity in *E. ampelina*. In multilocus phylogenetic analysis (TUB2, HIS3, TEF and ITS) of the genus *Ilyonectria*, the causal agent of black foot disease of grapevine, the HIS3 gene was also the most informative and the only gene able to separate all the species with high probabilities (Cabral *et al.*, 2012). Similarly, the HIS3 locus was also more informative than TUB2, ITS and TEF in a phylogenetic study of *Cercospora* spp. (Tessmann *et al.*, 2001).

Conidia of all *E. ampelina* isolates were similarly sized to those of Thai isolates (Sompong *et al.*, 2012). In the present study, *E. ampelina* colonies showed slow growth and high variability in colour, which was also reported for *E. ampelina* (Sompong *et al.*, 2012) and for *E. australis* (Miles *et al.*, 2015), *S. coryli* (Minutolo *et al.*, 2016) and *S. perseae* (Everett *et al.*, 2011). In this study, *E. ampelina* did not sporulate on culture media. Lesions produced by artificial inoculation sporulated poorly 9 days after inoculation. However, it is reported that, under field conditions, infected canes are the main inoculum source of

grapevine anthracnose (Thind, 2015). In spring, sclerotia or mycelium surviving in cane lesions become active and produce abundant conidia resulting in severe epidemics during rainy years (Thind *et al.*, 2004; Amorim *et al.*, 2016).

The incubation period of the disease on leaves was short, 2 to 3 days, as reported by Brook (1973) and Poolsawat *et al.* (2010). Leaves and young stems are highly susceptible to the disease, requiring 3-4 h of wetness at 21 °C for infection, while expanded leaves are highly resistant (Brook, 1973). In the greenhouse, with an average relative humidity of 60-70%, many lesions quantified on the fifth day after inoculation did not develop and were becoming less apparent as the leaf expanded. The highest severity of anthracnose in both cultivars was observed when relative humidity was higher than 95% ($P < 0.05$). Precipitation, relative humidity and temperature are the climatic factors that most influence the infection of *E. ampelina* (Thind *et al.*, 2004). In the present study, *E. ampelina* isolates caused reduction of shoot dry weight by up to 56% in 'Moscato Giallo' and 80% in 'Niagara Rosada' when compared to the control. In severe infections, when the lesions are numerous and deep, stems break, resulting in yield loss. Leaves and berries that are severely infected dry up and drop prematurely (Carisse & Lefebvre, 2011).

The results of the present study are in agreement with research in Australia and Japan that identified table grape cultivars as more susceptible to anthracnose than wine grape cultivars (Hart *et al.*, 1993; Kono *et al.*, 2013). Kono *et al.* (2013) attributed this result to the presence of larger-effect genes and/or more small-effect resistance genes within wine grape populations than within table grape populations. However, the potential sources and mechanisms of resistance to *E. ampelina* in grapevines are not clear.

The phylogenetic analysis of 13 *Colletotrichum* isolates obtained from anthracnose lesions resulted in four well-supported clades. The first clade contained six isolates belonging to the *C. gloeosporioides* species complex: *C. siamense*, *C. gloeosporioides*, *C. fructicola* and *C. viniferum*. *Colletotrichum viniferum* has been described in China as associated with ripe rot in *V. vinifera* (Yan *et al.*, 2015). The second largest group included four isolates clustered with *C. nymphaeae*, which was associated with anthracnose symptoms on stems of *V. vinifera* 'Red Globe' in China (Liu *et al.*, 2016). The third group included two isolates within the clade containing *C. truncatum* (synonym: *C. capsici*). *Colletotrichum capsici* has been reported to cause small dark brown spots on the leaves and petioles in table and wine grape in India (Sawant *et al.*, 2012b). Finally, a single isolate was clustered with *C. cliviae*. This

species showed high genetic diversity compared to other species of *Colletotrichum* obtained in this study.

Analysis based only on ITS sequences allowed the classification of *Colletotrichum* isolates only at the level of species complexes. Multilocus concatenation alignment (ITS, TUB2 and GAPDH) proved to be suitable for identification of the species belonging to different complexes, with clades being well supported. Similar results were observed in a study on identification of isolates belonging to *C. acutatum sensu lato* associated with anthracnose of *Carthamus tinctorius* (Baroncelli *et al.*, 2015). Although Sawant *et al.* (2012a,b) analysed hundreds of isolates of *C. gloeosporioides* and *C. capsici* associated with anthracnose of grapevine, there are only two ITS sequences of *C. gloeosporioides sensu lato* (accession nos. JN639880, JN639881) deposited in GenBank (Sawant *et al.*, 2012a). ITS sequences of *C. siamense* isolates obtained in this study (AV11 and AV19) showed 99% similarity to accession JN639881.

The wide range of cultural characteristics and conidial shape and size found in isolates of *Colletotrichum* spp. is due to the different species detected in this study. Similar conidial and cultural characteristics were reported in isolates of *C. gloeosporioides sensu lato* isolated from grapevines with anthracnose symptoms (Sawant *et al.*, 2012a) and ripe rot of grape (Yan *et al.*, 2015).

Colletotrichum viniferum (AV76) was the only species of *Colletotrichum* identified in this study that caused small necrotic spots on leaves of 'Moscato Giallo', resembling a hypersensitive reaction. Peng *et al.* (2013) reported that *C. viniferum* isolates obtained from grape berries with ripe rot symptoms showed nonspecific pathogenicity reactions on hosts when inoculated on leaves of *Citrus reticulata, Citrus sinensis, Ampelopsis sinica* and *Eriobotrya japonica*. Many species of *Colletotrichum* are associated with anthracnose in several crops and have demonstrated a lack of host specificity (Damm *et al.*, 2012; Weir *et al.*, 2012). *Colletotrichum* conidia may germinate on most surfaces, form an appressorium and remain attached to the surface as a viable propagule. *Colletotrichum* may also present latent infection and endophytic behaviour (Weir *et al.*, 2012). In grapevine, *C. acutatum* and *C. gloeosporioides* species complexes and *C. truncatum* are causal agents of ripe rot (Suzaki, 2011; Pan *et al.*, 2016). It is possible that isolates of *Colletotrichum* spp. obtained in this study survived in the plant endophytically or in the form of quiescent appressoria. Despite the isolation of multiple fungal species from grape tissues with anthracnose symptoms from the

different grape-growing regions of Brazil, only *E. ampelina* was identified as the causal agent of the disease.

References

Amorim L, Spósito MB, Kuniyuki H, 2016. Doenças da videira. In: Amorim L, Rezende JAM, Bergamin Filho A, Camargo LEA, eds. *Manual de Fitopatologia: doenças das plantas cultivadas*. São Paulo, SP, Brazil: Agronômica Ceres, 745–58.

Anderson HW, 1956. *Diseases of Fruit Crops*. New York, NY, USA: McGrawHill.

Baroncelli R, Sarrocco S, Zapparata A, Tavarini S, Angelini LG, Vannacci G, 2015. Characterization and epidemiology of *Colletotrichum acutatum sensu lato* (*C. chrysanthemi*) causing *Carthamus tinctorius* anthracnose. *Plant Pathology* **64**, 375–84.

Baroncelli R, Sreenivasaprasad S, Lane CR, Thon MR, Sukno SA, 2014. First report of *Colletotrichum acutatum sensu lato* (*Colletotrichum godetiae*) causing anthracnose on grapevine (*Vitis vinifera*) in the United Kingdom. *New Disease Reports* **29**, 26.

Barros LB, Biasi LA, Carisse O, May De Mio LL, 2015. Incidence of grape anthracnose on different *Vitis labrusca* and hybrid cultivars and rootstocks combination under humid subtropical climate. *Australasian Plant Pathology* **44**, 397–403.

Boratyn GM, Camacho C, Cooper PS *et al.*, 2013. BLAST: a more efficient report with usability improvements. *Nucleic Acids Research* **41**, 29–33.

Brook PJ, 1973. Epidemiology of grapevine anthracnose, caused by *Elsinoe ampelina*. *New Zealand Journal of Agricultural Research* **16**, 333–42.

Cabral A, Rego C, Nascimento T, Oliveira H, Groenewald JZ, Crous PW, 2012. Multi-gene analysis and morphology reveal novel *Ilyonectria* species associated with black foot disease of grapevines. *Fungal Biology* **116**, 62–80.

Carisse O, Lefebvre A, 2011. A model to estimate the amount of primary inoculum of *Elsinoë ampelina*. *Plant Disease* **95**, 1167–71.

Chowdappa P, Reddy GS, Kumar A, Rao BM, Rawal RD, 2009. Morphological and molecular characterization of *Colletotrichum* species causing anthracnose of grape in India. *The Asian and Australasian Journal of Plant Science and Biotechnology* **3**, 71–7.

Crous PW, Groenewald JZ, Risède JM, Philippe S, Hyde-Jones NL, 2004. *Calonectria* species and their *Cylindrocladium* anamorphs: species with clavate vesicles. *Studies in Mycology* **55**, 415–30.

Damm U, Cannon PF, Woudenberg JHC, Crous PW, 2012. The *Colletotrichum acutatum* species complex. *Studies in Mycology* **73**, 37–113.

Everett KR, Rees-George J, Pushparajah IPS, Manning MA, Fullerton RA, 2011. Molecular identification of *Sphaceloma perseae* (avocado scab) and its absence in New Zealand. *Journal of Phytopathology* **159**, 106–13.

Gene Codes Corporation, 2016. Sequencher® version 5.4.1 sequence analysis software. [http://www.genecodes.com]. Accessed 20 May 2016.

Giovaninni E, 2001. *Uva agroecológica*. Porto Alegre, RS, Brazil: Renascença.

Glass NL, Donaldson GC, 1995. Development of primer sets designed for use with the PCR to amplify conserved genes from filamentous ascomycetes. *Applied and Environmental Microbiology* **61**, 1323–30.

Guerber JC, Liu B, Correll JC, Johnston PR, 2003. Characterization of diversity in *Colletotrichum acutatum sensu lato* by sequence analysis of two gene introns, mtDNA and intron RFLPs, and mating compatibility. *Mycologia* **95**, 872–95.

Hall TA, 1999. BioEdit: a user-friendly biological sequence alignment editor and analysis program for Windows 95/98/NT. *Nucleic Acids Symposium Series* **41**, 95–8.

Hart KH, Magarey RD, Emmett RW, Magarey PA, 1993. Susceptibility of grapevine selections to black spot (anthracnose), *Elsinoe ampelina*. *Australian Grapegrower & Winemaker* **352**, 85–7.

Hyun JW, Yi SH, Mackenzie SJ *et al.*, 2009. Pathotypes and genetic relationship of worldwide collections of *Elsinoë* spp. causing scab diseases of citrus. *Phytopathology* **99**, 721–8.

IBGE - Instituto Brasileiro de Geografia e Estatística, 2016. Levantamento sistemático da produção agrícola. [ftp://ftp.ibge.gov.br/Producao_Agricola/Levantamento_Sistematico_da_Producao_Agricola_[mensal]/Fasciculo/lspa_201604.pdf]. Accessed 12 December 2016.

Kono A, Sato A, Ban Y, Mitani N, 2013. Resistance of *Vitis* germplasm to *Elsinoë ampelina* (de Bary) Shear evaluated by lesion number and diameter. *HortScience* **48**, 1433–9.

Kumar S, Third TS, Mohan C, 1994. Occurrence of *Gloeosporium ampelophagum* and *Colletotrichum gloeosporioides*, the incitants of grape anthracnose, during different months in Punjab. *Plant Disease Research* **9**, 222–4.

Liu M, Zhang W, Zhou Y *et al.*, 2016. First report of twig anthracnose on grapevine caused by *Colletotrichum nymphaeae* in China. *Plant Disease* **100**, 2530.

Lorenz DH, Eichhorn KW, Bleiholder H, Klose R, Meier U, Weber E, 1995. Phenological growth stages of the grapevine (*Vitis vinifera* L. ssp. *vinifera*)- Codes and descriptions according to the extended BBCH scale. *Australian Journal of Grape and Wine Research* **1**, 100–3.

Maddison WP, Maddison DR, 2011. Mesquite: a modular system for evolutionary analysis. Version 2.75. [http://mesquiteproject.org]. Accessed 20 January 2016.

Miles AK, Tan YP, Shivas RG, Drenth A, 2015. Novel pathotypes of *Elsinoë australis* associated with *Citrus australasica* and *Simmondsia chinensis* in Australia. *Tropical Plant Pathology* **40**, 26–34.

Minutolo M, Nanni B, Scala F, Alioto D, 2016. *Sphaceloma coryli*: A reemerging pathogen causing heavy losses on hazelnut in Southern Italy. *Plant Disease* **100**, 548–54.

Nirenberg H, 1976. Untersuchungen über die morphologische und biologische differenzierung in der *Fusarium*-Sektion Liseola. *Mitteilungen aus der Biologischen Bundesanstalt fur Land-und Forstwirtschaft* **169**, 1–117.

Nylander J, 2004. MrModeltest v2.3 Program distributed by the author. Evolutionary Biology Centre, Uppsala University.

Oliveira MDM, Silva PR, Amaro AA, Tecchio MA, 2008. Viabilidade econômica em tratamento antidegrana em uva “Niagara Rosada” no Estado de São Paulo. *Informações Econômicas* **38**, 59–68.

Page RDM, 1996. TreeView: an application to display phylogenetic trees on personal computers. *Computer Applications in the Biosciences* **12**, 357–8.

Pan FY, Huang Y, Lin L *et al.*, 2016. First report of *Colletotrichum capsici* causing grape ripe rot in Guangxi , China. *Plant Disease* **100**, 2531.

Pedro Júnior MJ, Pezzopane JRM, Martins FP, 1999. Uso da precipitação pluvial para previsão de épocas de pulverização visando controle de doenças fúngicas na videira "Niagara Rosada." *Revista Brasileira de Agrometeorologia* **7**, 107–11.

Peng L, Sun T, Yang Y *et al.*, 2013. *Colletotrichum* species on grape in Guizhou and Yunnan provinces, China. *Mycosciense* **54**, 29–41.

Poolsawat O, Tharapreuksapong A, Wongkaew S, Chaowiset W, Tantasawat P, 2012. Laboratory and field evaluations of resistance to *Sphaceloma ampelinum* causing anthracnose in grapevine. *Australasian Plant Pathology* **41**, 263–9.

Poolsawat O, Tharapreuksapong A, Wongkaew S, Reisch B, Tantasawat P, 2010. Genetic diversity and pathogenicity analysis of *Sphaceloma ampelinum* causing grape anthracnose in Thailand. *Journal of Phytopathology* **158**, 837–40.

Prakongkha I, Sompong M, Wongkaew S, Athinuwat D, Buensanteai N, 2013. Changes in salicylic acid in grapevine treated with chitosan and BTH against *Sphaceloma ampelinum*, the causal agent of grapevine anthracnose. *African Journal of Microbiology Research* **7**, 557–63.

Protas JFS, Camargo UA, 2011. *Vitivinicultura brasileira: panorama setorial de 2010*. Brasília, DF, Brazil; Bento Gonçalves, RS, Brazil: SEBRAE; IBRAVIN, Embrapa Uva e Vinho.

R Core Team, 2016. R: A Language and Environment for Statistical Computing. Vienna, Austria: R Foundation for Statistical Computing. [http://www.R-project.org]. Accessed 23 May 2016.

Rasband WS, 1997. Image J: Image Processing and Analysis in Java. [http://rsb.info.nih.gov/ij/]. Accessed 15 November 2015.

Rayner R, 1970. *A Mycological Colour Chart*. Kew, UK: Commonwealth Mycological Institute.

Ronquist F, Huelsenbeck J, 2003. MrBayes 3: Bayesian phylogenetic inference under mixed models. *Bioinformatics* **19**, 1572–4.

Sawant IS, Narkar SP, Shetty DS, Upadhyay A, Sawant SD, 2012a. Emergence of *Colletotrichum gloeosporioides sensu lato* as the dominant pathogen of anthracnose disease of grapes in India as evidenced by cultural, morphological and molecular data. *Australasian Plant Pathology* **41**, 493–504.

Sawant IS, Narkar SP, Shetty DS, Upadhyay A, Sawant SD, 2012b. First report of *Colletotrichum capsici* causing anthracnose on grapes in Maharashtra, India. *New Disease Reports* **25**, 2.

Schilder AMC, Smokevitch SM, Catal M, Mann WK, 2005. First report of anthracnose caused by *Elsinoë ampelina* on grapes in Michigan. *Plant Disease* **89**, 1011.

Sompong M, Wongkaew S, Tantasawat P, Buensanteai N, 2012. Morphological, pathogenicity and virulence characterization of *Sphaceloma ampelinum* the causal agent of grape anthracnose in Thailand. *African Journal of Microbiology Research* **6**, 2313–20.

Suzaki K, 2011. Improved method to induce sporulation of *Colletotrichum gloeosporioides*, causal fungus of grape ripe rot. *Journal of General Plant Pathology* **77**, 81–4.

Tessmann DJ, Charudattan R, Kistler HC, Rosskopf EN, 2001. A molecular characterization of *Cercospora* species pathogenic to water hyacinth and emendation of *C. piaropi*. *Mycologia* **93**, 323–34.

Thind TS, 2015. Anthracnose. In: Wilcox W, Gubler W, Uyemoto J, eds. *Compendium of grape diseases, disorders, and pests*. St Paul, MN, USA: APS Press, 17–9.

Thind TS, Arora JK, Moham C, Raj P, 2004. Epidemiology of powdery mildew, downy mildew and anthracnose diseases of grapevine. In: Naqvi SAMH, ed. *Diseases of fruits and vegetables*. Dordrecht, Netherlands: Kluwer Academic Publishers, 621–38.

Velho AC, Alaniz S, Casanova L, Mondino P, Stadnik MJ, 2015. New insights into the characterization of *Colletotrichum* species associated with apple diseases in southern Brazil and Uruguay. *Fungal Biology* **119**, 229–44.

Weir BS, Johnston PR, Damm U, 2012. The *Colletotrichum gloeosporioides* species complex. *Studies in Mycology* **73**, 115–80.

White TJ, Bruns T, Lee S, Taylor J, 1990. Amplification and direct sequencing of fungal ribosomal RNA genes for phylogenetics. In: Innis MA, Gelfand DH, Sninsky JJ, White TJ, eds. *PCR Protocols: A Guide to Methods and Applications*. New York, NY, USA: Academic Press, 315–22.

Whiteside JO, 1975. Biological characteristics of *Elsinoë fawcetti* pertaining to the epidemiology of sour orange scab. *Phytopathology* **65**, 1170–7.

Yan JY, Jayawardena MMRS, Goonasekara ID *et al.*, 2015. Diverse species of *Colletotrichum* associated with grapevine anthracnose in China. *Fungal Diversity* **71**, 233–46.

Supporting information

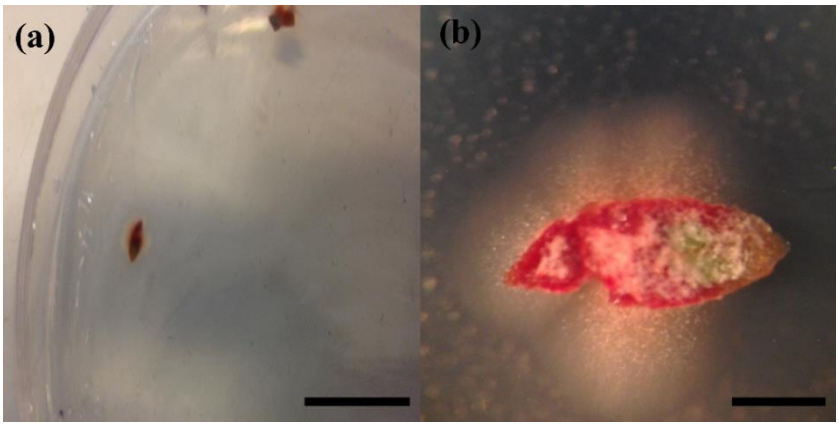

Figure S1 Isolation of *Elsinoë ampelina* 7 days after incubation on water agar (WA) medium: (a) small fragments of typical anthracnose lesions incubated on WA; and (b) initial mycelial growth of *E. ampelina* showing white to light coral colour. Scale bars: 1 cm for (a); and 1mm for (b).

3 PHYLOGENY, MORPHOLOGY AND PATHOGENICITY OF *ELSINOË AMPELINA*, THE CAUSAL AGENT OF GRAPEVINE ANTHRACNOSE IN BRAZIL AND AUSTRALIA

Abstract

Anthracnose caused by *Elsinoë ampelina* is one of the most important table grape diseases in humid regions in Brazil and Australia. The objective of this study was to characterize *E. ampelina* isolates from Brazil and Australia by means of phylogenetic analyses, morphological features and pathogenicity tests. Phylogenetic relationships among 35 isolates were determined based on a dataset of internal transcribed spacer (ITS), histone H3 (HIS3) and elongation factor 1-α (TEF) sequences. In phylogenetic tree analyses, using a combined ITS and TEF sequence alignment, all *E. ampelina* isolates were clustered together in a single well-supported clade. In contrast to the absence of genetic variability within ITS and TEF sequences, HIS3 sequences showed 54 polymorphic sites. The haplotype network generated from HIS3 dataset showed four distinct haplotypes. EA1 was the predominant haplotype including 29 isolates from both countries. High genetic variability was observed in two Brazilian isolates, haplotype EA4, which may have lost the intron region during species evolution. Colony colours differed between Brazilian and Australian isolates, but showed similar wrinkled colony texture, absence of spores, sparse to absent white aerial mycelium and slow growth (0.049-0.060 mm day^{-1}). Brazilian isolates produced conidia of 5.65 × 2.65 µm, larger than conidia from Australian isolates, which measured 5.14 × 2.30 µm. In pathogenicity tests, all Australian isolates inoculated were pathogenic on detached canes and potted vines of table grape.

Keywords: Table grape; Black spot; Fungal diversity: *Sphaceloma ampelinum*

3.1 Introduction

Grapevine anthracnose, also known as grapevine black spot and bird's-eye rot, is caused by the ascomycete fungus *Elsinoë ampelina* Shear (anamorph *Sphaceloma ampelinum* de Bary). The disease originated in Europe from where it spread around the world (Agrios, 2005). Historically, the disease has been reported in Australia, Brazil, Canada, India, New Zealand, Thailand and United States (de Castella & Brittlebank, 1917; Suhag & Grover, 1972; Brook, 1973; Mortensen, 1981; Pedro Júnior *et al.*, 1999; Poolsawat *et al.*, 2010; Carisse & Lefebvre, 2011). In Brazil, the first reports of anthracnose occurred after the introduction of American cultivars around 1840 (Sousa, 1996). In Australia, the disease was first observed in the late 18th century (Gregory, 1988). Anthracnose symptoms appear from bud burst until the end of the crop cycle, infecting all aboveground parts of the grapevine, and being more severe on younger tissues (Barros *et al.*, 2015). Infected leaves, petioles, stems, tendrils, rachises and

berries show small, reddish and circular spots that enlarge to become brownish and sunken lesions with a grey or dark centre (Thind, 2015).

In humid regions in Brazil and Australia, the disease reduces the fruit quality and can cause up to 100% crop loss (Magarey *et al.*, 1993a; Amorim *et al.*, 2016). In South (Rio Grande do Sul) and Southeast (São Paulo) Brazil, anthracnose is one of the main diseases during years with prolonged high relative humidity. In Australia, the disease has caused serious crop losses in Sunraysia (Victoria and New South Wales), Riverland (South Australia) and Murrumbidgee Irrigation Area (New South Wales) as well as other regions in years of high rainfall (Magarey *et al.*, 1993b). In infected vineyards, the fungus over-winters in dormant and dead canes, making it very difficult to control (Louime *et al.*, 2011). In both countries, the disease has been controlled with dormant treatments and foliar fungicide applications programmed at fixed intervals (Magarey *et al.*, 1993a; Amorim *et al.*, 2016).

Fungal species belonging to the genus *Elsinoë* cause anthracnose diseases in several other crops such as apple, cassava, citrus, hazelnut and rose (Alvarez *et al.*, 2003; Hyun *et al.*, 2009; Scheper *et al.*, 2013; Bagsic *et al.*, 2016; Minutolo *et al.*, 2016). A recent taxonomic study of *Elsinoë* spp. resulted in the recognition of 75 species from different hosts, including the description of eight new species (Fan *et al.*, 2017). However, little is known about the genetic variability and taxonomy of *E. ampelina* worldwide. The DNA sequences available in GenBank database are only from isolates collected in the United States and Brazil (Schilder *et al.*, 2005; Fan *et al.*, 2017; Santos *et al.*, 2017). Santos *et al.* (2017) analysing *E. ampelina* isolates from Brazil observed a wide range of cultural characteristics and different levels of pathogenicity. They also demonstrated that part of the histone H3 gene was the most informative locus for genetic diversity studies of this species. Poolsawat *et al.* (2010), using RAPD analysis, reported that *E. ampelina* isolates from Thailand were genetically different, but they could not be distinguished based on conidial morphology. Regarding the cultural features, *E. ampelina* isolates from Thailand were grouped into eight colony types according to their colours and showed slow colony growth on PDA, 2.12 to 3.82 cm in diameter at 35 days (Sompong *et al.*, 2012).

Grape species such as *Vitis labrusca*, *V. vinifera*, *V. rotundifolia*, *V. riparia* and *Vitis* sp. (hybrids) are susceptible to anthracnose (Yun *et al.*, 2007; Louime *et al.*, 2011; Kono *et al.*, 2013; Barros *et al.*, 2015). Generally, table grape cultivars are more susceptible to anthracnose than wine grape cultivars (Hart *et al.*, 1993; Kono *et al.*, 2013). The *V. vinifera* cv. Thompson Seedless (syn. Sultana and Sultanina) is one of the most common table grape

cultivars grown in the world. In addition, it plays a pivotal role in modern breeding, mainly due to the seedlessness (stenospermocarpy) phenotype (Di Genova *et al.*, 2014). However, 'Thompson Seedless' is highly susceptible to anthracnose (Sosnowski *et al.*, 2007; Kono *et al.*, 2013), but the variation in pathogenicity of different *E. ampelina* isolates is unknown. Therefore, the objective of this study was to characterize *E. ampelina* isolates from Brazil and Australia by means of phylogenetic analyses, morphological features and pathogenicity tests.

3.2 Materials and methods

3.2.1 Sampling and fungal isolation

Vineyards from two Brazilian States (Rio Grande do Sul and São Paulo) and four Australian States (Queensland, South Australia, Victoria and Western Australia) were inspected, and plant material showing anthracnose symptoms was collected in 2015 and 2016 (Fig. 1). Anthracnose symptoms were characterized by numerous brown, pinky purple or dark grey lesions on leaves, stems, rachises, tendrils and berries (Fig. 2). Symptomatic tissues were cut into small fragments (2-3 mm), disinfested by immersion in 70% alcohol (1 min) and 2.5% sodium hypochlorite (3 min), rinsed in sterile distilled water, and dried on sterilized filter paper. Fragments were then transferred to Petri dishes containing water agar medium (WA; Difco Laboratories) and incubated at 25 °C with a 12 h photoperiod for five days. Mycelium was transferred to potato dextrose agar medium (PDA; Difco Laboratories) and incubated under the same conditions for seven days. The isolates obtained were purified by cutting a small piece of mycelium (1 mm^2) from the margins of colonies and transferring them to PDA using a sterile needle for twice to three times (Bagsic *et al.*, 2016). Pure cultures were identified based on morphological characteristics. For storing, *E. ampelina* isolates were subcultured on PDA with fragments of 1 cm^2 sterilised filter paper on the surface. After growth appeared on the filter paper fragments, the isolates were removed from the culture medium, dried in a laminar flow cabinet and stored in envelopes in a plastic box (13 × 13 × 4 cm) containing silica gel, sealed with parafilm and kept at -4 °C.

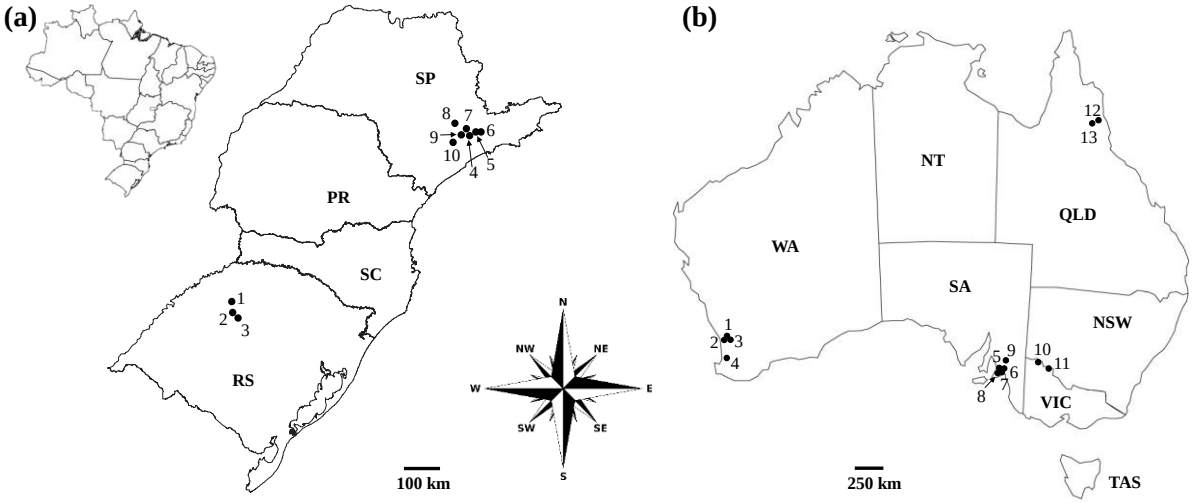

Figure 1 Collection sites of *Elsinoë ampelina* isolates associated with grapevine anthracnose symptoms in Brazil (a) and Australia (b). Locations where samples were collected are indicated on the maps by numbers. (a) Brazil: 1- Catuípe; 2- Boa Vista do Cadeado; 3- Augusto Pestana; 4- Jundiaí; 5- Jarinu; 6- Atibaia; 7- Louveira; 8- Piracicaba; 9-Indaiatuba; 10- Porto Feliz. Brazilian States: PR - Paraná; RS - Rio Grande do Sul; SC - Santa Catarina and; SP - São Paulo. (b) Australia: 1- The Vines; 2- Caversham; 3- Herne Hill; 4- Donnybrook; 5- Adelaide (Campbelltown, Kensington, Norwood and Urrbrae suburbs); 6- Lobethal; 7- Aldgate; 8- McLaren Vale; 9- Nuriootpa; 10- Mildura; 11- Robinvale; 12- Mareeba; 13- Mutchilba. Australian States and Territories: NSW- New South Wales; NT- Northern Territory; QLD- Queensland; SA- South Australia; TAS- Tasmania; VIC- Victoria and; WA- Western Australia.

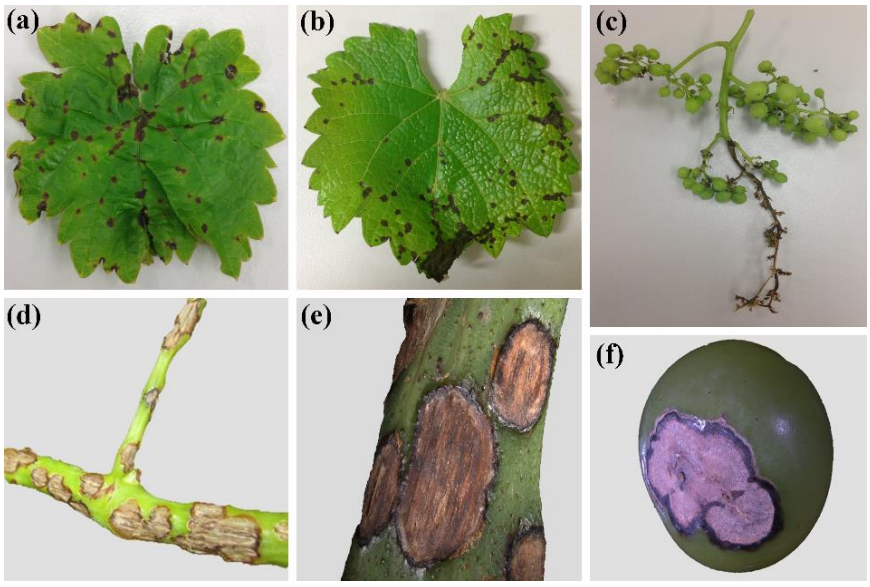

Figure 2 Anthracnose symptoms on grapevines: (a, c, d) symptoms on *Vitis vinifera* cv. Thompson Seedless in Australia; (b, e, f) symptoms on *Vitis labrusca* cv. Niagara Rosada in Brazil; (a, b) brown and dark-grey lesions on leaves; (c) a dry rachis from the lesion point; (d, e) numerous cankers on stems; and (f) berry showing pinky purple lesion.

3.2.2 DNA isolation, PCR amplification and sequencing

For each *E. ampelina* isolate, a small amount of mycelium (0.5 cm^2) was removed from the surface of 14-day-old cultures grown on PDA at 25 °C with a 12 h photoperiod, using a sterile scalpel. DNA extraction and purification were performed using the Wizard Genomic DNA Purification kit (Promega) following the manufacturer's instructions. Three DNA regions were amplified including: internal transcribed spacer (ITS) and partial sequences of the histone H3 (HIS3) and elongation factor 1-α (TEF) regions using the primer pairs ITS1 and ITS4 (White *et al.*, 1990); CYLH3F and CYLH3R (Crous *et al.*, 2004) and; elongation-1-F e elongation-1-R (Hyun *et al.*, 2009), respectively.

Each 25 µL PCR reaction contained 2 µL DNA (25 ng μL^{-1}), 8.5 µL Nuclease Free Water, 1 µL each primer (10 µM) and 12.5 µL GoTaq Colorless Master Mix 2x (Promega). PCR reactions were carried out in a thermal cycler (SuperCycler Trinity, Kyratec or TC-512, Techne). The cycling parameters for ITS consisted of an initial denaturation at 94 °C for 2 min; followed by 35 cycles of denaturation at 94 °C for 1 min, annealing at 55 °C for 1 min and extension at 72 °C for 1 min; and final extension at 72 °C for 5 min. For TEF, initial denaturation at 94 °C for 2 min was followed by 40 cycles of amplification (94 °C for 30 s, 55 °C for 1 min and 72 °C for 1 min) and a final extension at 72 °C for 3 min. For HIS3, initial denaturation at 95 °C for 3 min was followed by 34 cycles of amplification (95 °C for 1 min, 56.9 °C for 1 min and 72 °C for 1 min) and a final extension at 72 °C for 4 min. The amplicons were analysed in 2% agarose gel stained with GelRed (Biotium) in 1× Tris Acetate EDTA (TAE) buffer and purified using the Wizard SV Gel and PCR Clean-Up System kit (Promega), following the manufacturer's instructions. PCR products sequencing was performed using a 3130xl Genetic Analyzer (Applied Biosystems) at the Centro de Biotecnologia Agrícola (CEBTEC, Piracicaba, Brazil) and a 3730 DNA Analyzer (Applied Biosystems) at the Australian Genome Research Facility (AGRF, Adelaide, Australia). PCR products were sequenced in both directions, and consensus sequences were obtained using Sequencher 5.4.1 (Gene Codes Corporation, 2016). All sequences generated in this study were deposited in GenBank (Table 1).

3.2.3 Phylogenetic analyses

Consensus sequences obtained were aligned and compared with those of the genus *Elsinoë* from previous studies available in GenBank using BioEdit (Hall, 1999). Due to the lack of HIS3 sequences from *Elsinoë* species available in GenBank, the phylogeny was conducted for a combined ITS and TEF sequence alignment using the Maximum Likelihood (ML) and Bayesian Inference (BI) methods. ML analysis was performed using Kimura 2-parameter model as the nucleotide substitution model in MEGA v.7.0.14 (Kumar *et al.*, 2016). Nearest-Neighbour-Interchange (NNI) was used as the heuristic method for phylogenetic inference, and 1000 bootstrap replicates were performed. For BI method, the best nucleotide substitution model was determined by MrModeltest v. 2.3 (Nylander, 2004) using Akaike information criterion (AIC). Bayesian posterior probabilities were determined by Markov Chain Monte Carlo (MCMC) algorithm using MrBayers v.3.1.1 (Ronquist & Huelsenbeck, 2003). Four MCMC chains were run simultaneously for random trees for 10^7 generations and trees were sampled every 1000 generations. The first 25% of the trees were discarded as the burn-in phase. For each phylogenetic method, the analysis was conducted twice. Trees were viewed and edited in TreeView (Page, 1996).

3.2.4 Intraspecific diversity

To characterize intraspecific genetic diversity of *E. ampelina* isolates, haplotype analyses were determined for each locus and for a combined multilocus dataset (ITS, TEF and HIS3) using DnaSP v.5.10.01 (Librado & Rozas, 2009). To identify the evolutionary relationship of the population analysed, a haplotype network was built for each locus and for a combined multilocus dataset using TCS v1.21 (Clement *et al.*, 2000). The connection limit was set to 95% of confidence (Templeton *et al.*, 1992) and gaps were included for haplotype construction.

3.2.5 Morphological characterization

For cultural observations, 6.5 mm diameter mycelial plugs excised from a 30-day-old colony of each isolate were placed in the centre of Petri dishes containing PDA. Plates were incubated at 25 °C and 12 h photoperiod for four weeks. Then, cultural characteristics such as

texture, density, colour and growth were assessed. Colony colours were rated using the mycological colour charts of Rayner (1970). Colony diameter was assessed weekly to obtain the mycelial growth rate (mm day^{-1}). The experiment was performed twice using three replicates for each isolate

Due to the absence of sporulation of *E. ampelina in vitro*, colonies grown on PDA for four weeks were mashed, sterilized distilled water added, and the mycelial suspension was calibrated to 2×10^5 CFU mL^{-1}. The suspension of each isolate was sprayed to the point of runoff on young leaves (10-day-old) of grapevines *V. labrusca* cv. Niagara Rosada to analyse Brazilian isolates and on young leaves of grapevines *V. vinifera* cv. Thompson Seedless to assess Australian isolates. The inoculations were carried out in the respective countries that the isolates were collected. Grapevines were incubated in a moisture chamber at room temperature (22-25 °C) for 48 h. Seven days after inoculation, leaves showing anthracnose symptoms were detached from the vines and placed in the Petri dishes. Over each lesion, a 50 µL drop of sterile distilled water was deposited. After 4 h, the drop was removed and conidia were measured. For each isolate, length and width were measured for 30 randomly selected conidia and the ratio of length/width (L/W) calculated. Measurements were carried out at × 400 magnification using an Axiocam 503 color (Carl Zeiss) and Dino-Eye Eyepiece AM423 (Dino-Eye) cameras coupled to an Axio Lab.A1 (Carl Zeiss) and Olympus BX41 (Olympus) microscope, respectively.

Data of conidial measurements and mycelial growth rate were subjected to *F* test ($P < 0.05$) to determine whether there were morphological differences between Australian and Brazilian isolates, using 'R' v. 3.3.0 (R Core Team, 2016).

3.2.6 Pathogenicity tests

Nine *E. ampelina* isolates collected in different locations in Australia were used in potted vine and detached cane assays to determinate their pathogenicity on *Vitis vinifera* cv. Thompson Seedless. Dormant canes (1-year-old) from an anthracnose-free vineyard were collected from the Loxton Research Centre (South Australian Research and Development Institute, Australia) and stored in a cold room at 4 °C for eight months.

For the potted vine assay (PVA), 4 node cuttings were sectioned from the canes, rooted for 45 days in plastic trays containing vermiculite and maintained in a greenhouse at 25 °C. After the rooting period, vines were removed from the trays, planted in individual pots

and placed in a shadehouse for four months. Vines were pruned 15 days before they were used in the assay. For inoculation, vines with two young shoots with three to four unfolded leaves, from the third and fourth nodes, were sprayed with a suspension of spores of *E. ampelina* (10^5 conidia mL^{-1}) until runoff, covered with plastic bags for 48 h and kept at 25 °C in a humidity chamber (plastic tent measuring: 160 × 80 × 80 cm) containing automatic nebulizers to maintain high relative humidity (80-90%). The humidity chamber was located within a greenhouse. Conidial suspensions were obtained by placing *E. ampelina* cultures in rainwater and shaking on an orbital shaker (Ratek Instruments) at 200 rpm in darkness for seven days to induce sporulation (Chapter 4). Vines sprayed with sterile distilled water were used as a control. Six and nine days after inoculation, vines were assessed for number of lesions per leaf and leaf disease severity, respectively, on the top two leaves per shoot on each potted vine. The experiment was arranged in a completely randomized design with five replicates per isolate and two shoots were assessed per replicate. The experiment was performed twice.

The second pathogenicity test was a detached cane assay (DCA) (Sosnowski *et al.*, 2007). Single-node cuttings were sectioned from the canes and inserted into pre-holed polystyrene sheets. The sheets with cuttings were placed in plastic trays containing tap water and kept at 25 °C for 14 days to allow for bud burst before inoculation. Single-young shoots with two to three unfolded leaves were sprayed with a suspension of 10^5 conidia mL^{-1} until runoff. Cuttings sprayed only with sterile distilled water were used as a control. Each tray was covered with plastic bags and kept at 25 °C. After 48 h, the plastic bags were removed and the vines kept in a humidity chamber. Six and nine days after inoculation, the shoots were assessed for the number of lesions per leaf and leaf disease severity, respectively. The experimental design was completely randomized with 10 replicates per isolate and the two top leaves on each cutting were assessed. The experiment was performed twice.

For both pathogenicity tests, the number of lesions per leaf was rated visually and leaf disease severity was quantified based on the percentage of leaf area covered by lesions using a standard area diagram set (Chapter 5). Re-isolations were performed by incubating symptomatic tissue fragments on PDA at 25 °C for three weeks and the pathogen was identified based on cultural and morphological features (Sompong *et al.*, 2012).

The *F* test ($P < 0.05$) was used to determine if pooling of the two experiments of each pathogenicity test was allowed. To compare the nine *E. ampelina* isolates in PVA and DCA, the number of lesions per leaf and leaf disease severity were subjected to analysis of variance

(ANOVA), and the means compared by Fisher's least significant difference (LSD) test ($P < 0.05$). The relationships between the variables assessed and between pathogenicity methods were verified using Pearson Correlation coefficient ($P < 0.05$). Data for the non-inoculated vines (control) were excluded from the analyses. All statistical analyses were performed using 'R' v. 3.3.0 (R Core Team, 2016).

3.3 Results

3.3.1 Phylogenetic analyses

PCR amplifications of ITS, TEF, and HIS3 regions from 18 Brazilian and 17 Australian isolates gave amplicons of 602, 398, and 351-400 bp, respectively (Table 1). Phylogenetic trees built using a combined ITS and TEF sequence alignment were comprised of 50 taxa and 910 characters including gaps. For BI analysis, the best nucleotide substitution models were HKY+I for ITS and GTR+G for TEF. ML and BI analyses produced nearly identical topologies (BI tree not shown). The ITS and TEF sequences obtained from 35 isolates of this study were 100% identical to those of *E. ampelina* isolates from the United States and Brazil (EAMI-1, AV25 and CBS 208.25). The BI and ML analyses revealed a clear separation of the *E. ampelina* isolates from the others species of the genus *Elsinoë*. All *E. ampelina* isolates were grouped in a single clade with ML bootstrap support value of 96% and Bayesian posterior probability value of 0.94 (Fig. 3).

Table 1 *Elsinoë* spp. used in this study with isolation details, haplotype and GenBank accessions

Species	Isolate code	Host	Tissue	Location[b]	Haplotype[c]	GenBank accession numbers[d]		
						ITS	TEF	HIS3
Elsinoë ampelina	AVBR118	*V. labrusca* cv. Niagara Rosada	Leaf	Jarinu, SP, Brazil	EA3	**KY684866**	**KY684901**	**KY684831**
	AVBR119	*V. labrusca* cv. Niagara Rosada	Leaf	Jundiaí, SP, Brazil	EA3	**KY684867**	**KY684902**	**KY684832**
	AVBR120	*V. labrusca* cv. Niagara Rosada	Leaf	Jundiaí, SP, Brazil	EA1	**KY684868**	**KY684903**	**KY684833**
	AVBR121	*V. labrusca* cv. Niagara Rosada	Leaf	Porto Feliz, SP, Brazil	EA1	**KY684869**	**KY684904**	**KY684834**
	AVBR122	*V. labrusca* cv. Niagara Rosada	Leaf	Porto Feliz, RS, Brazil	EA1	**KY684870**	**KY684905**	**KY684835**
	AVBR123	*V. labrusca* cv. Niagara Rosada	Leaf	Atibaia, RS Brazil	EA1	**KY684871**	**KY684906**	**KY684836**
	AVBR124	*V. labrusca* cv. Niagara Rosada	Leaf	Atibaia, RS, Brazil	EA1	**KY684872**	**KY684907**	**KY684837**
	AVBR125	*V. labrusca* cv. Niagara Rosada	Leaf	Atibaia, RS, Brazil	EA1	**KY684873**	**KY684908**	**KY684838**
	AVBR126	*V. labrusca* cv. Niagara Rosada	Leaf	Louveira, SP, Brazil	EA1	**KY684874**	**KY684909**	**KY684839**
	AVBR127	*V. labrusca* cv. Niagara Rosada	Leaf	Louveira, SP, Brazil	EA1	**KY684875**	**KY684910**	**KY684840**
	AVBR128	*V. labrusca* cv. Niagara Rosada	Leaf	Indaiatuba, SP, Brazil	EA1	**KY684876**	**KY684911**	**KY684841**
	AVBR129	*V. labrusca* cv. Niagara Rosada	Leaf	Indaiatuba, SP, Brazil	EA1	**KY684877**	**KY684912**	**KY684842**
	AVBR130	*Vitis riparia* × *(V. rupestris* × *V. cordifolia*) cv. Riparia do Traviú[a]	Leaf	Catuípe, RS, Brazil	EA1	**KY684878**	**KY684913**	**KY684843**
	AVBR131	*V. labrusca* cv. Niagara Rosada	Leaf	Boa Vista do Cadeado, RS, Brazil	EA3	**KY684879**	**KY684914**	**KY684844**
	AVBR133	*V. vinifera* cv. Moscato Branco	Leaf	Augusto Pestana, RS, Brazil	EA4	**KY684880**	**KY684915**	**KY684845**
	AVBR134	*V. riparia* × *V. labrusca* cv. Baco Blanc	Stem	Augusto Pestana, RS, Brazil	EA4	**KY684881**	**KY684916**	**KY684846**
	AVBR136	*Vitis riparia* × *(V. rupestris* × *V. cordifolia*) cv. Riparia do Traviú[a]	Leaf	Augusto Pestana, RS, Brazil	EA1	**KY684882**	**KY684917**	**KY684847**
	AVBR137	*V. labrusca* cv. Niagara Rosada	Leaf	Piracicaba, SP, Brazil	EA1	**KY684883**	**KY684918**	**KY684848**
	GAAUS1	*V. vinifera* cv. unknown	Leaf	The Vines, Perth, WA, Australia	EA1	**KY684884**	**KY684919**	**KY684849**
	GAAUS9	*V. vinifera* cv. unknown	Leaf	Caversham, Perth, WA, Australia	EA1	**KY684885**	**KY684920**	**KY684850**
	GAAUS10	*V. vinifera* cv. Thompson Seedless	Leaf	Kensington, Adelaide, SA, Australia	EA1	**KY684886**	**KY684921**	**KY684851**
	GAAUS11	*V. vinifera* cv. Thompson Seedless	Leaf	Norwood, Adelaide, SA, Australia	EA1	**KY684887**	**KY684922**	**KY684852**
	GAAUS12	*V. vinifera* cv. Muscat Hamburg	Leaf	Urrbrae, Adelaide, SA, Australia	EA1	**KY684888**	**KY684923**	**KY684853**

(continued)

Table 1 (continued)

Species	Isolate code	Host	Tissue	Location[b]	Haplotype[c]	GenBank accession numbers[d]		
						ITS	TEF	HIS3
	GAAUS14	*V. vinifera* cv. Thompson Seedless	Leaf	Mildura, VIC, Australia	EA1	**KY684889**	**KY684924**	**KY684854**
	GAAUS16	*V. vinifera* cv. Flame Seedless	Stem	Herne Hill, Perth, WA, Australia	EA2	**KY684890**	**KY684925**	**KY684855**
	GAAUS18	*V. vinifera* cv. unknown	Leaf	Lobethal, SA, Australia	EA1	**KY684891**	**KY684926**	**KY684856**
	GAAUS19	*V. vinifera* cv. unknown	Tendril	McLaren Vale, SA, Australia	EA1	**KY684892**	**KY684927**	**KY684857**
	GAAUS21	*V. vinifera* cv. Thompson Seedless	Stem	Robinvale, VIC, Australia	EA1	**KY684893**	**KY684928**	**KY684858**
	GAAUS23	*V. vinifera* cv. Thompson Seedless	Berry	Nuriootpa, SA, Australia	EA1	**KY684894**	**KY684929**	**KY684859**
	GAAUS24	*V. vinifera* cv. Red Globe	Stem	Donnybrook, WA, Australia	EA1	**KY684895**	**KY684930**	**KY684860**
	GAAUS26	*V. vinifera* cv. Perlette	Stem	Caversham, Perth, WA, Australia	EA1	**KY684896**	**KY684931**	**KY684861**
	GAAUS27	*V. vinifera* cv. Maroo Seedless	Leaf	Mareeba, QLD, Australia	EA1	**KY684897**	**KY684932**	**KY684862**
	GAAUS30	*V. vinifera* cv. Maroo Seedless	Berry	Mutchilba, QLD, Australia	EA1	**KY684898**	**KY684933**	**KY684863**
	GAAUS31	*V. vinifera* cv. Thompson Seedless	Rachis	Campbelltown, Adelaide, SA, Australia	EA1	**KY684899**	**KY684934**	**KY684864**
	GAAUS32	*Vitis* sp. cv. Ornamental grapevine	Tendril	Aldgate, SA, Australia	EA1	**KY684900**	**KY684935**	**KY684865**
	EAMI-1	*Vitis* spp. cv. Marquis	-	USA	-	AY826762	-	-
	AV25	*V. labrusca* cv. Niagara Rosada	Leaf	Jundiaí, SP, Brazil	-	KX786350	KX786389	-
	CBS 208.25	*V. vinifera*	-	Brazil	-	KX887186	KX886832	-
E. barleriicola	CBS 471.62	*Barleria gibsonii*	-	India	-	KX887200	KX886846	-
E. brasiliensis	CPC 18528	*Chamaesyce hyssopifolia*	-	Brazil	-	KX887204	KX886850	-
E. euphorbiae	CBS 401.63	*Euphorbia parviflora*	-	India	-	KX887217	KX886863	-
E. genipae	CBS 342.39	*Genipa americana*	-	Brazil	-	KX887227	KX886873	-
E. glycines	CBS 389.64	*Glycine soja*	-	Japan	-	KX887229	KX886875	-
	CBS 390.64	*G. soja*	-	Japan	-	KX887230	KX886876	-
E. menthae	CBS 321.37	*Mentha piperita*	-	USA	-	KX887252	KX886897	-
	CBS 322.37	*M. piperita*	-	USA	-	KX887253	KX886898	-
E. mimosae	CBS 141943	*Mimosa invisa*	-	Ecuador	-	KX887254	KX886899	-
	CPC 19478	*M. invisa*	-	Brazil	-	KX887255	KX886900	-
E. rhois	CBS 519.50	*Toxicodendron vernix*	-	Brazil	-	KX887280	KX886925	-
E. ricini	CBS 403.63	*Ricinus communis*	-	India	-	KX887281	KX886926	-

[a]Rootstock.
[b]QLD - Queensland; RS - Rio Grande do Sul; SP - São Paulo; SA - South Australia; WA - Western Australia; VIC – Victoria.
[c]Haplotypes based on histone H3 sequences.
[d]Sequence numbers in bold were obtained in the present study.

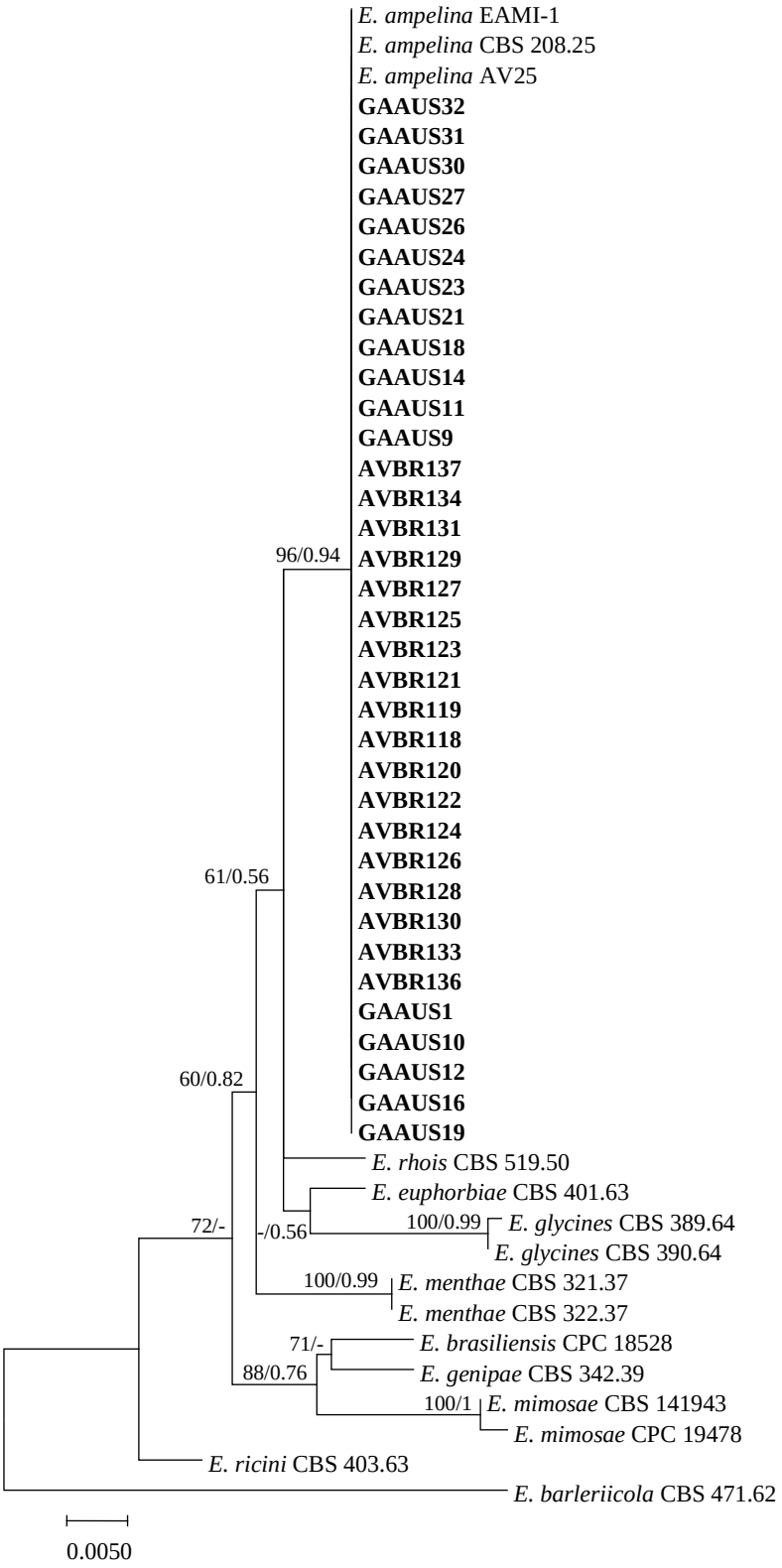

Figure 3 Maximum Likelihood (ML) phylogenetic tree showing the relationship among *Elsinoë* isolates generated from the combined analysis of ITS and TEF sequence data. ML bootstrap support values ≥ 50% and Bayesian posterior probabilities values ≥ 0.50 are shown at the nodes. Isolates in bold were obtained in the present study.

3.3.2 Intraspecific diversity

ITS and TEF sequences of all Brazilian and Australian isolates were monomorphic, therefore were not used in intraspecific diversity analyses. However, there were 54 polymorphic sites within the HIS3 gene. The haplotype network generated from HIS3 dataset showed four distinct haplotypes (Fig. 4). EA1 was the predominant haplotype in the population analysed including 29 isolates, 13 isolates from Brazil and 16 isolates from Australia. Haplotype EA2 included only the isolate GAAUS16 (Australia) showing T to C base substitution at position 50. The isolates AVBR118, AVBR119 and AVBR131 from Brazil represented by EA3 showed two base substitutions and one base deletion if compared to the EA1. Finally, two Brazilian isolates represented by haplotype EA4 showed four base substitutions and absence of the intron region (alignment position 315-365).

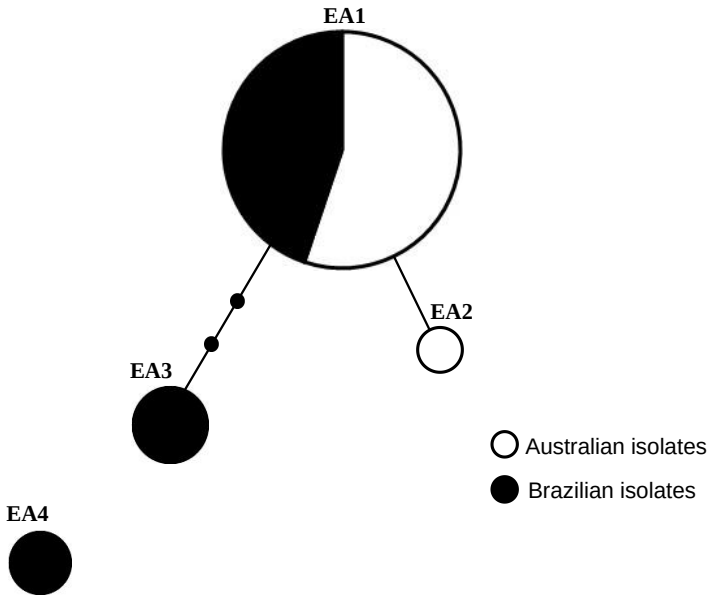

Figure 4 Haplotype network (95% of confidence) for the histone H3 locus based on 351-400 bp sequences of *Elsinoë ampelina* isolates from Brazil and Australia. Geographic origin of isolates from each haplotype are shown in Table 1. Each circle represents distinct haplotypes (EA1-4) and the size corresponds to the number of isolates included in the haplotype. The two small black dots indicate hypothetical haplotypes not detected in the dataset.

3.3.3 Morphological characterization

Colony colour on PDA was very heterogeneous such as sulphur yellow, coral, red, dark brick and leaden black (Fig. 5). In general, Brazilian isolates were brighter red than Australian isolates. All isolates showed wrinkled texture, absence of spores in cultures and

sparse to absent white aerial mycelium. Colonies of *E. ampelina* isolates grew slowly, the mean growth rate of Brazilian isolates was 0.056 mm day^{-1} and for Australian isolates was 0.055 mm day^{-1}, not statistically different (P = 0.06) (Table S1). After four weeks on PDA, colony diameter varied from 1.93 to 2.50 cm.

Elsinoë ampelina isolates from both countries produced conidia that were cylindrical to oblong, hyaline, aseptate and with both ends rounded (Fig. 5i). Brazilian isolates produced conidia of 5.65 ± 0.61 × 2.65 ± 0.26 µm, bigger than conidia from Australian isolates, which measured 5.14 ± 0.52 × 2.30 ± 0.18 µm. L/W ratio was 2.13 and 2.24 for isolates from Brazil and Australia, respectively. Length, width and L/W ratio were significantly different between Brazilian and Australian isolates (P < 0.05). No teleomorph structures were observed during this study.

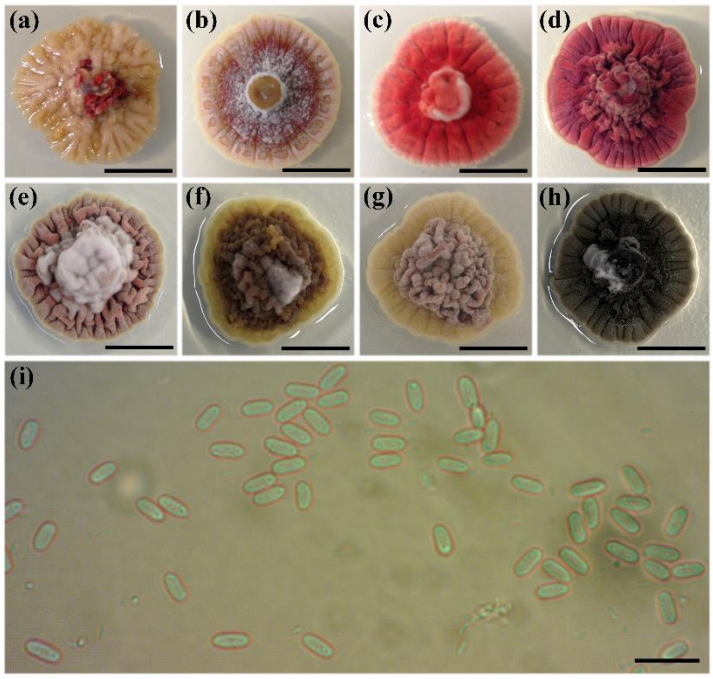

Figure 5 *Elsinoë ampelina* colony and conidial morphology: (a-d) colony morphology of 28-day-old Brazilian isolates; (e-h) colony morphology of 28-day-old Australian isolates; and (i) hyaline conidia. Scale bars: a-h: 1 cm; i: 10 µm.

3.3.4 Pathogenicity

All isolates inoculated on ‘Thompson Seedless’ caused anthracnose symptoms occurring first on leaves followed by symptoms on stems and tendrils in PVA and DCA. The symptoms on leaves and stems appeared 3 and 5 to 6 days after inoculation, respectively, in both assays. Tendrils were only formed on vines in the PVA, and symptoms appeared on

them 5 to 6 days after inoculation. The initial symptoms were characterized as small brown spots, which rapidly grew and, sometimes, coalesced into larger lesions. Control (non-inoculated) vines were not observed with any anthracnose symptoms.

There were no differences between the variances of the two PVA experiments (P = 0.82 for the number of lesions per leaf and P = 0.61 for the leaf disease severity) and of the two DCA experiments (P = 0.33 for the number of lesions per leaf and P = 0.65 for the leaf disease severity). Therefore, a pooled analysis of the two experiments was performed for each assessment (lesion number and severity). Isolates showed different levels of pathogenicity with both methods (Fig. 6). In the PVA, isolate GAAUS23 showed the highest number of lesions per leaf (69.09), significantly higher than all other isolates except GAAUS21, GAAUS30 and GAAUS32. The leaf disease severity varied significantly among the nine isolates, ranging from 8.24 to 14.32%. In the DCA, the number of lesions per leaf and leaf disease severity varied between 21.95 to 49.58 and 6.02 to 13.63%, respectively. Correlation was observed between number of lesions per leaf and leaf disease severity in PVA (r = 0.76) and DCA (r = 0.77). However, there was no significant correlation ($P > 0.05$) between PVA and DCA. *Elsinoë ampelina* was reisolated from infected tissues in both pathogenicity methods, fulfilling Koch's postulates.

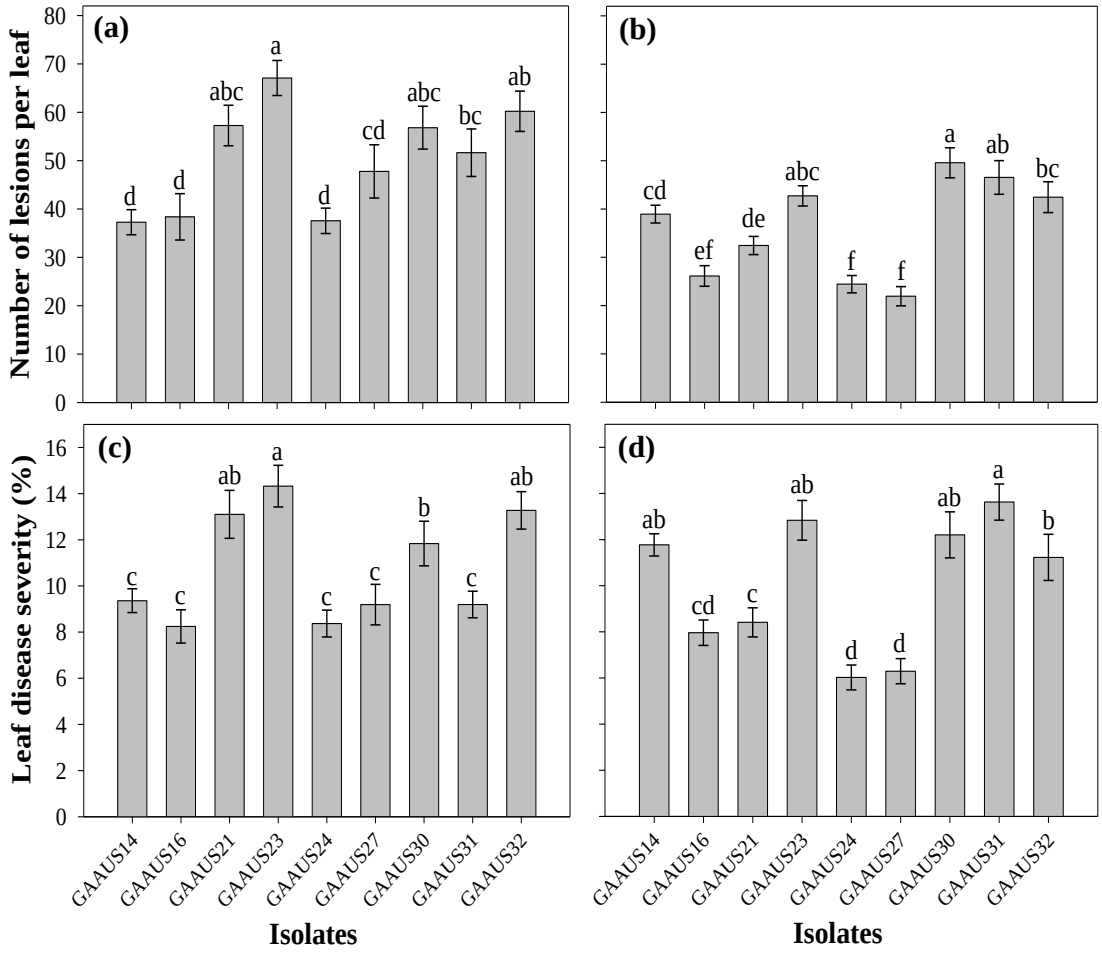

Figure 6 Pathogenicity of Australian *Elsinoë ampelina* isolates on *Vitis vinifera* cv. Thompson Seedless in the potted vine assay (PVA) (a, c) and the detached cane assay (DCA) (b, d): (a, b) number of lesions per leaf assessed six days after inoculation; and (c, d) leaf disease severity assessed nine days after inoculation. Columns with the same letter do not differ significantly, according to Fisher's LSD test ($P < 0.05$). Bars correspond to the standard error of the mean.

3.4 Discussion

Elsinoë ampelina, the causal agent of grapevine anthracnose, has been the subject of limited research worldwide. This work constitutes the first study comparing molecular and morphological data of *E. ampelina* populations from two countries. Molecular analyses, including phylogeny and haplotype network, were conducted to determine the level of genetic variability among and between Brazilian and Australian isolates. In the ML and BI analyses, using combined ITS and TEF sequence alignment, all *E. ampelina* isolates were clustered together in a single well-supported clade. *Elsinoë ampelina* was closely related to *E. rhois*, *E. euphorbiae* and *E. glycines*, also observed by Fan *et al.* (2017). ITS sequences from all *E. ampelina* isolates analysed were monomorphic. Likewise, all TEF sequences also were

monomorphic. Furthermore, ITS sequences obtained in our study showed 100% identity to sequences of isolates collected in the United States and Brazil (Schilder *et al.*, 2005; Fan *et al.*, 2017). Minutolo *et al.* (2016), studying 24 *E. coryli* isolates from hazelnut, observed that ITS sequences showed 99% identity to each other. However, the ITS is a useful locus for distinguishing most species of the genus *Elsinoë*, resolving 61/74 (82.4%) of the species included in the phylogenetic tree (Fan *et al.*, 2017).

Our results suggest that ITS and TEF regions are highly conserved in Brazilian and Australian *E. ampelina* populations, as was also observed by Santos *et al.* (2017). These authors studied Brazilian isolates collected in 2014 from different vineyards than those sampled in 2015 and analysed in this study. The absence of genetic variability for these two genomic regions may be associated with absence of sexual reproduction in Brazil and Australia (Magarey *et al.*, 1993a; Amorim *et al.*, 2016). The reason for nonexistence of the sexual stage may be related to lack of harsh winter or the lack of suitable mating types (Magarey *et al.*, 1993a). In pathogens reproducing only asexually, in which no recombination occurs, entire genotypes can be transferred from one population to another, a process known as genotype flow (Agrios, 2005). Unlike rust and downy mildew fungi that can spread propagules over long distances, sometimes encompassing entire continents, *E. ampelina* spreads propagules up to 7 m in wind-borne rain-splash drops, distributing its genomes only over short distances (Brook, 1973; Agrios, 2005).

In contrast with absence of variability of the ITS and TEF regions, HIS3 locus showed 54 polymorphic sites within the 351-400 bp. HIS3 haplotype analysis revealed some genetic differences among isolates resulting in the formation of four distinct haplotypes. EA1 was the predominant haplotype including 29 isolates (82.9%) collected in different regions of Brazil and Australia. For the haplotypes EA2, EA3 and EA4, a relationship was observed between the geographical origin (country) of the isolates and the haplotype network structure. Two Brazilian isolates, represented by haplotype EA4, showed four base substitutions and absence of the intron region (alignment position 315-365). Due to the high genetic diversity (< 95% of confidence), this haplotype did not have connection with the others. Our results suggest that isolates belonging to haplotype EA4 may have lost the intron region during species evolution, while EA1 is a highly conserved haplotype. In the same way, Yun & Nishida (2011) reported that in the course of fungal evolution, some species of Saccharomycotina and Taphrinomycotina lost the histone introns (histone H2A, H2B, H3 and H4 genes). In an overall analysis of different lineages of eukaryotes, it was observed that evolution of

eukaryotic genes was dominated by intron loss (Csuros *et al.*, 2011).

In previous studies, morphological features were used partially to characterize *E. ampelina* (Schilder *et al.*, 2005; Yun *et al.*, 2007; Poolsawat *et al.*, 2010; Sompong *et al.*, 2012). In this study, cultural and conidial features from Brazilian and Australian isolates also offered substantial information to support the species identification. Moreover, no relationship was observed between the haplotype network structure and morphological characteristics of the isolates. Isolates from both countries showed wrinkled texture, slow growth, absence of spores and sparse to absent white aerial mycelium in cultures on PDA. These results agree with the findings regarding several species of the genus *Elsinoë* (Miles *et al.*, 2015; Bagsic *et al.*, 2016; Fan *et al.*, 2017). Furthermore, *E. ampelina* isolates from Brazil showed different colony colours to those collected in Australia. However, no colony colour pattern was observed among and between different regions sampled in Brazil or Australia. In Thailand, Poolsawat *et al.* (2009) reported that colony colour variation of *E. ampelina* isolates was more pronounced among different geographic regions than that within the same region.

Although many *Elsinoë* species were described in a recent taxonomic study (Fan *et al.*, 2017), no morphological description of *E. ampelina* was provided, probably due to the lack of fresh isolates. In the sexual stage, *E. ampelina* produces hyaline and 3-septate ascospores measuring 15-16 × 4-4.5 µm (Shear, 1929). The asexual stage produces small hyaline conidia with mucilaginous walls, 3-7 × 2-4 µm, in acervuli on the exterior of the lesions (Thind, 2015). In our study, Brazilian isolates showed greater length and width of conidia than those from Australian isolates. Conidia dimensions of the isolates analysed varied, at 3.50-7.01 × 1.79-3.42 µm, similar to those observed by Sompong *et al.* (2012) in Thailand. In another study in Thailand, conidia measured 4.51-5.12 × 1.74-1.85 µm and no difference in conidial size was observed among *E. ampelina* isolates from different regions (Eastern, Northern, Northeastern and Western) (Poolsawat *et al.*, 2010).

Pathogenicity tests showed that Australian *E. ampelina* isolates obtained from different geographical regions and vine organs caused typical anthracnose symptoms on ‘Thompson Seedless’. Different levels of pathogenicity were also observed in the nine isolates analysed. However, no relationship was observed between levels of pathogenicity and origin of the isolates. Leaf disease severity varied between 8.24 to 14.32% in the PVA and 6.02 to 13.63% in the DCA. These results are in agreement with those reported by Wang *et al.* (1998), who analysed 108 clones of Chinese *Vitis* species. Sosnowski *et al.* (2007), using the DCA in Australia, observed that susceptibility to anthracnose ranged considerably among five

table grape cultivars including Blush Seedless, Christmas Rose, Fantasy Seedless, Red Globe and Thompson Seedless. The same authors reported that 'Thompson Seedless' showed leaf disease severity around 28%, greater than that observed in our study.

Development of anthracnose epidemics is governed by susceptibility of the vine tissue, dispersal of conidia and favourable weather conditions (Thind, 2015). Major outbreaks occur during rainy years, since relative humidity and rainfall are important factors related to anthracnose growth in the vineyard (Barros *et al.*, 2015). Temperature also influences anthracnose development, and wetness periods necessary for infection range from 7 to 10 h at l2 °C and 3 to 4 h at 21 °C (Brook, 1973). In both pathogenicity methods used in this study, a positive correlation was observed between leaf disease severity and number of lesions per leaf. Kono *et al.* (2013) analysing 133 grapevine genotypes reported positive correlation between lesion number and lesion diameter in American and Japanese hybrids, whereas there was no correlation between these parameters in *V. vinifera*. In general, anthracnose studies involving inoculations are performed on potted vines; however, potted vines require propagation and maintenance. On the other hand, detached canes are an effective and rapid method for anthracnose research, as was also reported by Sosnowski *et al.* (2007). Although the environmental condition was similar for both pathogenicity methods performed in this study, some isolates showed different levels of pathogenicity between the methods. The reasons for this are not fully understood and further studies are required. In conclusion, this study gives new information related to anthracnose aetiology in Brazil and Australia. This knowledge will help provide a better understanding of epidemiology, and assist with the establishment of integrated control strategies and breeding for resistant cultivars in both countries.

References

Agrios GN, 2005. *Plant Pathology*. Burlington, MA, USA: Elsevier Academic Press.

Alvarez E, Mejia JF, Valle TL, 2003. Molecular and pathogenicity characterization of *Sphaceloma manihoticola* isolates from South-Central Brazil. *Plant Disease* **87**, 1322–28.

Amorim L, Spósito MB, Kuniyuki H, 2016. Doenças da videira. In: Amorim L, Rezende JAM, Bergamin Filho A, Camargo LEA, eds. *Manual de Fitopatologia: doenças das plantas cultivadas*. São Paulo, SP, Brazil: Agronômica Ceres, 745–58.

Bagsic I, Linde M, Debener T, 2016. Genetic diversity and pathogenicity of *Sphaceloma rosarum* (teleomorph *Elsinoë rosarum*) causing spot anthracnose on roses. *Plant Pathology* **65**, 978–86.

Barros LB, Biasi LA, Carisse O, May De Mio LL, 2015. Incidence of grape anthracnose on different *Vitis labrusca* and hybrid cultivars and rootstocks combination under humid subtropical climate. *Australasian Plant Pathology* **44**, 397–403.

Brook PJ, 1973. Epidemiology of grapevine anthracnose, caused by *Elsinoe ampelina*. *New Zealand Journal of Agricultural Research* **16**, 333–42.

Carisse O, Lefebvre A, 2011. A model to estimate the amount of primary inoculum *of Elsinoë ampelina*. *Plant Disease* **95**, 1167–71.

Clement M, Posada D, Crandall K, 2000. TCS: a computer program to estimate gene genealogies. *Molecular Ecology* **9**, 1657–60.

Crous PW, Groenewald JZ, Risède JM, Philippe S, Hyde-Jones NL, 2004. *Calonectria* species and their *Cylindrocladium* anamorphs: Species with clavate vesicles. *Studies in Mycology* **55**, 415–30.

Csuros M, Rogozin IB, Koonin EV, 2011. A detailed history of intron-rich eukaryotic ancestors inferred from a global survey of 100 complete genomes. *PLoS Computational Biology* **7**, e1002150.

de Castella F, Brittlebank C, 1917. Anthracnose or black spot of the vine. *The Journal of the Department of Agriculture of Victoria*, 1–19.

Di Genova A, Almeida AM, Muñoz-Espinoza C *et al.*, 2014. Whole genome comparison between table and wine grapes reveals a comprehensive catalog of structural variants. *BMC Plant Biology* **14**, 7.

Fan XL, Barreto RW, Groenewald JZ *et al.*, 2017. Phylogeny and taxonomy of the scab and spot anthracnose fungus *Elsinoë* (Myriangiales, Dothideomycetes). *Studies in Mycology* **87**, 1–41.

Gene Codes Corporation, 2016. Sequencher® version 5.4.1 sequence analysis software. [http://www.genecodes.com]. Accessed 20 May 2016.

Gregory GR, 1988. Development and status of Australian viticulture. In: Coombe BG, Dry PR, eds. *Viticulture, Volume 1: Resources in Australia*. Adelaide, SA, Australia: Australian Industrial Publishers, 1–37.

Hall TA, 1999. BioEdit: a user-friendly biological sequence alignment editor and analysis program for Windows 95/98/NT. *Nucleic acids symposium series* **41**, 95–8.

Hart KH, Magarey RD, Emmett RW, Magarey PA, 1993. Susceptibility of grapevine selections to black spot (anthracnose) *Elsinoe ampelina*. *Australian Grapegrower & Winemaker* **352**, 85–7.

Hyun JW, Yi SH, Mackenzie SJ *et al.*, 2009. Pathotypes and genetic relationship of worldwide collections of *Elsinoë* spp. causing scab diseases of citrus. *Phytopathology* **99**, 721–8.

Kono A, Sato A, Ban Y, Mitani N, 2013. Resistance of *Vitis* germplasm to *Elsinoë ampelina* (de Bary) Shear evaluated by lesion number and diameter. *HortScience* **48**, 1433–9.

Kumar S, Stecher G, Tamura K, 2016. MEGA7: Molecular evolutionary genetics analysis version 7.0 for Bigger Datasets. *Molecular Biology and Evolution* **33**, 1870–4.

Librado P, Rozas J, 2009. DnaSP v5: A software for comprehensive analysis of DNA polymorphism data. *Bioinformatics* **25**, 1451–2.

Louime C, Lu J, Onokpise O *et al.*, 2011. Resistance to *Elsinoë ampelina* and expression of related resistant genes in *Vitis rotundifolia* Michx. grapes. *International Journal of Molecular Sciences* **12**, 3473–88.

Magarey RD, Coffey BE, Emmett RW, 1993a. Anthracnose of grapevines, a review. *Plant Protection Quarterly* **8**, 106–10.

Magarey RD, Emmett RW, Magarey PA, Franz PR, 1993b. Evaluation of control of grapevine anthracnose caused by *Elsinoe ampelina* by pre-infection fungicides. *Australasian Plant Pathology* **22**, 48–52.

Miles AK, Tan YP, Shivas RG, Drenth A, 2015. Novel pathotypes of *Elsinoë australis* associated with *Citrus australasica* and *Simmondsia chinensis* in Australia. *Tropical Plant Pathology* **40**, 26–34.

Minutolo M, Nanni B, Scala F, Alioto D, 2016. *Sphaceloma coryli* : A reemerging pathogen causing heavy losses on hazelnut in Southern Italy. *Plant Disease* **100**, 548–54.

Mortensen JA, 1981. Sources and inheritance of resistance to anthracnose in *Vitis*. *The Journal of Heredity* **72**, 423–6.

Nylander J, 2004. MrModeltest v2.3 Program distributed by the author. Evolutionary Biology Centre, Uppsala University.

Page RDM, 1996. TreeView: an application to display phylogenetic trees on personal computers. *Computer Applications in the Biosciences* **12**, 357–8.

Pedro Júnior MJ, Pezzopane JRM, Martins FP, 1999. Uso da precipitação pluvial para previsão de épocas de pulverização visando controle de doenças fúngicas na videira 'Niagara Rosada'. *Revista Brasileira de Agrometeorologia* **7**, 107–11.

Poolsawat O, Tharapreuksapong A, Wongkaew S, Reisch B, Tantasawat P, 2010. Genetic diversity and pathogenicity analysis of *Sphaceloma ampelinum* causing grape anthracnose in Thailand. *Journal of Phytopathology* **158**, 837–40.

Poolsawat O, Tharapreuksapong A, Wongkaew S, Tantasawat P, 2009. Cultural characteristics of *Sphaceloma ampelinum*, causal pathogen of grape anthracnose on different media. *Suranaree Journal of Science and Technology* **16**, 149–57.

R Core Team, 2016. R: A Language and Environment for Statistical Computing. Vienna, Austria: R Foundation for Statistical Computing. [http://www.R-project.org]. Accessed 23 May 2016.

Rayner R, 1970. *A Mycological Colour Chart*. Kew, UK: Commonwealth Mycological Institute.

Ronquist F, Huelsenbeck J, 2003. MrBayes 3: Bayesian phylogenetic inference under mixed models. *Bioinformatics* **19**, 1572–4.

Santos RF, Ciampi-Guillardi M, Amorim L, Massola Júnior NS, Spósito MB, 2017. Aetiology of anthracnose on grapevine shoots in Brazil. *Plant Pathology*, in press.

Scheper RWA, Wood PN, Fisher BM, 2013. Isolation, spore production and Koch's postulates of *Elsinoe pyri*. *New Zealand Plant Protection* **66**, 308–16.

Schilder AMC, Smokevitch SM, Catal M, Mann WK, 2005. First report of anthracnose caused by *Elsinoë ampelina* on grapes in Michigan. *Plant Disease* **89**, 1011.

Shear CL, 1929. The life history of *Sphaceloma ampelinum* de Bary. *Phytopathology* **19**, 673–9.

Sompong M, Wongkaew S, Tantasawat P, Buensanteai N, 2012. Morphological, pathogenicity and virulence characterization of *Sphaceloma ampelinum* the causal agent of grape anthracnose in Thailand. *African Journal of Microbiology Research* **6**, 2313–20.

Sosnowski M, Emmett B, Clarke K, Wicks T, 2007. Susceptibility of tablegrapes to black spot (anthracnose) disease. *The Australasian & New Zealand Grapegrower & Winemaker* **521**, 8–11.

Sousa JSI, 1996. *Uvas para o Brasil*. Piracicaba, SP, Brazil: FEALQ.

Suhag LS, Grover RK, 1972. Overwintering and control of *Elsinoe ampelina*, the cause of grapevine anthracnose. In: Chadha K, Randhowa G, Pal R, eds. *Viticulture in the Tropics*. New Delhi, India: Horticultural Society of India, 294–299.

Templeton AR, Crandall KA, Sing CF, 1992. A cladistic analysis of phenotypic associations with haplotypes inferred from restriction endonuclease mapping and DNA sequence data. III. Cladogram estimation. *Genetics* **132**, 619–33.

Thind TS, 2015. Anthracnose. In: Wilcox W, Gubler W, Uyemoto J, eds. *Compendium of grape diseases, disorders, and pests*. St Paul, MN, USA: APS Press, 17–9.

Wang Y, Liu Y, He P, Lamikanra O, Lu J, 1998. Resistance of Chinese *Vitis* species to *Elsinoë ampelina* (de Bary) Shear. *HortScience* **33**, 123–6.

White TJ, Bruns T, Lee S, Taylor J, 1990. Amplification and direct sequencing of fungal ribosomal RNA genes for phylogenetics. In: Innis MA, Gelfand DH, Sninsky JJ, White TJ, eds. *PCR Protocols: A Guide to Methods and Applications*. New York, NY, USA: Academic Press, 315–22.

Yun HK, Louime C, Lu J, 2007. First report of anthracnose caused by *Elsinoe ampelina* on Muscadine Grapes (*Vitis rotundifolia*) in Northern Florida. *Plant Disease* **91**, 905.

Yun CS, Nishida H, 2011. Distribution of introns in fungal histone genes. *PLoS ONE* **6**, e16548.

Supporting information

Table S1 Morphological description of *Elsinoë ampelina* isolates from Brazil and Australia

Country	Isolate	Mycelial growth (mm day^{-1})	Conidial dimensions		
			Length (µm)	Width (µm)	Length/width ratio
Brazil	AVBR118	0.059	5.33 ± 0.49	2.74 ± 0.26	1.95
	AVBR119	0.060	6.07 ± 0.49	2.76 ± 0.21	2.20
	AVBR120	0.060	5.67 ± 0.54	2.63 ± 0.35	2.16
	AVBR121	0.055	5.18 ± 0.43	2.38 ± 0.27	2.17
	AVBR122	0.058	5.91 ± 0.54	2.70 ± 0.16	2.19
	AVBR123	0.057	5.52 ± 0.67	2.61 ± 0.21	2.11
	AVBR124	0.056	5.13 ± 0.45	2.43 ± 0.26	2,11
	AVBR125	0.053	5.39 ± 0.90	2.64 ± 0.35	2.04
	AVBR126	0.059	5.79 ± 0.61	2.45 ± 0.24	2.36
	AVBR127	0.053	6.03 ± 0.60	2.75 ± 0.26	2.19
	AVBR128	0.052	5.40 ± 0.67	2.68 ± 0.29	2.02
	AVBR129	0.059	5.91 ± 0.76	2.75 ± 0.30	2.15
	AVBR130	0.054	5.83 ± 0.55	2.72 ± 0.19	2.14
	AVBR131	0.056	5.75 ± 0.67	2.94 ± 0.33	1.96
	AVBR133	0.059	5.71 ± 0.76	2.73 ± 0.25	2.09
	AVBR134	0.053	5.69 ± 0.78	2.61 ± 0.33	2.18
	AVBR136	0.053	5.42 ± 0.52	2.51 ± 0.22	2.16
	AVBR137	0.056	5.91 ± 0.54	2.70 ± 0.16	2.19
	Mean	0.056	5.65 ± 0.61	2.65 ± 0.26	2.13
Australia	GAAUS1	0.055	5.21 ± 0.85	2.42 ± 0.28	2.15
	GAAUS9	0.055	5.28 ± 0.40	2.45 ± 0.31	2.15
	GAAUS10	0.058	4.89 ± 0.59	2.32 ± 0.15	2.10
	GAAUS11	0.055	5.16 ± 0.47	2.34 ±0.16	2.20
	GAAUS12	0.055	5.27 ± 0.40	2.28 ± 0.14	2.31
	GAAUS14	0.053	5.07 ± 0.44	2.26 ± 0.18	2.25
	GAAUS16	0.058	5.22 ± 0.85	2.30 ± 0.20	2.27
	GAAUS18	0.054	4.95 ± 0.44	2.29 ± 0.16	2.16
	GAAUS19	0.056	4.96 ± 0.58	2.17 ± 0.14	2.29
	GAAUS21	0.052	5.23 ± 0.55	2.27 ± 0.21	2.30
	GAAUS23	0.056	5.18 ± 0.60	2.30 ± 0.17	2.25
	GAAUS24	0.051	5.08 ± 0.36	2.28 ± 0.15	2.23
	GAAUS26	0.049	5.41 ± 0.43	2.47 ± 0.22	2.19
	GAAUS27	0.056	4.98 ± 0.43	2.25 ± 0.21	2.21
	GAAUS30	0.059	5.14 ± 0.47	2.26 ± 0.12	2.27
	GAAUS31	0.055	5.12 ± 0.52	2.21 ± 0.18	2.32
	GAAUS32	0.057	5.27 ± 0.39	2.23 ± 0.11	2.36
	Mean	0.055	5.14 ± 0.52	2.30 ± 0.18	2.24

4 *IN VITRO* PRODUCTION OF CONIDIA OF *ELSINOË AMPELINA*, THE CAUSAL FUNGUS OF GRAPEVINE ANTHRACNOSE

Abstract

Anthracnose, caused by *Elsinoë ampelina*, is an important disease of grapevines. Colonies of *E. ampelina* grow slowly and rarely produce conidia on artificial media. To facilitate studies involving *E. ampelina*, our objective was to develop a method to induce significant conidial production of this fungus. In the present study, we induced the *in vitro* production of conidia of 10 Australian isolates by shake-incubation of mycelial fragments in rainwater under continuous light and darkness. Furthermore, seven Brazilian isolates were shake-incubated in rainwater and distilled water under continuous darkness. In both experiments, cultures were shaken at 200-rpm and kept at room temperature (22 – 25 °C) for 7 days. Conidial production, germination, and infectivity were quantified. Australian and Brazilian isolates showed different levels of conidial production. All Australian isolates sporulated in rainwater ranging from 4.20×10^3 to 5.91×10^6 conidia mL^{-1} and the conidia germination was more than 90% on water agar medium. All the Brazilian isolates produced conidia in rainwater and distilled water, showing high germination, except for one isolate that did not sporulate. Conidial suspensions from Australian and Brazilian *E. ampelina* isolates caused typical anthracnose symptoms on grapevine leaves. This study describes an efficient method, using rainwater or distilled water associated with shaking, to induce the conidia production of *E. ampelina*.

Keywords: Black spot; Sporulation; Rainwater; Shaking; *Sphaceloma ampelinum*

4.1 Introduction

Anthracnose, also known as black spot and bird's eye rot, is found in most grape-growing regions of the world (Thind, 2015). The symptoms are characterized by circular necrotic lesions on all green plant tissue. In years with high rainfall, grapevine anthracnose can cause delayed development and berry ripening, severe crop losses and low fruit quality for the fresh market (Carisse & Lefebvre, 2011a; Carisse & Morissete-Tomas, 2013; Amorim *et al.*, 2016). The causal organism is the ascomycete *Elsinoë ampelina* Shear (anamorph *Sphaceloma ampelinum* de Bary). The sexual stage does not occur as regularly as the asexual stage and has not been reported in a number of countries including India, Australia and Brazil (Suhag & Grover, 1972; Magarey *et al.*, 1993a; Amorim *et al.*, 2016). In the asexual stage, the fungus produces acervuli containing short and cylindrical conidiophores bearing small, ovoid and hyaline conidia (3 - 7 × 2 - 4 µm) on the exterior of lesions (Thind, 2015).

Epidemiological and disease management studies related to grapevine anthracnose require a large quantity of inoculum. However, Brazilian *E. ampelina* isolates grow slowly and do not sporulate on solid artificial media (Santos *et al.*, 2017). Moreover, Kono *et al.*

(2009) reported that Japanese isolates showed poor and unstable sporulation in culture. *Elsinoë fawcettii* and *E. australis*, the causal agents of citrus scab, also do not sporulate on artificial media (Hyun *et al.*, 2015). Likewise, conidia production in culture of *E. veneta* is sparse and variable (Williamson *et al.*, 1989).

Generally, *in vitro* production of conidia of *Elsinoë* species is based on the method of Whiteside (1975) (Swart *et al.*, 2001; Hyun *et al.*, 2009; Miles *et al.*, 2015; Bagsic *et al.*, 2016). In this method, portions of mycelium are extracted from colonies on PDA, fragmented in small pieces and deposited in Petri dishes containing Fries' medium. After 2-3 days at 25 °C, the affixed colonies are flushed with sterile distilled water, then incubated in sterile distilled water for 24 h to induce conidial production (Whiteside, 1975). However, conidial production using this method is still limited, especially for some isolates of *E. fawcettii* and *E. australis* (Hyun *et al.*, 2015). This result agrees with the findings for *E. ampelina*, where isolates rarely produced conidia (Santos *et al.*, 2017). Therefore, Hyun *et al.* (2015) developed an efficient method for sporulation of citrus scab pathogens using rainwater and shaking, resulting in conidia production approximately 13 times higher than that from Whiteside's method.

As *E. ampelina* rarely sporulates *in vitro*, many studies have been carried out using conidia from infected grapevine tissues (Mortensen, 1981; Magarey *et al.*, 1993b; Carisse & Lefebvre, 2011b; Sosnowski *et al.*, 2012). In these studies, infected tissues were obtained either directly from naturally infected vineyard material or from greenhouse-grown grapevines previously inoculated with mycelium or spores. However, the resulting conidial suspension could contain spores from different *E. ampelina* strains, or contaminants such as yeasts. Yeasts, commonly found on grape tissues, show conidial morphology resembling that of *E. ampelina* (Shear, 1929). Thus, trials using conidial suspension derived from infected shoots may lead to inaccurate or unreliable results. Therefore, the objective of this study was to develop an efficient method for production of conidia of *E. ampelina*.

4.2 Materials and methods

4.2.1 Fungal isolates

Elsinoë ampelina isolates were collected in 2015 and 2016 from grapevines showing anthracnose symptoms in vineyards in Australia and Brazil (Table 1). Symptomatic tissues

were cut into small fragments (2-3 mm), disinfested, transferred to water agar (WA; Difco Laboratories), and then to potato dextrose agar (PDA; Difco Laboratories) where the isolates were purified (Chapter 3). Isolates were placed onto PDA adjacent to filter paper discs so that cultures grew over them. Cultures on filter paper were dried and stored at -4 °C until the commencement of experiments at the South Australian Research and Development Institute (Adelaide, Australia) and University of São Paulo (Piracicaba, Brazil). In a preliminary study to confirm fungal identification, morphological characterization and sequencing of the internal transcribed spacer region (ITS) of all *E. ampelina* isolates were performed (Chapter 3). ITS sequences were deposited in the GenBank database.

Table 1. Isolates of *Elsinoë ampelina* used in the *in vitro* conidial production study

Isolate	Host	Location[a]	GenBank accession number (ITS)
GAAUS9	*V. vinifera* cv. unknown	Perth, WA, Australia	**KY684885**
GAAUS14	*V. vinifera* cv. Thompson Seedless	Mildura, VIC, Australia	**KY684889**
GAAUS16	*V. vinifera* cv. Flame Seedless	Perth, WA, Australia	**KY684890**
GAAUS21	*V. vinifera* cv. Thompson Seedless	Robinvale, VIC, Australia	**KY684893**
GAAUS23	*V. vinifera* cv. Thompson Seedless	Nuriootpa, SA, Australia	**KY684894**
GAAUS24	*V. vinifera* cv. Red Globe	Donnybrook, WA, Australia	**KY684895**
GAAUS27	*V. vinifera* cv. Maroo Seedless	Mareeba, QLD, Australia	**KY684897**
GAAUS30	*V. vinifera* cv. Maroo Seedless	Mutchilba, QLD, Australia	**KY684898**
GAAUS31	*V. vinifera* cv. Thompson Seedless	Adelaide, SA, Australia	**KY684899**
GAAUS32	*Vitis* sp. cv. Ornamental grapevine	Aldgate, SA, Australia	**KY684900**
AVBR118	*V. labrusca* cv. Niagara Rosada	Jarinu, SP, Brazil	**KY684866**
AVBR120	*V. labrusca* cv. Niagara Rosada	Jundiaí, SP, Brazil	**KY684868**
AVBR124	*V. labrusca* cv. Niagara Rosada	Atibaia, RS, Brazil	**KY684872**
AVBR129	*V. labrusca* cv. Niagara Rosada	Indaiatuba, SP, Brazil	**KY684877**
AVBR130	*Vitis riparia* × *(V. rupestris* × *V. cordifolia)* cv. Riparia do Traviú	Catuípe, RS, Brazil	**KY684878**
AVBR134	*V. riparia* × *V. labrusca* cv. Baco Blanc	Augusto Pestana, RS, Brazil	**KY684881**
AVBR136	*Vitis riparia* × *(V. rupestris* × *V. cordifolia)* cv. Riparia do Traviú	Augusto Pestana, RS, Brazil	**KY684882**

[a]QLD - Queensland; RS - Rio Grande do Sul; SA - South Australia; SP - São Paulo; VIC – Victoria; WA - Western Australia.

4.2.2 *In vitro* production of conidia

Ten *E. ampelina* isolates collected from various locations in Australia were used in this study (Table 1). Due to the slow growth on artificial media, a 1 cm^2 mycelial fragment excised from a 14-day-old colony was gently streaked over the entire surface of Petri dishes containing PDA amended with streptomycin sulphate (100 mg L^{-1}, Sigma-Aldrich). Plates

were incubated at 25 °C with a 12 h photoperiod for 14 days. To induce sporulation, a colony fragment (4 × 4 cm) was removed, placed in a sterile Petri dish and mashed using a pestle, resulting in fragments smaller than 2 mm. The small fragments were transferred to a 50 mL conical flask containing 40 mL sterile rainwater and incubated on an orbital shaker (Ratek Instruments) at 200-rpm and room temperature (22 - 25 °C) for 7 days (adapted from Hyun *et al.*, 2015). The rainwater was collected and filtered through four layers of gauze to remove the debris prior to sterilization. The experiments were carried out with two light regimes: continuous light or dark. The experimental design was a completely randomized 10 (isolates) × 2 (light regimes) factorial design with three replicates per treatment. As a control, only rainwater was used. The experiment was performed twice.

Additionally, seven *E. ampelina* isolates collected from Brazilian vineyards were tested in this study (Table 1). Using the methodology described above, isolates were grown on PDA, colonies were mashed, small mycelial fragments were transferred to a 125 mL conical flask and incubated on an orbital shaker (Tecnal) at 200-rpm and room temperature (22 - 25 °C) for 7 days in the dark. The experiment was performed using 40 mL sterile rainwater (pH = 5.9; Ca = 0.05 $mmol_c\ L^{-1}$; Mg = 0 $mmol_c\ L^{-1}$; K_2O = 0.02 $mmol_c\ L^{-1}$; Na = 0.02 $mmol_c\ L^{-1}$; Cl = 0.91 $mmol_c\ L^{-1}$; CO_3 = 0 $mmol_c\ L^{-1}$; and HCO_3 = 0.08 $mmol_c\ L^{-1}$) or 40 mL sterile distilled water (pH = 6.3 ; Ca = 0.05 $mmol_c\ L^{-1}$; Mg = 0 $mmol_c\ L^{-1}$; K_2O = 0 $mmol_c\ L^{-1}$; Na = 0 $mmol_c\ L^{-1}$; Cl = 0.48 $mmol_c\ L^{-1}$; CO_3 = 0 $mmol_c\ L^{-1}$; and HCO_3 = 0.06 $mmol_c\ L^{-1}$) in each conical flash. The experimental design was a completely randomized 7 (isolates) × 2 (water media) factorial design with three replicates per treatment. In control flasks, only rainwater or distilled water was used. The experiment was performed twice.

4.2.3 Conidia quantification and germination

The suspension obtained in each flask was filtered through two layers of gauze, and the conidial concentration was estimated (conidia mL^{-1}) four times using a haemocytometer. To evaluate conidia germination from the first experiment with both the Australian and Brazilian isolates, four 50 µL drops of a 10^4 conidia mL^{-1} suspension were deposited on WA. The plates were incubated at 25 °C with a 12 h photoperiod for 24 h. Percentage of conidia germination was assessed by counting the number of germinated conidia out of 100 conidia in each drop using an Olympus BX41 (Olympus) and Eclipse E200 (Nikon Instruments Inc.)

microscope (× 400) for Australian and Brazilian isolates, respectively. A conidium was considered germinated when the germ tube was more than half of the conidium's length.

4.2.4 Infectivity of conidia produced *in vitro*

To assess the infectivity of the conidia produced by Australian isolates in the first experiment, single-node cuttings of cv. Thompson Seedless (*Vitis vinifera*) were sectioned from dormant canes (1-year-old) and inserted into pre-holed polystyrene sheets, with at least 1 cm of the cane protruding below the sheet (Sosnowski *et al.*, 2007). The sheets were then floated on tap water in plastic trays for 14 days to allow for budburst before inoculation in a greenhouse at approximately 25 °C. Single-young shoots with two to three unfolded leaves were sprayed, until runoff, with a suspension of 10^5 conidia mL^{-1} for all isolates, except for isolate GAAUS9, which was applied at 5×10^3 conidia mL^{-1} due to low sporulation. The conidial suspension of each treatment was obtained from only one replicate of the *in vitro* conidia production experiment. Cuttings sprayed only with sterile rainwater were used as a control. For each treatment, 10 cuttings were inoculated. Each tray was covered with a plastic bag and kept in the greenhouse. After 48 h, the plastic bags were removed and the plants were placed in a humidity chamber located within the greenhouse (plastic tent measuring: 160 × 80 × 80 cm) containing automatic nebulizers to maintain high relative humidity (80-90%). Nine days after inoculation, the leaf disease severity was assessed using a standard area diagram set (Chapter 5).

For Brazilian isolates, the infectivity of conidia from the first *in vitro* production experiment was assessed using detached leaves of cv. Niagara Rosada (*V. labrusca*). Young leaves (10 day-old) were removed from healthy potted vines and sprayed with a suspension of 10^4 conidia mL^{-1} until runoff. The conidial suspension of each treatment was obtained from only one replicate. After inoculation, four leaves for each treatment were deposited on WA (0.5%) in Petri dishes with the petioles embedded in the agar. The dishes were incubated at 25 °C with a 12 h photoperiod. Leaves sprayed only with sterile rainwater and sterile distilled water were used as a control. Seven days after inoculation the leaf disease severity was assessed using a standard area diagram set (Chapter 5).

4.2.5 Statistical analyses

Analysis of variance (ANOVA) and means comparisons using Scott Knott test ($P < 0.05$) were performed using 'R' v. 3.3.0 (R Core Team, 2016). The sporulation data were transformed to the $\log_{10}$ (number of conidia +1) for statistical analysis. For conidia germination and leaf disease severity data analysis, the original data set were used.

4.3 Results

All *E. ampelina* colonies used in the experiments for induction of sporulation were analysed before commencement and none had conidia. After 7 days in rainwater, all Australian isolates produced micro colonies (1 - 3 mm in diameter; Fig. 1a) and an abundant number of conidia under both continuous light and dark. Brazilian isolates incubated in rainwater and distilled water also produced numerous micro colonies and, for all but one isolate, there was conidial production. Isolates from both countries produced cylindrical to oblong, hyaline and aseptate conidia (Fig. 1b), measuring 3.8 - 5.7 × 2.1 - 2.8 µm (Australian isolates) and 4.3 - 6.9 × 2.4 - 3.3 µm (Brazilian isolates). The conidia were produced singly (Fig. 1c) or in chains (Fig. 1d) from hyphal tips. In control flasks, no conidia were observed.

Australian isolates showed various levels of conidial production. In the first experiment, conidia production by the isolates was similar for both light regimes, except for the isolates GAAUS9, GAAUS23 and GAAUS30, where the first two isolates had a significantly higher number of conidia in continuous dark than continuous light and GAAUS30 showed highest conidia production in light (Table 2). Conidial production in continuous light and dark varied between 0.42 to 73.50 × 10^4 and 3.67 to 155.83 × 10^4 conidia mL^{-1}, respectively. In the repeated experiment, the isolates GAAUS16 and GAAUS 31 showed a significantly higher number of conidia in continuous dark than continuous light, while for the others there was no difference between light regimes. The GAAUS31 isolate, in continuous dark, showed the highest number of conidia (591.33 × 10^4 conidia mL^{-1}) followed by GAAUS14 and GAAUS16 (118.17 and 141.92 × 10^4 conidia mL^{-1}, respectively). The conidial production mean of all isolates was not significantly different between light and dark.

There were no significant differences between the light regimes for percentage of conidial germination ($P = 0.81$; Fig. 1e) and leaf disease severity ($P = 0.53$) of Australian isolates. Therefore, a pooled analysis was performed. After 24 h on WA, conidial germination

varied between 90.00 to 99.13% (Table 2). Conidial suspensions from all isolates caused typical anthracnose symptoms on leaves from 3 days after inoculation showing leaf disease severity ranging from 3.22 to 13.63% at 9 days (Fig. 1f).

Table 2 Sporulation, conidial germination and leaf disease severity of Australian *Elsinoë ampelina* isolates obtained by incubation in rainwater under continuous light and darkness

Isolate	Sporulation ($\times 10^4$ conidia mL^{-1})				Germination (%)[a]	Severity (%)[a]
	Experiment 1		Experiment 2		Experiment 1	Experiment 1
	Light	Dark	Light	Dark		
GAAUS9	0.42 bD	3.67 aB	0.42 aC	2.00 aC	99.13 A	3.22 D
GAAUS14	11.34 aB	16.77 aB	106.33 aA	118.17 aB	91.00 D	11.77 A
GAAUS16	15.17 aB	57.67 aA	5.25 bB	141.92 aB	99.00 A	7.69 B
GAAUS21	73.50 aA	155.83 aA	56.25 aA	14.67 aC	95.00 B	8.41 B
GAAUS23	8.25 bC	33.41 aB	19.08 aA	4.50 aC	92.50 C	12.84 A
GAAUS24	22.75 aA	12.83 aB	6.83 aB	9.75 aC	93.38 C	6.02 C
GAAUS27	4.83 aC	13.17 aB	22.50 aA	5.67 aC	92.13 C	6.30 C
GAAUS30	48.25 aA	9.83 bB	30.33 aA	26.67 aC	90.00 D	12.21 A
GAAUS31	62.50 aA	17.75 aB	59.58 bA	591.33 aA	95.38 B	13.63 A
GAAUS32	2.92 aC	6.42 aB	20.75 aA	9.58 aC	97.25 A	11.23 A
Mean	24.99 a	32.73 a	32.73 a	92.43 a	94.48	9.36

Means within each row followed by the same lowercase letter and within each column followed by uppercase letter are not different by the Scott Knott test ($P < 0.05$).
[a]There was no significant difference between the experiments carried out with conidial suspensions for the two light regimes (continuous light and darkness) so a pooled analysis was performed.

Brazilian isolate AVBR120 did not produce conidia in either experiment (Table 3). Of the six Brazilian isolates that produced conidia, different amounts of conidia were produced in rainwater and distilled water. In the first experiment, the sporulation ranged from 0.75 to 821.92 × 10^4 conidia mL^{-1} in rainwater and from 1.00 to 791.67 × 10^4 conidia mL^{-1} in distilled water. In the repeated experiment, the average number of conidia produced by the seven isolates in rainwater was 54.02 × 10^4 and 49.99 × 10^4 conidia mL^{-1} in distilled water, which were not significantly different as also observed in the first experiment. In both experiments and media, the isolate AVBR118 had significantly higher conidia production than all other isolates.

There were no significant differences between media when comparing percentage of conidia germination ($P = 0.18$) and leaf disease severity ($P = 0.65$) of Brazilian isolates. Therefore, data from both media were pooled and analysed. Conidia germination varied among the six isolates ranging from 88.50 to 97.50% (Table 3). Detached leaves inoculated

with the conidial suspensions produced visible necrotic lesions showing leaf disease severity from 2.50 to 7.15%.

Table 3 Sporulation, conidial germination and leaf disease severity of Brazilian *Elsinoë ampelina* isolates obtained by incubation in rainwater (RW) and distilled water (DW) under continuous darkness

Isolate	Sporulation ($\times 10^4$ conidia mL^{-1})				Germination (%)[a]	Severity (%)[a]
	Experiment 1		Experiment 2		Experiment 1	Experiment 1
	RW	DW	RW	DW		
AVBR118	821. 92 aA	791.67 aA	300.67 aA	285.83 aA	88.50 C	3.89 B
AVBR120	0.00 aF	0.00 aE	0.00 aD	0.00 aF	-	-
AVBR124	36.42 aC	27.00 aB	39.08 aB	4.33 bD	97.50 A	4.28 B
AVBR129	1.50 aE	1.08 aD	1.75 aC	1.25 aE	94.63 B	3.29 B
AVBR130	10.92 aD	1.00 bD	1.08 bC	9.67 aC	94.75 B	6.07 A
AVBR134	0.75 bE	4.67 aC	0.75 bC	30.92 aB	95.13 B	2.50 B
AVBR136	202.50 aB	41.58 bB	34.83 aB	17.92 aB	96.63 A	7.15 A
Mean	153.43 a	123.86 a	54.02 a	49.99 a	94.52	4.53

Means within each row followed by the same lowercase letter and within each column followed by uppercase letter are not different by the Scott Knott test ($P < 0.05$).
[a]There was no significant difference between the experiments carried out with conidial suspensions from the two media (rainwater and distilled water), so a pooled analysis was performed.

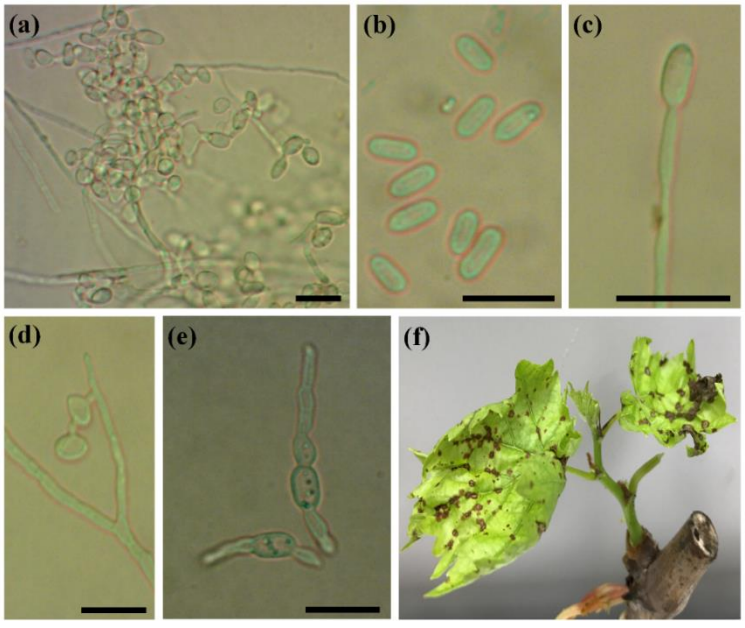

Figure 1 Sporulation in rainwater, conidia germination and symptoms of *Elsinoë ampelina*: (a) micro colonies producing hyaline conidia; (b) conidia released in rainwater after 7 days; (c) production of single conidium from a hyphal tip; (d) conidia produced in chains from a hypha; (e) conidia germinated after 24 h on water agar; and (f) single-node cutting cv. Thompson Seedless showing anthracnose symptoms 9 days after inoculation with conidia produced in rainwater. Scale bars = 10 µm.

4.4 Discussion

In this study, the combination of either rainwater or distilled water and shaking for 7 days induced abundant sporulation of *E. ampelina* in pure cultures. Species of the genus *Elsinoë* are pathogens causing scab and anthracnose on many economically important crops (Fan *et al.*, 2017). However, many species including *E. ampelina* rarely produce conidia *in vitro* (Williamson *et al.*, 1989; Swart *et al.*, 2001; Hyun *et al.*, 2015; Santos *et al.*, 2017). Therefore, a method to induce abundant conidial production of *E. ampelina* will facilitate studies involving grapevine anthracnose.

The use of rainwater resulted in sporulation of around 10^7 conidia colony^{-1} of *E. fawcettii* and *E. australis* (Hyun *et al.*, 2015). In both liquid substrates tested in our study, the first conidia were observed after 4 h incubation. In the method of Whiteside (1975), colonies of *E. fawcetti* started to release conidia in 2 to 3 h. Under natural conditions, conidia of *E. ampelina* are produced in abundance 5 days after inoculation at 21 °C (Brook, 1973). In our experiments, the conidia were produced in chains or singly from hyphal tips, being morphologically identical to the conidia produced on anthracnose lesions. The production of conidia in chains was also reported by Whiteside (1975) on citrus scab lesions.

To induce sporulation of Japanese *E. ampelina*, Kono *et al.* (2009) inoculated small amounts of conidia scraped from the surface of colonies grown on PDA at 24 °C in the dark as a pre-culture. Then, approximately 10 colonies from the pre-culture were incubated in 200 µl of sterile water in a 2 mL tube with shaking for up to 24 h. However, Australian and Brazilian isolates used in our experiments did not produce any conidia on PDA, making it impossible to form pre-cultures from conidia. In the experiments carried out with Australian isolates incubated in rainwater, the sporulation from some isolates was statistically different between continuous light and dark. However, the results were not congruent between the experiments. Lazarotto *et al.* (2014), studying effects of 0, 12 and 24 h photoperiods on sporulation of *Fusarium chlamydosporum*, reported that light regimes had an effect on sporulation for some isolates, while for others it had no effect. Yun *et al.* (2003) described a methodology, where *E. ampelina* cultures were grown on V-8 juice agar medium at 28 °C under a near-ultraviolet light for 2 days to produce conidia. However, this method was performed with the Brazilian isolates and none produced conidia, possibly due to differences in fungal isolates requirements to sporulate (data not shown).

According to Su *et al.* (2012), factors such as low nutrient media and light should be considered in the induction of fungal sporulation in artificial media. Elson *et al.* (1998) analysed the influence of carbon (carbohydrate) concentration on conidial production of *Helminthosporium solani*, and observed that higher carbon concentrations inhibited the conidiation. Physical force by shaking was reported to improve the sporulation of *Penicillium cyclopium* (Roncal *et al.*, 2002). Furthermore, shaking influenced mycelial detachment and helped the release of conidia, which increased conidial production of *E. fawcettii* and *E. australis* (Hyun *et al.*, 2015). The lack of a carbon source in rainwater and distilled water, along with shaking, were most likely the main factors that induced abundant sporulation of *E. ampelina.*

In the present study, conidia production varied among isolates. Hyun *et al.* (2015) associated the variation of the conidial production with texture, toughness, and gelatinous stickiness of cultures, which could potentially limit mycelial fragmentation during maceration and homogenization. These features may be also associated with the variation of conidia production between the repetitions in our experiments. We did not identify any evidence to explain the absence of sporulation from isolate AVBR120. Additionally, the variation in conidial production among the isolates may be also related to their genetic variability.

The production of high quantity and quality of pathogen inoculum is essential for studying many aspects of fungal species (Rodrigues *et al.*, 2010). The methodology used in this study led to the abundant production of conidia by *E. ampelina*. In both rainwater and distilled water, conidial germination was higher than 88.5% after 24 h on WA. Conidia usually had one to two germ tubes; however, in some conidia up to four germ tubes were observed. In addition, conidia of all isolates were infective on grapevine, causing typical anthracnose symptoms on leaves. This study is the first report that the method using mycelial fragments shake-incubated in rainwater or distilled water is effective for production of abundant infective conidia of *E. ampelina*.

References

Amorim L, Spósito MB, Kuniyuki H, 2016. Doenças da videira. In: Amorim L, Rezende JAM, Bergamin Filho A, Camargo LEA, eds. *Manual de Fitopatologia: doenças das plantas cultivadas*. São Paulo, SP, Brazil: Agronômica Ceres, 745–58.

Bagsic I, Linde M, Debener T, 2016. Genetic diversity and pathogenicity of *Sphaceloma rosarum* (teleomorph *Elsinoë rosarum*) causing spot anthracnose on roses. *Plant Pathology* **65**, 978–86.

Brook PJ, 1973. Epidemiology of grapevine anthracnose, caused by *Elsinoe ampelina*. *New Zealand Journal of Agricultural Research* **16**, 333–42.

Carisse O, Lefebvre A, 2011a. A model to estimate the amount of primary inoculum of *Elsinoë ampelina*. *Plant Disease* **95**, 1167–71.

Carisse O, Lefebvre A, 2011b. Evaluation of Northern grape hybrid cultivars for their susceptibility to anthracnose caused by *Elsinoe ampelina*. *Plant Health Progress*, doi:10.1094/PHP-2011-0805-01-RS.

Carisse O, Morissete-Tomas V, 2013. Epidemiology of grape anthracnose: factors associated with defoliation of grape leaves infected by *Elsinoë ampelina*. *Plant Disease* **97**, 222–30.

Elson MK, Schisler DA, Jackson MA, 1998. Carbon-to-nitrogen ratio, carbon concentration, and amino acid composition of growth media influence conidiation of *Helminthosporium solani*. *Mycologia* **90**, 406–13.

Fan XL, Barreto RW, Groenewald JZ *et al.*, 2017. Phylogeny and taxonomy of the scab and spot anthracnose fungus *Elsinoë* (Myriangiales, Dothideomycetes). *Studies in Mycology* **87**, 1–41.

Hyun JW, Paudyal DP, Hwang R, 2015. Improved method to increase conidia production from isolates of different pathotypes of citrus scab pathogen *Elsinoe* spp. *Research in Plant Disease* **21**, 231–4.

Hyun JW, Yi SH, Mackenzie SJ *et al.*, 2009. Pathotypes and genetic relationship of worldwide collections of *Elsinoë* spp. causing scab diseases of citrus. *Phytopathology* **99**, 721–8.

Kono A, Nakaune R, Yamada M, Nakano M, Mitani N, Ueno T, 2009. Effect of culture conditions on conidia formation by *Elsinoë ampelina*, the causal organism of grapevine anthracnose. *Plant Disease* **93**, 481–4.

Lazarotto M, Mezzomo R, Maciel CG, Finger G, Muniz MFB, 2014. Mycelia growth and sporulation of *Fusarium chlamydosporum* species complex under different culture conditions. *Amazonian Journal of Agricultural and Environmental Sciences* **35**, 35–40.

Magarey RD, Coffey BE, Emmett RW, 1993a. Anthracnose of grapevines, a review. *Plant Protection Quarterly* **8**, 106–10.

Magarey RD, Emmett RW, Magarey PA, Franz PR, 1993b. Evaluation of control of grapevine anthracnose caused by *Elsinoe ampelina* by pre-infection fungicides. *Australasian Plant Pathology* **22**, 48–52.

Miles AK, Tan YP, Shivas RG, Drenth A, 2015. Novel pathotypes of *Elsinoë australis* associated with *Citrus australasica* and *Simmondsia chinensis* in Australia. *Tropical Plant Pathology* **40**, 26–34.

Mortensen JA, 1981. Sources and inheritance of resistance to anthracnose in *Vitis*. *The Journal of Heredity* **72**, 423–6.

R Core Team, 2016. R: A Language and Environment for Statistical Computing. Vienna, Austria: R Foundation for Statistical Computing. [http://www.R-project.org]. Accessed 23 May 2016.

Rodrigues TTM, Maffia LA, Dhingra OD, Mizubuti ES, 2010. *In vitro* production of conidia of *Alternaria solani*. *Tropical Plant Pathology* **35**, 203–12.

Roncal T, Cordobés S, Sterner O, Ugalde U, 2002. Conidiation in *Penicillium cyclopium* is induced by conidiogenone, an endogenous diterpene. *Eukaryotic cell* **1**, 823–9.

Santos RF, Ciampi-Guillardi M, Amorim L, Massola Júnior NS, Spósito MB, 2017. Aetiology of anthracnose on grapevine shoots in Brazil. *Plant Pathology*, in press.

Shear CL, 1929. The life history of *Sphaceloma ampelinum* de Bary. *Phytopathology* **19**, 673–9.

Sosnowski M, Emmett B, Clarke K, Wicks T, 2007. Susceptibility of tablegrapes to black spot (anthracnose) disease. *The Australasian & New Zealand Grapegrower & Winemaker* **521**, 8–11.

Sosnowski MR, Emmett RW, Wilcox WF, Wicks TJ, 2012. Eradication of black rot (*Guignardia bidwellii*) from grapevines by drastic pruning. *Plant Pathology* **61**, 1093–102.

Su Y, Qi Y, Cai L, 2012. Induction of sporulation in plant pathogenic fungi. *Mycology* **3**, 195–200.

Suhag LS, Grover RK, 1972. Overwintering and control of *Elsinoe ampelina*, the cause of grapevine anthracnose. In: Chadha K, Randhowa G, Pal R, eds. *Viticulture in the Tropics*. New Delhi, India: Horticultural Society of India, 294–9.

Swart L, Crous PW, Kang J-C, Mchau GRA, Pascoe I, Palm ME, 2001. Differentiation of species of *Elsinoë* associated with scab disease of Proteaceae based on morphology, symptomatology, and ITS sequence phylogeny. *Mycologia* **93**, 366–79.

Thind TS, 2015. Anthracnose. In: Wilcox W, Gubler W, Uyemoto J, eds. *Compendium of grape diseases, disorders, and pests*. St Paul, MN, USA: APS Press, 17–9.

Whiteside JO, 1975. Biological characteristics of *Elsinoë fawcetti* pertaining to the epidemiology of sour orange scab. *Phytopathology* **65**, 1170–7.

Williamson B, Hof L, Mcnicol RJ, 1989. A method for *in vitro* production of conidia of *Elsinoe veneta* and the inoculation of raspberry cultivars. *Annals of Applied Biology* **114**, 23–33.

Yun HK, Park KS, Roh JH, Kwon BO, Jeong SB, 2003. Development of an efficient screening system for anthracnose resistance in grapes. *Journal of the Korean Society for Horticultural Science* **44**, 809–12.

5 DEVELOPMENT AND VALIDATION OF A STANDARD AREA DIAGRAM SET FOR ASSESSMENT OF ANTHRACNOSE SEVERITY ON GRAPEVINE LEAVES

Abstract

Anthracnose, caused by *Elsinoë ampelina*, is an important grapevine disease in humid regions that causes serious crop losses in different parts of the world. The objective of this study was to develop and validate a standard area diagram set (SADs) to aid the visual estimates of the severity of anthracnose on grapevine leaves. The SADs comprises six true colour diagrams with anthracnose severity ranging from 1.1 to 27.4%. The intermediate values are 2.1, 4.3, 8.3 and 15.6%. To validate the SADs, 12 raters assessed 50 images of grapevine leaves with a range of anthracnose severities. Initially, the raters estimated the severity without the use of the SADs. One week later, the raters provided estimates for the same set of images using the SADs as an aid. For all raters, the estimates of grapevine anthracnose severity using the SADs were closer to the actual values than the unaided estimates. Significant improvements in accuracy (coefficient of bias, C_b = 0.90 without the SADs and 0.99 with the SADs), precision (Pearson correlation coefficient, r = 0.89 without the SADs and 0.96 with the SADs) and agreement (Lin's concordance correlation coefficient, ρ_c = 0.80 without the SADs and 0.96 with the SADs) were observed. Moreover, the SADs also significantly improved the inter-rater reliability of the estimates (R^2 = 0.70 without the SADs and 0.89 with the SADs). The SADs proposed in this study was proven to be adequate for estimates of anthracnose severity on grapevine leaves.

Keywords: *Vitis labrusca*; *Elsinoë ampelina*; Disease assessment; Phytopathometry

5.1 Introduction

Grapevine (*Vitis* spp.) is an important crop in Brazil, occupying 75,906 ha (IBGE, 2017). The annual Brazilian grapevine production is more than 1.5 million tons, half of which is sold as table grapes and the other half as grapes for processing (Buffara *et al.*, 2014). Table grapes, belonging to the species *Vitis labrusca*, include the cultivars Niagara Rosada, Niagara Branca, Concord and Isabel that are commonly cultivated in the southeastern and southern regions. In these regions, anthracnose caused by *Elsinoë ampelina* Shear (anamorph *Sphaceloma ampelinum* de Bary) is one of the most important grapevine diseases (Santos *et al.*, 2017).

The fungus *E. ampelina* infects the aerial parts of the vine, including the young shoots, leaves, petioles, tendrils and berries. On leaves, the symptoms are dark brown to dark grey, slightly depressed circular or angular spots, which enlarge and coalesce to cover an extensive part of the leaf blade, mainly along the veins (Thind, 2015). As the disease develops, the lesions on the stems, petioles and tendrils may coalesce and form brown to dark grey cankers

(Amorim *et al.*, 2016). Infected berries show sunken spots with greyish centres and black edges. Severely infected berries dry up and drop prematurely (Carisse & Lefebvre, 2011). In infected vineyards, during rainy years, the pathogen causes severe epidemics that reduce the quality and quantity of grape production (Thind, 2015; Amorim *et al.*, 2016).

The quantification of plant disease is fundamental to the study and analysis of disease epidemics as well as the assessment of different control strategies (Campbell & Madden, 1990). However, the quantification needs to be accurate and precise to provide reliable and reproducible estimates. The accuracy and precision of disease assessments can be improved by selecting the most appropriate method, including standard area diagrams and training raters to evaluate the disease (Nutter & Schultz, 1995). A standard area diagram set (SADs), also known as a diagrammatic scale, is a set of illustrations of diseased plants or plant parts that exhibit different severity levels (Amorim & Bergamin Fillho, 2011). It is considered a simple and fast method to quantify the severity of diseases (Paula *et al.*, 2016). In plant breeding, a SADs is a valuable tool for identifying the genetic variations in disease resistance among plant genotypes (Vieira *et al.*, 2014).

In the literature, the first SADs that was developed showed five illustrations with different severities of rust (*Puccinia recondita* f.sp. *tritici*) on wheat leaves (Cobb, 1892). Since then, several SAD sets have been developed and published using logarithmic increments to determine intermediate values of disease severity (Mesquini *et al.*, 2009; Vieira *et al.*, 2014; Ortega-Acosta *et al.*, 2016). Moreover, some researchers have published SAD sets using linear increments (Capucho *et al.*, 2011; Rios *et al.*, 2013; Debona *et al.*, 2015). However, Schwanck & Del Ponte (2014) analysed linear and logarithmic SAD sets in true colour and black and white and developed a SADs to assess the severity of rice brown spot disease (*Bipolaris oryzae*). The study verified that all sets had similar accuracies and precisions. Ideally, a SADs should be accurate, precise and improve the inter-rater reliability (reproducibility) of visual estimates. Accuracy measures the degree of closeness between the estimates and the actual severity and precision measures the variability of the estimates (Nutter & Schultz, 1995; Madden *et al.*, 2007; Yadav *et al.*, 2013).

Estimates of grapevine anthracnose symptoms on leaves are normally performed by counting the number of lesions per leaf or leaf area (Poolsawat *et al.*, 2012; Kono *et al.*, 2013; Santos *et al.*, 2017), estimating the leaf disease severity using image-based software (Santos *et al.*, 2017) or using a scale index (Wang *et al.*, 1998; Shetty *et al.*, 2014). As grapevine anthracnose studies involve the analysis of hundreds of leaves, these assessment methods can

be time consuming. As simple, accurate, precise and fast tools, SAD sets have long been used to aid the estimations of disease severity in several crops (Del Ponte *et al.*, 2017). However, no SADs has been proposed to aid the estimation of anthracnose severity. Therefore, the objective of this study was to develop and validate a SADs for assessing anthracnose severity on grapevine leaves.

5.2 Materials and methods

5.2.1 Development of the SADs

To develop the SADs, 50 leaves of 'Niagara Rosada' showing different levels of anthracnose severity were collected from a vineyard located in Jundiaí, São Paulo, Brazil (23°7'24.31"S; 46°51'47.68"W). In addition, 50 symptomatic leaves were obtained from inoculations of *E. ampelina* isolates on potted vines of 'Niagara Rosada' (Santos *et al.*, 2017). Then, 100 leaves with a range of anthracnose severity were individually photographed using a digital camera (Sony Cyber-shot DSC-W570 – 16.1 megapixels, Sony) mounted 30 cm from the leaf. For each leaf, the proportion of diseased area was estimated using ImageJ (Schneider *et al.*, 2012). The minimum and maximum values of severity observed in the samples were used to determine the lower and upper limits of the SADs. Four other severity values were determined based on logarithmic increments. A representative image of a grapevine leaf was used as the template to develop the SADs in PAINT.NET 4.0.9 image editing software (http://www.getpaint.net/). The shape, size, colour and spatial pattern of the lesions were added manually to each diagram, copying those observed on an actual diseased leaf.

5.2.2 Validation of the SADs

To validate the SADs, a group of 12 raters without experience evaluating grapevine anthracnose assessed 50 images of leaves with different disease severities. The images were displayed on individual Microsoft PowerPoint slides in a random sequence in two phases. In the first phase, the raters estimated the severity without using the SADs. One week later, in the second phase, the raters provided estimates for the same set of images with the aid of the SADs.

5.2.3 Data analyses

The precision, accuracy, bias and agreement of the estimates without and with the use of the SADs were determined for each rater. The precision was calculated using the Pearson correlation coefficient (r) between actual severity (x) and estimated severity (y), where 1 = perfect correlation. The accuracy, bias and agreement were determined by Lin's concordance correlation (LCC) analysis (Lin, 1989). The accuracy was determined using the coefficient of bias (C_b), which measures how far the best-fit line deviates from the 45° line of concordance, where 1 = perfect relationship between x and y. C_b is calculated based on scale bias (υ) and location bias (μ) (Yadav *et al.*, 2013). Scale bias measures the difference between line slopes, where 1 = equal slopes, and location bias measures the difference between line heights, where 0 = equal heights, between the fitted line from y and the concordance line from x. Lin's concordance correlation coefficient (LCCC, ρ_c) was used to determine the agreement (combines the precision and accuracy; $\rho_c = r \times C_b$), where 1 = perfect concordance between x and y.

The inter-rater reliability of the estimates was determined using the coefficient of determination (R^2) obtained from a linear regression between the severity estimates from all pairs of raters (Nutter & Schultz, 1995). In addition, the inter-rater reliability was also calculated using the intra-class correlation coefficient (ICC), which is based on the variance estimates for all raters combined (without and with the use of the SADs) using a two-way random effects analysis of variance (ANOVA) model (Nita *et al.*, 2003).

The 95% confidence intervals (95% CIs), which were based on the differences between the means of each group (without and with the use of the SADs), were calculated for the statistics r, C_b, υ, μ, ρ_c and R^2 by bootstrapping using the percentile method (Yadav *et al.*, 2013). In the analyses, 10,000 bootstrap samples were used. If the 95% CIs included zero, the difference is not significant ($P < 0.05$). To calculate the LCCC statistics, the epi.ccc function in the epiR package (Stevenson *et al.*, 2017) was used. The ICC was determined using the icc function in the irr package (Gamer *et al.*, 2012). All statistical analyses were performed using 'R' v. 3.4.1 (R Core Team, 2017).

5.3 Results

The SADs developed in this study comprises six values of anthracnose severity ranging from 1.1 to 27.4%. The intermediate values are 2.1, 4.3, 8.3 and 15.6% (Fig. 1). The first symptoms on the leaves were characterized by small, dark grey lesions that enlarged and coalesced as the disease developed and occurred mainly along the veins. Coalescence of lesions was commonly observed on leaves with more than 4% severity values. Thus, these features were represented in the diagrams.

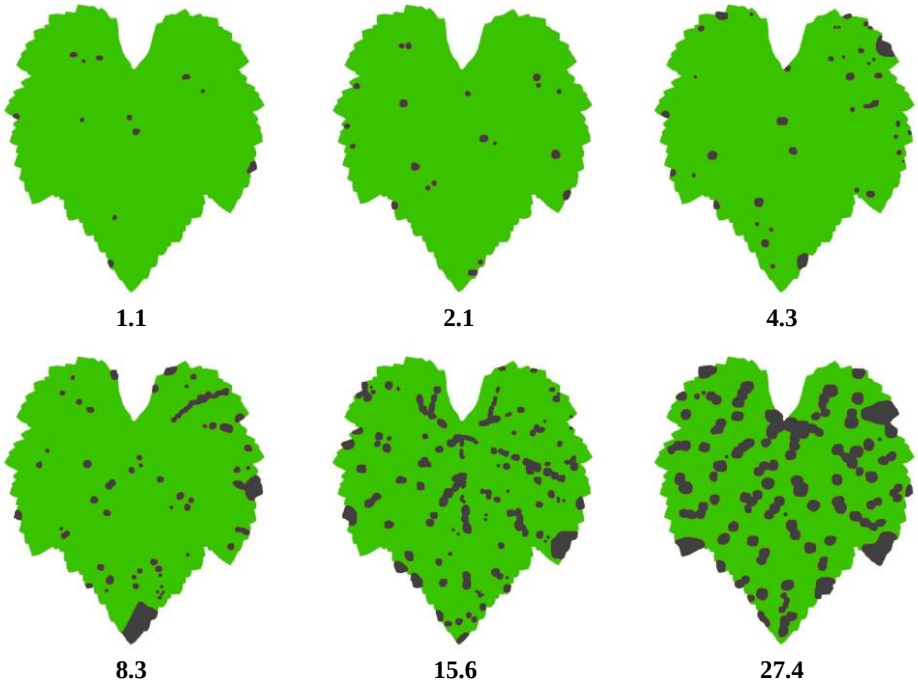

Figure 1 Standard area diagram set developed as an aid for the assessment of grapevine anthracnose severity on leaves. The numbers in the diagrams represent the percentages (%) of leaf disease severity.

The visual estimates of anthracnose severity on leaves, from the pooled data from 12 raters, were closer to the actual values when the SADs was employed than the unaided estimates (Fig. 2a, b). An overall tendency to overestimate anthracnose severity was observed for severity values < 10%, especially for estimates without the use of the SADs. In addition, the absolute errors (the estimated severity minus the actual severity) of the estimates aided by the SADs were lower than those estimates that did not utilize the diagrams (Fig. 2c, d). Without the use of the SADs, the absolute errors ranged from -18.42 to 22.58, but when the SADs was employed, the errors decreased and varied from -7.42 to 6.60.

The LCC analysis demonstrated a range of scale bias (υ) location bias (μ), coefficient of bias (C_b), Pearson correlation coefficient (r) and LCCC (ρ_c) among raters without and with the SADs (Fig. 3). For most raters, the statistical parameters υ and μ were closer to 1 and 0, respectively, when the SADs was used. At the same time, the measures C_b, r and ρ_c were improved for all raters when the SADs was employed. When the estimates from the raters were pooled, significant improvements in accuracy (C_b = 0.90 and 0.99 without and with the SADs, respectively), precision (r = 0.89 and 0.96 without and with the SADs, respectively) and agreement (ρ_c = 0.80 and 0.96 without and with the SADS, respectively) were observed (Table 1). Although there were numerical improvements in scale bias (υ = 1.11 to 0.98 without and with the SADs, respectively) and location bias (μ = 0.05 to < 0.01 without and with the SADs, respectively), they were not statistically significant. Moreover, the use of the SADs also reduced the standard deviation for all parameters analysed (υ, μ, C_b, r and ρ_c) (Table 1).

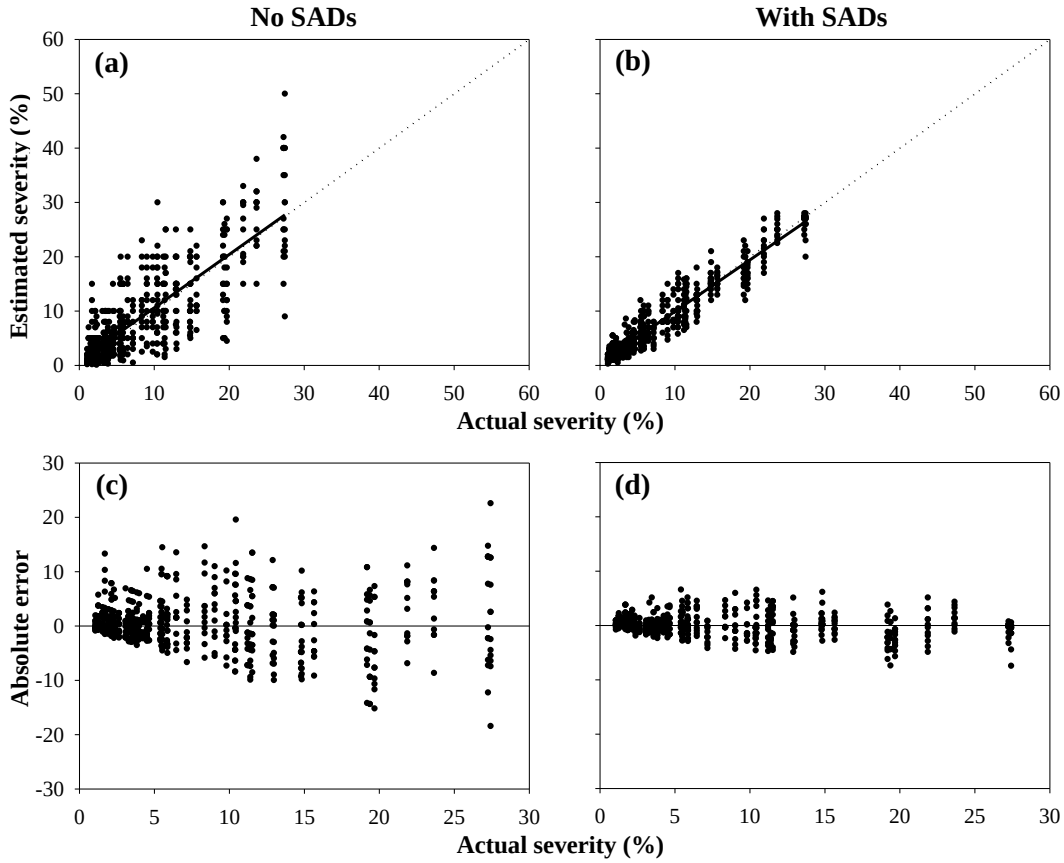

Figure 2 Relationship between the actual and estimated severity of anthracnose on grapevine leaves estimated by 12 raters for a set of 50 leaves (n = 600) without (a) and with (b) the use of a standard area diagram set (SADs). The solid line represents the best-fitting line. The dotted line represents the concordance line. The absolute error (the estimated minus the actual severity) of the anthracnose estimates by the same raters without (c) and with (d) the use of the SADs. The solid line represents the no-error line.

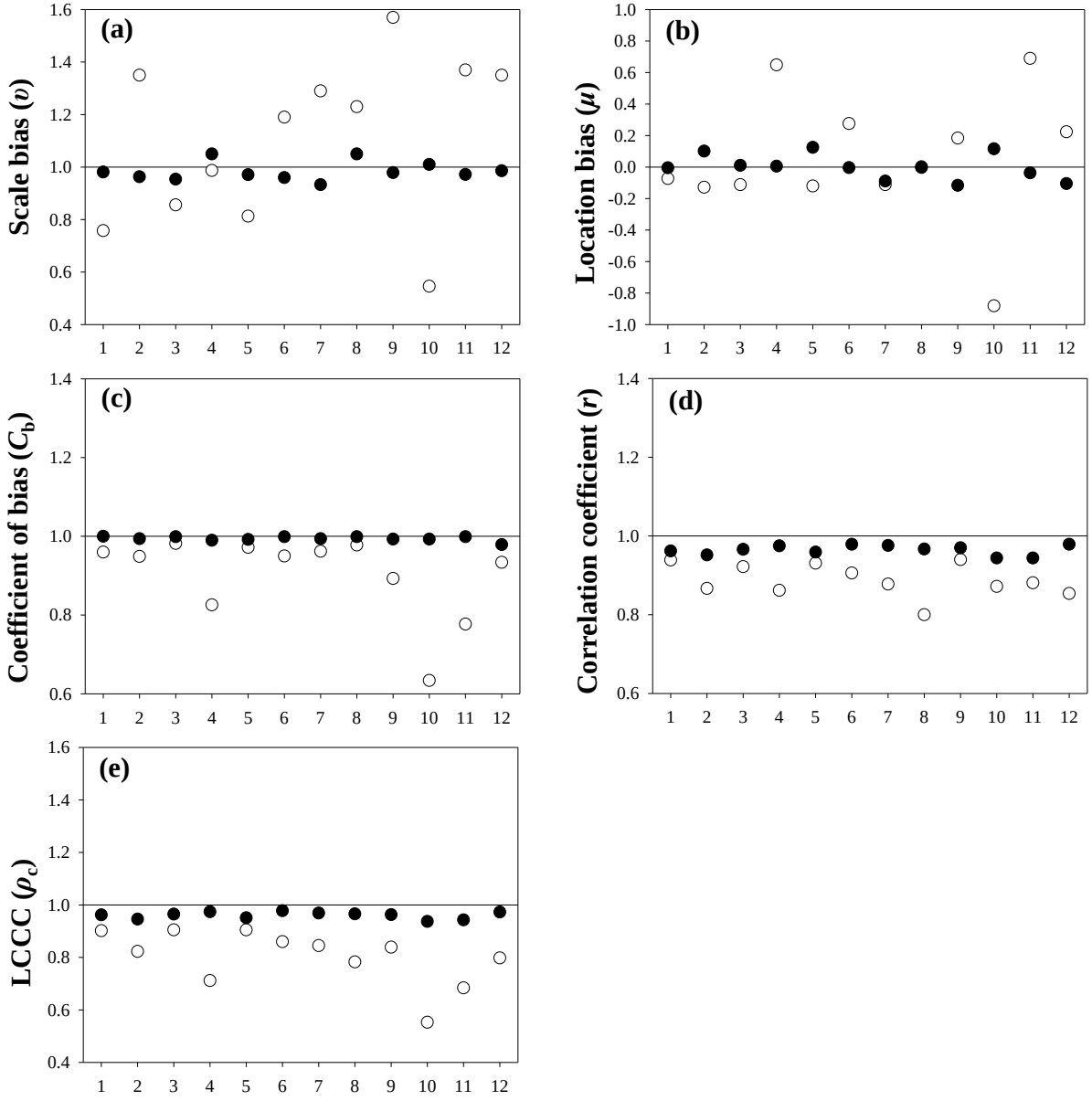

Figure 3 Scale bias (υ) (a), location bias (μ) (b), coefficient of bias (C_b) (c), Pearson correlation coefficient (r) (d) and Lin's concordance correlation coefficient - LCCC (ρ_c) (e) of the estimates of anthracnose severity on grapevine leaves from 12 raters without (white circles) or with (black circles) the use of a standard area diagram set. Perfect agreement between actual severity (x) and estimated severity (y) occurs when $\upsilon = 1$, $\mu = 0$, $C_b = 1$, $r = 1$ and $\rho_c = 1$.

Table 1 Bias, accuracy, precision and agreement related to the estimates of anthracnose severity on grapevine leaves conducted by 12 raters without and with the use of a standard area diagram set (SADs)

Statistic	**Means**[a]		**95% CIs**[b] **of the difference between means**
	No SADs	**With SADs**	
Scale (υ)[c]	1.11 (0.31)	0.98 (0.04)	-0.29, 0.05
Location (μ)[d]	0.05 (0.41)	< 0.01 (0.08)	-0.27, 0.19
Coefficient of bias (C_b)[e]	0.90 (0.11)	0.99 (0.01)	**0.05, 0.16**
Correlation coefficient (r)[f]	0.89 (0.04)	0.96 (0.01)	**0.05, 0.10**
LCCC (ρ_c)[g]	0.80 (0.11)	0.96 (0.01)	**0.11, 0.22**

[a]Standard deviation in parentheses.
[b]Confidence intervals (CIs) were based on 10,000 bootstrap samples. If the CIs include zero, there were no significant differences between the means ($P < 0.05$). The values in bold represent a significant difference.
[c]Scale bias or slope shift [1 = perfect relationship between the actual severity (x) and the estimated severity (y)].
[d]Location bias or height shift (0 = perfect relationship between x and y).
[e]Coefficient of bias (C_b) measures how far the best-fit line deviates from the line of concordance (1 = perfect relationship between x and y). C_b is calculated based on υ, and μ and is a measure of accuracy.
[f]Pearson correlation coefficient measures the precision (1 = perfect correlation between x and y).
[g]Lin's concordance correlation coefficient (LCCC) combines both measures of precision (r) and accuracy (C_b) to measure agreement (1 = perfect concordance between x and y).

The inter-rater reliability of the assessments measured by the coefficient of determination (R^2) and intra-class correlation coefficient (ICC) was improved with the use of the SADs. Without the SADs, 46.97, 34.85 and 18.18% of the pairwise comparisons had an $R^2 < 0.70$, 0.70-0.79 and 0.80-0.89, respectively. However, when the SADs was employed, 46.97% of the pairwise comparisons had R^2 values between 0.80-0.89 and 53.03% resulted in an $R^2 > 0.90$ (Table 2). The mean R^2 among the raters significantly increased from 0.70 to 0.89 when the SADs was used to aid the visual estimations. Moreover, the ICC improved from 0.69 to 0.94 when the SADs was used.

Table 2 Inter-rater reliability of the estimates measured by coefficient of determination (R^2) of a linear regression between the severity estimates from the pairwise comparisons among 12 raters when assessing anthracnose severity on grapevine leaves without and with the use of a standard area diagram set (SADs)

Rater	**1**	**2**	**3**	**4**	**5**	**6**	**7**	**8**	**9**	**10**	**11**	**12**
No SADs												
1	-	0.69	0.77	0.71	0.80	0.80	0.76	0.58	0.80	0.77	0.72	0.63
2		-	0.85	0.51	0.83	0.65	0.77	0.74	0.78	0.73	0.65	0.77
3			-	0.63	0.85	0.69	0.85	0.71	0.86	0.75	0.71	0.78
4				-	0.75	0.74	0.47	0.61	0.57	0.56	0.78	0.50
5					-	0.80	0.68	0.71	0.81	0.77	0.80	0.69
6						-	0.55	0.65	0.67	0.68	0.79	0.56
7							-	0.51	0.81	0.76	0.52	0.69
8								-	0.57	0.60	0.69	0.57
9									-	0.73	0.68	0.73
10										-	0.63	0.58
11											-	0.67
12												-
With SADs												
1	-	0.88	0.90	0.95	0.91	0.89	0.91	0.94	0.90	0.83	0.87	0.90
2		-	0.90	0.89	0.90	0.87	0.90	0.89	0.85	0.80	0.84	0.87
3			-	0.91	0.95	0.91	0.92	0.90	0.89	0.88	0.90	0.90
4				-	0.91	0.91	0.92	0.91	0.91	0.86	0.86	0.93
5					-	0.91	0.90	0.88	0.85	0.85	0.88	0.87
6						-	0.93	0.89	0.89	0.83	0.85	0.93
7							-	0.92	0.92	0.83	0.91	0.93
8								-	0.91	0.81	0.87	0.89
9									-	0.87	0.90	0.92
10										-	0.86	0.87
11											-	0.90
12												-

Statistic	**No SADs**	**With SADs**	**95% CI[a] of the difference**
Mean inter-rater coefficient of determination (R^2)	0.70 (0.10)	0.89 (0.03)	**0.17, 0.22**

[a] Confidence interval (CI) was based on 10,000 bootstrap samples. If the CI includes zero, the difference between the means was not significant ($P < 0.05$). The values in bold represent significant differences.

5.4 Discussion

The SADs that was developed and validated in the present study improved the accuracy, precision, agreement and inter-rater reliability of the visual estimates of anthracnose severity on grapevine leaves. SAD sets have been used as tools to aid the estimation of several crop diseases, including blast (*Pyricularia oryzae*) on wheat (Rios *et al.*, 2013), brown eye spot (*Cercospora coffeicola*) on coffee (Paula *et al.*, 2016), leaf blight (*Setosphaeria turcica*)

on corn (Vieira *et al.*, 2014) and brown spot (*Bipolaris oryzae*) on rice (Schwanck & Del Ponte, 2014). For grapevine diseases, SAD sets have been demonstrated to improve the visual estimates of the severity of downy mildew (*Plasmopora viticola*) (Buffara *et al.*, 2014), rust (*Phakopsora euvitis*) (Angelotti *et al.*, 2008), isariopsis leaf spot (*Pseudocercospora vitis*) (Lenz *et al.*, 2009) and botrytis bunch rot (*Botrytis cinerea*) (Hill *et al.*, 2010).

In this study, the minimum anthracnose severity in the SADs was 1.1%, even though this level may be lower in a vineyard. Severities lower than 1.1% were not included in the SADs because they did not seem practical, since the first symptoms are few small spots that are difficult to see, which has also been reported for the SAD sets used to assess grapevine rust (Angelotti *et al.*, 2008) and grapevine downy mildew (Buffara *et al.*, 2014). The maximum anthracnose severity that was observed on the leaves was 27.4%. In Australia, Sosnowski *et al.* (2007) observed that the anthracnose severity on *Vitis vinifera* cv. Thompson Seedless leaves was between 23 and 28%, which fell among the other six *V. vinifera* cultivars analysed, which ranged from 8 to 24%. The severity intervals in the proposed SADs were determined based on a logarithmic function (nonlinear) due to the higher frequency of severity values between 1.1 to 15.6%, where anthracnose severity levels are typically more common in Brazil. Thus, more reference values in the diagrams were concentrated within this range. In the field, the variation in the severity of grapevine anthracnose may be related to the susceptibility of grape cultivars, canopy management, climatic variation, dormant treatments and foliar fungicide applications (Thind, 2015; Amorim *et al.*, 2016).

For all raters, the estimates of grapevine anthracnose severity using the SADs as a visual aid were closer to the actual values than the estimates that did not use the SADs. The absolute errors of the estimates decreased when the SADs was used, falling within ±8% of the actual value compared to -18 to +23% when the estimates were performed without the SADs. In a study with peach rust (*Tranzschelia discolour*), the use of a SADs reduced the absolute errors of the estimates, with most errors falling within ±10% compared to -16 to +54% when the estimates were carried out without the use of a SADs (Dolinski *et al.*, 2017). In our study, we observed that raters tended to overestimate severities less than 10%, which was also observed by Spolti *et al.* (2011) in the estimations of sooty blotch and flyspeck severity on apple fruit. According to Campbell & Madden (1990), errors in the quantification of plant disease may be magnified in subsequent epidemiological analyses, resulting in erroneous conclusions. In this context, the magnitude of the errors may be reduced by training the raters

to use the SADs (Belasque Júnior *et al.*, 2005) and with the aid of specialized computer software (Nutter & Schultz, 1995).

The measures of precision, accuracy and agreement (r, C_b and ρ_c) were significantly improved when the SADs was used, indicating that the estimates were very close to the actual values, which has been described in other studies (Rios *et al.*, 2013; Yadav *et al.*, 2013; Schwanck & Del Ponte, 2014; Dolinski *et al.*, 2017). Although the scale bias (υ) and location bias (μ) statistics were closer to 1 and 0, respectively, when the raters used the SADs, there were no significant differences in the values from the unaided estimates, which was also reported by González-Domínguez *et al.* (2014). These authors compared inexperienced and experienced raters during assessments of scab (*Fusicladium eriobotryae*) severity on loquat fruit and observed significant improvements in r, C_b and ρ_c with the use of a SADs in only the group of inexperienced raters. However, the use of a SADs to assess the severity of frogeye leaf spot (*Cercospora sojina*) on soybean plants resulted in increases in r, C_b and ρ_c for both inexperienced and experienced raters (Debona *et al.*, 2015).

The reproducibility of the anthracnose estimates (R^2) among raters increased considerably when they used the SADs, from 0.70 (unaided estimates) to 0.89 (aided estimates). This result indicates that the use of the SADs improved the precision of the assessments performed by different raters. Similarly, Nuñez *et al.* (2017) found improvements from 0.77 to 0.89 for raters assessing the severity of black rot of crucifers (*Xanthomonas campestris* pv. *campestris*) in kale. The improvements in the reproducibility of the results are critical to ensuring that disease estimations from multiple raters in the same experiment are uniform (Correia *et al.*, 2017). Thus, the SADs proposed in this study will be useful for assessments of grapevine anthracnose severity in epidemiological and control studies.

References

Amorim L, Bergamin Fillho A, 2011. Fenologia, patometria e quantificação de danos. In: Amorim L, Rezende JAM, Bergamin Filho A, eds. *Manual de Fitopatologia: princípios e conceitos*. São Paulo, SP, Brazil: Agronômica Ceres, 517–42.

Amorim L, Spósito MB, Kuniyuki H, 2016. Doenças da videira. In: Amorim L, Rezende JAM, Bergamin Filho A, Camargo LEA, eds. *Manual de Fitopatologia: doenças das plantas cultivadas*. São Paulo, SP, Brazil: Agronômica Ceres, 745–58.

Angelotti F, Scapin CR, Tessmann D, 2008. Diagrammatic scale for assessment of grapevine rust. *Tropical Plant Pathology* **33**, 439–43.

Belasque Júnior J, Bassanezi RB, Spósito MB, Ribeiro LM, Jesus Junior WC, Amorim L, 2005. Escalas diagramáticas para avaliação da severidade do cancro cítrico. *Fitopatologia Brasileira* **30**, 387–93.

Buffara CRS, Angelotti F, Vieira RA, Bogo A, Tessmann D, Bem BP, 2014. Elaboration and validation of a diagrammatic scale to assess downy mildew severity in grapevine. *Ciência Rural* **44**, 1384–91.

Campbell CL, Madden LV, 1990. *Introduction to plant disease epidemiology*. New York, NY, USA: Wiley.

Capucho AS, Zambolim L, Duarte HSS, Vaz GRO, 2011. Development and validation of a standard area diagram set to estimate severity of leaf rust in *Coffea arabica* and *C. canephora*. *Plant Pathology* **60**, 1144–50.

Carisse O, Lefebvre A, 2011. A model to estimate the amount of primary inoculum of *Elsinoë ampelina*. *Plant Disease* **95**, 1167–71.

Cobb N, 1892. Contribution to an economic knowledge of the Australian rusts (Uredinae). *Agricultural Gazette (NSW)* **3**, 60.

Correia KC, Queiroz JVJ, Martins RB, Nicoli A, Del Ponte EM, Michereff SJ, 2017. Development and evaluation of a standard area diagram set for the severity of phomopsis leaf blight on eggplant. *European Journal of Plant Pathology* **149**, 269–76.

Debona D, Nascimento KJT, Rezende D *et al.*, 2015. A set of standard area diagrams to assess severity of frogeye leaf spot on soybean. *European Journal of Plant Pathology* **142**, 603–14.

Del Ponte EM, Pethybridge SJ, Bock CH, Michereff SJ, Machado FJ, Spolti P, 2017. Standard area diagrams for aiding severity estimation : scientometrics, pathosystems and methodological trends in the last 25 years. *Phytopathology*, in press.

Dolinski MA, Duarte HSS, Silva JB, May de Mio LL, 2017. Development and validation of a standard area diagram set for assessment of peach rust. *European Journal of Plant Pathology* **148**, 817–24.

Gamer M, Lemon J, Fellows I, Singh P, 2012. irr: Various coefficients of interrater reliability and agreement. R package version 0.84. [http://www.R-project.org]. Accessed 07 July 2017.

González-Domínguez E, Martins RB, Del Ponte EM, Michereff SJ, García-Jiménez J, Armengol J, 2014. Development and validation of a standard area diagram set to aid assessment of severity of loquat scab on fruit. *European Journal of Plant Pathology* **139**, 413–22.

Hill GN, Beresford RM, Evans KJ, 2010. Tools for accurate assessment of botrytis bunch rot (*Botrytis cinerea*) on wine grapes. *New Zealand Plant Protection* **63**, 174–81.

IBGE - Instituto Brasileiro de Geografia e Estatística, 2017. Levantamento sistemático da produção agrícola [ftp://ftp.ibge.gov.br/Producao_Agricola/Levantamento_ Sistematico_da_Producao_Agricola_[mensal]/Fasciculo/lspa_201706.pdf]. Accessed 19 August 2017.

Kono A, Sato A, Ban Y, Mitani N, 2013. Resistance of *Vitis* germplasm to *Elsinoë ampelina* (de Bary) Shear evaluated by lesion number and diameter. *HortScience* **48**, 1433–9.

Lenz G, Costa ID, Balardin RS *et al.*, 2009. Elaboração e validação de escala diagramática para quantificação da mancha de isariopsis da videira. *Ciência Rural* **39**, 2301–8.

Lin LIK, 1989. A concordance correlation coefficient to evaluate reproducibility. *Biometrics* **45**, 255–68.

Madden LV, Hughes G, van den Bosch F, 2007. *The study of plant disease epidemics*. St. Paul, MN, USA: APS Press.

Mesquini RM, Schwan-Estrada KRF, Godoy CV, Vieira RA, Zarate NAH, Vieira MC, 2009. Escala diagramática para a quantificação de *Septoria apiicola* e *Cercospora arracacina* em mandioquinha-salsa. *Tropical Plant Pathology* **34**, 250–5.

Nita M, Ellis MA, Madden LV, 2003. Reliability and accuracy of visual estimation of Phomopsis leaf blight of strawberry. *Phytopathology* **93**, 995–1005.

Nuñez AMP, Monteiro FP, Pacheco LP *et al.*, 2017. Development and validation of a diagrammatic scale to assess the severity of black rot of crucifers in kale. *Journal of Phytopathology* **165**, 195–203.

Nutter FW, Schultz PM, 1995. Improving the accuracy and precision of disease assessments: selection of methods and use of computer-aided training programs. *Canadian Journal of Plant Pathology* **17**, 174–84.

Ortega-Acosta SA, Velasco-Cruz C, Hernández-Morales J, Ochoa-Martinez DL, Hernández-Ruiz J, 2016. Diagrammatic logarithmic scales for assess the severity of spotted leaves and calyces of roselle. *Revista Mexicana de Fitopatología* **34**, 270–85.

Paula PVAA, Pozza EA, Santos LA, Chaves E, Maciel MP, Paula JCA, 2016. Diagrammatic scales for assessing brown eye spot (*Cercospora coffeicola*) in red and yellow coffee cherries. *Journal of Phytopathology* **164**, 791–800.

Poolsawat O, Tharapreuksapong A, Wongkaew S, Chaowiset W, Tantasawat P, 2012. Laboratory and field evaluations of resistance to *Sphaceloma ampelinum* causing anthracnose in grapevine. *Australasian Plant Pathology* **41**, 263–9.

R Core Team, 2017. R: A Language and Environment for Statistical Computing. Vienna, Austria: R Foundation for Statistical Computing. [http://www.R-project.org]. Accessed 07 July 2017.

Rios JA, Debona D, Duarte HSS, Rodrigues FA, 2013. Development and validation of a standard area diagram set to assess blast severity on wheat leaves. *European Journal of Plant Pathology* **136**, 603–11.

Santos RF, Ciampi-Guillardi M, Amorim L, Massola Júnior NS, Spósito MB, 2017. Aetiology of anthracnose on grapevine shoots in Brazil. *Plant Pathology*, in press.

Schneider CA, Rasband WS, Eliceiri KW, 2012. NIH Image to ImageJ: 25 years of image analysis. *Nature Methods* **9**, 671–5.

Schwanck AA, Del Ponte EM, 2014. Accuracy and reliability of severity estimates using linear or logarithmic disease diagram sets in true colour or black and white: a study case for rice brown spot. *Journal of Phytopathology* **162**, 670–82.

Shetty DS, Narkar SP, Sawant IS, Sawant SD, 2014. Efficacy of quinone outside inhibitors (QoI) and demethylation inhibitors (DMI) fungicides against grape anthracnose. *Indian Phytopathology* **67**, 174–8.

Sosnowski M, Emmett B, Clarke K, Wicks T, 2007. Susceptibility of tablegrapes to black spot (anthracnose) disease. *The Australasian & New Zealand Grapegrower & Winemaker* **521**, 8–11.

Spolti P, Schneider L, Sanhueza RMV, Batzer JC, Gleason ML, Del Ponte EM, 2011. Improving sooty blotch and flyspeck severity estimation on apple fruit with the aid of standard area diagrams. *European Journal of Plant Pathology* **129**, 21–9.

Stevenson M, Nunes T, Heuer C *et al.*, 2017. epiR: Tools for the analysis of epidemiological data. R package version 0.9-87. [http://www.R-project.org]. Accessed 07 July 2017.

Thind TS, 2015. Anthracnose. In: Wilcox W, Gubler W, Uyemoto J, eds. *Compendium of grape diseases, disorders, and pests*. St Paul, MN, USA: APS Press, 17–9.

Vieira RA, Mesquini RM, Silva CN, Hata FT, Tessmann DJ, Scapim CA, 2014. A new diagrammatic scale for the assessment of northern corn leaf blight. *Crop Protection* **56**, 55–7.

Wang Y, Liu Y, He P, Lamikanra O, Lu J, 1998. Resistance of Chinese *Vitis* species to *Elsinoë ampelina* (de Bary) Shear. *HortScience* **33**, 123–6.

Yadav NVS, Vos SM, Bock CH, Wood BW, 2013. Development and validation of standard area diagrams to aid assessment of pecan scab symptoms on fruit. *Plant Pathology* **62**, 325–35.

6 TEMPORAL AND SPATIAL DYNAMICS OF ANTHRACNOSE IN A BRAZILIAN VINEYARD

Abstract

Grapevine anthracnose (*Elsinoë ampelina*) is an economically important grapevine disease in south and southeast Brazil. The objective of this work was to study the temporal and spatial progression of anthracnose in a Brazilian vineyard. The experiment was carried out in a 'Niagara Rosada' vineyard in São Paulo State, Brazil over 2014 and 2015 growing seasons. The incidence of vines with diseased leaves, stems and berries and also disease severity on leaves were recorded from the bud break to the véraison. Monomolecular, logistic and Gompertz models were fitted by non-linear regression to the incidence and severity data over time to characterize the temporal progress. The dispersion index and Taylor′s power law were used to characterize the spatial pattern. Anthracnose symptoms occurred rapidly after bud break and ontogenic resistance was observed for all organs assessed. The monomolecular model showed the best fit to the incidence progress, which had progress rates ranging from 0.051 to 0.136 per day. In both seasons, the leaf disease severity was lower than 5%, showing a linear progress. Spatial analyses showed a predominantly random spatial pattern. Our analyses suggest that the progress of anthracnose incidence and severity over time is governed mainly by the primary inoculum due to age-related resistance of the vine organs; once the pathogen is established in a vineyard, seasonal infection is randomly distributed; and *E. ampelina* survives efficiently between seasons in the vineyard. Therefore, anthracnose control measures in Brazilian vineyards should be focused on reduction of the inoculum within the vineyard.

Keywords: *Vitis labrusca*; Black spot; *Elsinoë ampelina*; Disease progress; Monomolecular model

6.1 Introduction

Grapevine anthracnose, caused by *Elsinoë ampelina* Shear (anamorph *Sphaceloma ampelinum* de Bary), is an important disease in southern and southeastern Brazil (Bardin *et al.*, 2010; Barros *et al.*, 2015). These regions are responsible for 78% of the Brazilian grape production (IBGE, 2016). Anthracnose symptoms appear on all the green and succulent parts of vine, including leaves, stems, petioles, rachises, tendrils and berries. *Elsinoë ampelina* causes numerous circular or angular, dark brown to dark grey lesions on shoots and on rachis (Thind, 2015). On berries, small, reddish circular spots initially develop and the lesion may extend into the pulp causing crack on fruit. Clusters are susceptible to infection from flowering to the véraison. In high disease severity, anthracnose causes stem breakage, delayed development and berry ripening, premature leaf and berry drop, low fruit quality for the fresh market and wine production, loss of photosynthetic activity and reduction of vine vigor in the subsequent season (Thind *et al.*, 2004; Naves *et al.*, 2006; Carisse & Lefebvre, 2011; Carisse

& Morissete-Tomas, 2013; Amorim *et al.*, 2016). Once established in the vineyard, anthracnose can be very destructive and difficult to manage (Thind, 2015).

Elsinoë ampelina survives between seasons on diseased canes, tendrils, rachises and mummified berries, as well as vine debris on the ground (Amorim *et al.*, 2016). Although the pathogen survives on different organs, the greatest persistence is observed on cane cankers (Suhag & Grover, 1972). At the end of season, sclerotia may be formed on the canker's edge (Naves *et al.*, 2006). In the spring, under conditions of high humidity, conidia are formed from mycelium or sclerotia. Conidia are spread by rain splash, causing the primary infection concomitantly with the bud break (Thind *et al.*, 2004). Optimum conidia germination occurs at 25 to 30 °C, with a minimum of 3 to 4 h of leaf wetness (Thind, 2015). Susceptible cultivars show symptoms within 2 days after inoculation (Poolsawat *et al.*, 2010).

In São Paulo State, the largest Brazilian producer of table grapes, where the cultivar Niagara Rosada (*Vitis labrusca*) corresponds to approximately 90% of the plants (Oliveira *et al.*, 2008; IEA, 2016), anthracnose epidemics are considered a limiting factor for grape production (Costa *et al.*, 2012). The disease is controlled by protective fungicide applications starting during bud break and continuing at 7 to 14-day intervals until the berries formation, which is the critical period for infection (Balardin *et al.*, 1994). Additionally, winter treatments with lime sulphur or copper-containing products are required to reduce the inoculum produced within the vineyard (Du Plessis, 1940).

Despite the importance of grapevine anthracnose, little is known about its epidemiology. The quantification of disease intensity over time is essential in epidemiological studies to characterize the disease dynamics, as well as for evaluation and comparison of different treatments (Campbell & Madden, 1990). The knowledge of the spatial patterns of disease spread can provide useful information on the growth and dispersal of pathogen populations (Luo *et al.*, 2012). The relative importance of the origin of the initial inoculum, for example, whether it originates from inside or outside the orchard and its possible dispersal mechanisms can be partially inferred from a spatial dynamic analysis (Spósito *et al.*, 2008; Keske *et al.*, 2013; Silva-Junior *et al.*, 2014). However, the importance of the primary and secondary inoculum and the temporal and spatial dynamics of grapevine anthracnose are unknown in Brazil. Therefore, a thorough investigation of grapevine anthracnose epidemiology will provide relevant information about the inoculum, dispersal and growth of the disease in the vineyard. These information will help Brazilian grape growers in decision-making to manage the disease. If the primary inoculum is more important than the secondary

inoculum for epidemics development, control measures should be reinforced to eradicate the pathogen during the dormant period.

Thus, the objective of this work was to study the temporal and spatial progression of anthracnose in a Brazilian vineyard to better understand the disease epidemiology.

6.2 Materials and methods

6.2.1 Experimental area

The experiment was carried out over 2014 and 2015 growing seasons in a vineyard of cv. Niagara Rosada (*V. labrusca*) grafted on 'IAC-766 [*V. riparia* × (*V. cordifolia* × *V. rupestris*) × *V. caribaea*] rootstock, planted in 2002. The experimental vineyard located in São Paulo State, Brazil (23°7'24.31"S; 46°51'47.68"W, 626 m a.s.l.), consisted of 590 plants (10 rows with 59 plants) in 2014 and 472 plants (8 rows with 59 plants) in 2015. The experimental design was randomized blocks, each block containing 2 rows. Grapevines were trained in a vertical shoot positioning system at a spacing of 2 m between rows and 1 m between plants.

Lime sulphur application during the winter was performed until 2012. The vines were spur-pruned (5 to 8 spurs per vine with 1 to 2 buds per spur) on 22 August in both seasons. Shortly thereafter, the grapevines pruning debris were removed from the vineyard. Three days after pruning, hydrogen cyanamide at 4% (Dormex, BASF) was sprayed to enhanced bud opening. During the experiment, downy mildew (*Plasmopara viticola*) was controlled using fosetyl (Aliette, Bayer) at a standard rate of 2 g a. i. L^{-1}. Temperature, relative humidity, rainfall and leaf wetness period were recorded by a meteorological station (Campbell Scientific) located near the vineyard.

6.2.2 Disease assessment

Anthracnose monitoring in the vineyard began after the bud break. Incidence quantification was sectorized per vine organ: leaf, stem and berry. Presence of the disease was considered when the vine presented one or more lesions in the respective organ. Disease incidence was assessed in all vines and disease severity was assessed in 12 (2014) and 15 (2015) plants per block. One shoot from each vine was selected and marked with a tag to

quantify the disease severity on leaves. Images were captured of four leaves from middle third of each shoot and disease severity was quantified based on the percentage of leaf area covered by lesions using Quant (Vale *et al.*, 2003). The disease incidence and severity were assessed every 2 to 13 days from the bud break to the véraison (Table 1). Comparisons between disease incidence and severity against growing seasons were performed by *t* test ($P < 0.05$).

Table 1 Assessment dates of anthracnose incidence and severity in a *Vitis labrusca* cv. Niagara Rosada vineyard in Jundiaí, São Paulo State, Brazil, 2014 and 2015

Organ	**2014**	**2015**
Leaf	23, 30 Sept 7, 14, 21, 30 Oct 7, 15, 18 Nov 1 Dec	17, 19, 21, 24, 30 Sep 7, 12, 19 Oct 5, 18, 28 Nov
Stem	7, 14, 21, 30 Oct 7, 12, 18 Nov 1, 10 Dec	30 Sept 7, 12, 19, 26 Oct 5, 12, 18, 28 Nov 8, 14 Dec
Berry	18 Nov 1, 10 Dec	26 Oct 5, 12, 18, 28 Nov 8, 14 Dec

6.2.3 Temporal analysis

Monomolecular [$y(t) = y_{max} - (y_{max} - y_0)* \exp(-r* t)$], logistic [$y(t) = y_{max}/(1 + ((y_{max} - y_0)/ y_0)* \exp(-r* t))$] and Gompertz [$y(t) = y_{max}* (\exp(-(-\log (y_0/ y_{max}))* \exp(-r* t)))$] models were fitted by non-linear regression to the disease incidence and severity data over time using STATISTICA v.7 (StatSoft, 2004). In these models, $y(t)$ is the proportion of disease intensity, y_0 is the initial inoculum, r is the disease progress rate, y_{max} is the maximum asymptote and t is the time in days. The best model to describe disease progress curves was selected based on the coefficients of determination (R^2), distribution of the residuals and the standard error of the parameters estimated by each model (Madden *et al.*, 2007). When the disease incidence reached 100%, the y_{max} was fixed at 1 (proportion). Comparisons among parameters estimated for each model were performed by *t* test ($P < 0.05$). When necessary, the disease progress rate parameter was multiplied by the maximum asymptote parameter ($r* y_{max}$) (Madden *et al.*, 2007).

6.2.4 Spatial analysis

Maps showing the cumulative anthracnose incidence of vines with symptoms on leaves, stems and berries were built and transformed into a matrix (*x*, *y*, *z*), where *x* represents the vineyard row, *y* the vine in the row and *z* the vine condition (0 to asymptomatic vine and 1 to symptomatic vine). The incidence of grapevines with anthracnose symptoms in quadrats of 2×2 and 3×2 (2 to 3 vines per row × 2 rows) were chosen to determine the spatial pattern of the epidemic. For each assessment, disease incidence (*p*) was determined in both quadrats sizes using the equation: $p = \sum (Xi) / nN$, where, *X* is the total number of symptomatic plants in each quadrat *i*, *n* is the total number of plants in each quadrat and *N* is the total number of quadrats in the experimental field (Madden & Hughes, 1995). The disease incidence (*p*) was used to calculate the dispersion index (*D*) and Taylor's power law.

The dispersion index was determined for each assessment by equation $D = V_{obs}/V_{bin}$, where, V_{obs} is the observed variance and V_{bin} is the binomial variance determined by equations $V_{obs} = \sum[(X_i - np)^2 / (n^2(N - 1))]$ and $V_{bin} = [p(1 - p)] /n$, respectively (Madden *et al.*, 2007). The significance of the dispersion index was verified using chi-square test ($P < 0.05$). *D* values significantly equal to 1.0 indicate random distribution of symptomatic plants at a given assessment date (null hypothesis). *D* values greater than 1.0 indicate aggregation (Madden & Hughes, 1995; Madden *et al.*, 2007).

The Taylor's power law $\log(V_{obs}) = \log(A) + b \log(V_{bin})$ was determined for incidence data of grapevines with symptoms on leaves, stems and berries, using pooled data from 2014 and 2015. The Taylor's power law is based on the linear relationship between the $\log(V_{bin})$ and the $\log(V_{obs})$ (Madden & Hughes, 1995) and the significance was determined by *F* test ($P < 0.05$). The appropriateness of the relationship was assessed by the coefficient of determination (R^2) and distribution of the residuals. The equality of the parameters $b = 1$ and $\log(A) = 0$ was tested using *t* test ($P < 0.05$) (Madden & Hughes, 1995). A random spatial distribution is indicated by $\log(A) = 0$ and $b = 1$. Values of $b > 1$ indicate aggregation, which varied with disease incidence. Furthermore, when $\log(A) > 0$ and $b = 1$ symptomatic plants show a constant aggregated pattern of distribution (Madden & Hughes, 1995).

6.3 Results

6.3.1 Temporal analysis

The bud break started on 09 September in 2014 and on 07 September in 2015, 18 and 16 days after pruning, respectively. In 2014, the first anthracnose symptoms on leaves appeared at 14 days after bud break (DAB) and 1.4% of the vines had symptoms. Seven days later, disease incidence increased to 54.8% (Fig. 1a). In 2015, the first symptoms on leaves were observed at 10 DAB and the incidence reached 100% at 42 DAB (Fig. 1b). The first symptoms on stems appeared at 28 DAB in 2014. At 59 DAB, the incidence of vines with diseased stems was 58.9% and then, it had a small increase, reaching 64.0% at 92 DAB (Fig. 1c). Likewise, in 2015 the first anthracnose lesions on stems were observed at 23 DAB and the disease incidence had a small increment after 66 DAB (Fig. 1d). In 2014, less than 4% of vines showed symptoms on berries until 70 DAB (46th day after the beginning of the fruit development), which increased to 13.8% after heavy rains (92 mm) on days 77-80 DAB (Fig. 1e, g). Otherwise, in 2015, symptoms on berries appeared earlier than in 2014 and the final disease incidence was 81.9% at 98 DAB (Fig. 1f). During 2015, the incidence of vines with diseased stems and berries at the end of the growing season were higher than in 2014 ($P < 0.05$).

The monomolecular model showed the best fit to the disease incidence progress for all organs assessed during the two growing seasons (Table 2). The maximum asymptote, initial inoculum and disease progress rate varied among plant organs and between seasons. The asymptotes ranged from 0.13 to 1 and they were significantly higher in 2015 than in 2014 ($P < 0.05$) for vines with diseased stems and berries. For all epidemics, the initial inoculum was lower than 0.155. The disease progress rates for all epidemics ranged from 0.067 to 0.608 per day. However, when the scaled rate (r^*y_{max}) was employed, the progress rates varied from 0.051 to 0.136 per day.

In both growing seasons, the anthracnose severity on leaves was lower than 5% showing a linear progress over time. Thus, the data were not fitted to the monomolecular, logistic and Gompertz models.

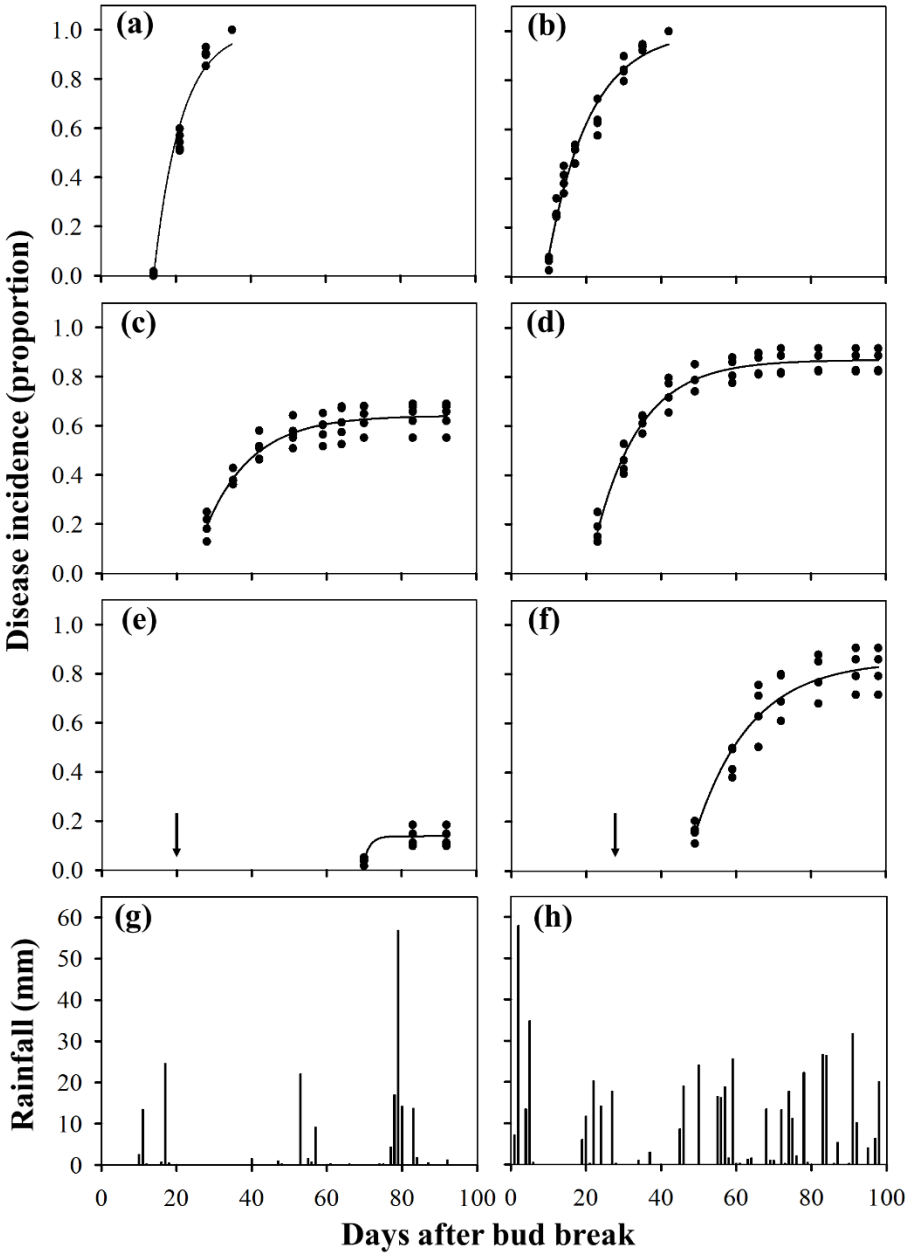

Figure 1 Cumulative incidence (proportion) of grapevines with anthracnose symptoms (dark circles) on leaves (a, b), stems (c, d) and berries (e, f) in a *Vitis labrusca* cv. Niagara Rosada vineyard in Jundiaí, São Paulo State, Brazil, 2014 (a, c, e) and 2015 (b, d, f). Solid lines indicate the monomolecular model fitted to the disease incidence. Arrows indicate the beginning of anthesis in 2014 (e) and in 2015 (f). Bars indicate rainfall events during the experiment in 2014 (g) and 2015 (h).

Table 2 Parameters and respective standard errors estimated by non-linear regression of monomolecular, logistic and Gompertz models fitted to the incidence of grapevines with anthracnose symptoms on leaves, stems and berries in a *Vitis labrusca* cv. Niagara Rosada vineyard in Jundiaí, São Paulo State, Brazil, 2014 and 2015

			Parameter							
Season	**Organ**	**Model**[a]	R^2	y_{max}	y_{max} **SE**	y_0	y_0 **SE**	r	r **SE**	r^*y_{max}[b]
		Monomolecular	0.98	1	-	-0.152	0.033	0.136	0.007	0.136
2014	Leaf	Logistic	0.98	1	-	0.037	0.013	0.423	0.044	0.423
		Gompertz	0.99	1	-	0.005	0.003	0.269	0.014	0.269
		Monomolecular	0.97	1	-	0.005	0.025	0.088	0.004	0.088
2015	Leaf	Logistic	0.95	1	-	0.171	0.018	0.165	0.013	0.165
		Gompertz	0.96	1	-	0.124	0.017	0.126	0.008	0.126
		Monomolecular	0.90	0.64	0.013	0.155	0.025	0.080	0.010	0.051
2014	Stem	Logistic	0.89	0.62	0.011	0.186	0.021	0.151	0.019	0.094
		Gompertz	0.90	0.63	0.011	0.173	0.022	0.113	0.014	0.071
		Monomolecular	0.95	0.86	0.011	0.111	0.026	0.083	0.006	0.071
2015	Stem	Logistic	0.95	0.85	0.009	0.178	0.020	0.172	0.014	0.146
		Gompertz	0.95	0.85	0.009	0.151	0.020	0.125	0.009	0.106
		Monomolecular	0.77	0.13	0.013	-0.047	6.537	0.608	> 1	0.079
2014	Berry	Logistic	0.77	0.13	0.013	0.020	0.811	0.757	> 1	0.098
		Gompertz	0.77	0.13	0.013	0.012	0.550	0.612	> 1	0.080
		Monomolecular	0.90	0.85	0.037	0.099	0.045	0.067	0.011	0.057
2015	Berry	Logistic	0.90	0.81	0.024	0.144	0.023	0.158	0.022	0.128
		Gompertz	0.90	0.83	0.027	0.124	0.035	0.109	0.015	0.090

[a]Monomolecular, logistic and Gompertz models were fitted to the incidence data using $[y(t) = y_{max} - (y_{max} - y_0)^* \exp(-r^* t)]$, $[y(t) = y_{max}/(1 + ((y_{max} - y_0)/ y_0)^* \exp(-r^* t))]$ and $[y(t) = y_{max}^* (\exp(-(-\log (y_0/ y_{max}))^* \exp(-r^* t)))]$, respectively; where, $y(t)$ is the proportion of disease incidence, y_0 is the initial inoculum, r is the disease progress rate, y_{max} is the maximum asymptote of diseased vines, t is the time in days. R^2 is the coefficient of determination and SE corresponds to the standard error of the mean.
[b]Scaled rate ($r^* y_{max}$) (Madden *et al.*, 2007).

6.3.2 Spatial analysis

The values of the dispersion index (D) varied according to the evaluation date, organ and quadrat size. In 2014, the distribution of vines with anthracnose symptoms on leaves was random (quadrats 2×2) for all assessments. Similarly, in 2015 87.5% of the maps presented a random pattern for quadrats 2×2 and 3×2. In 2014, the distribution of vines with symptoms on stems became aggregated when the incidence was higher than 58.9% in quadrats 2×2 (Fig. 2). However, in 2015 the aggregated pattern was firstly observed in the incidence of 17.9 and 45.4% for quadrats 2×2 and 3×2, respectively. The distribution of vines with symptoms on berries was random. An aggregated pattern was observed only in one (I = 15.9%) over 20 maps assessed in both seasons and quadrat sizes (Fig. 3).

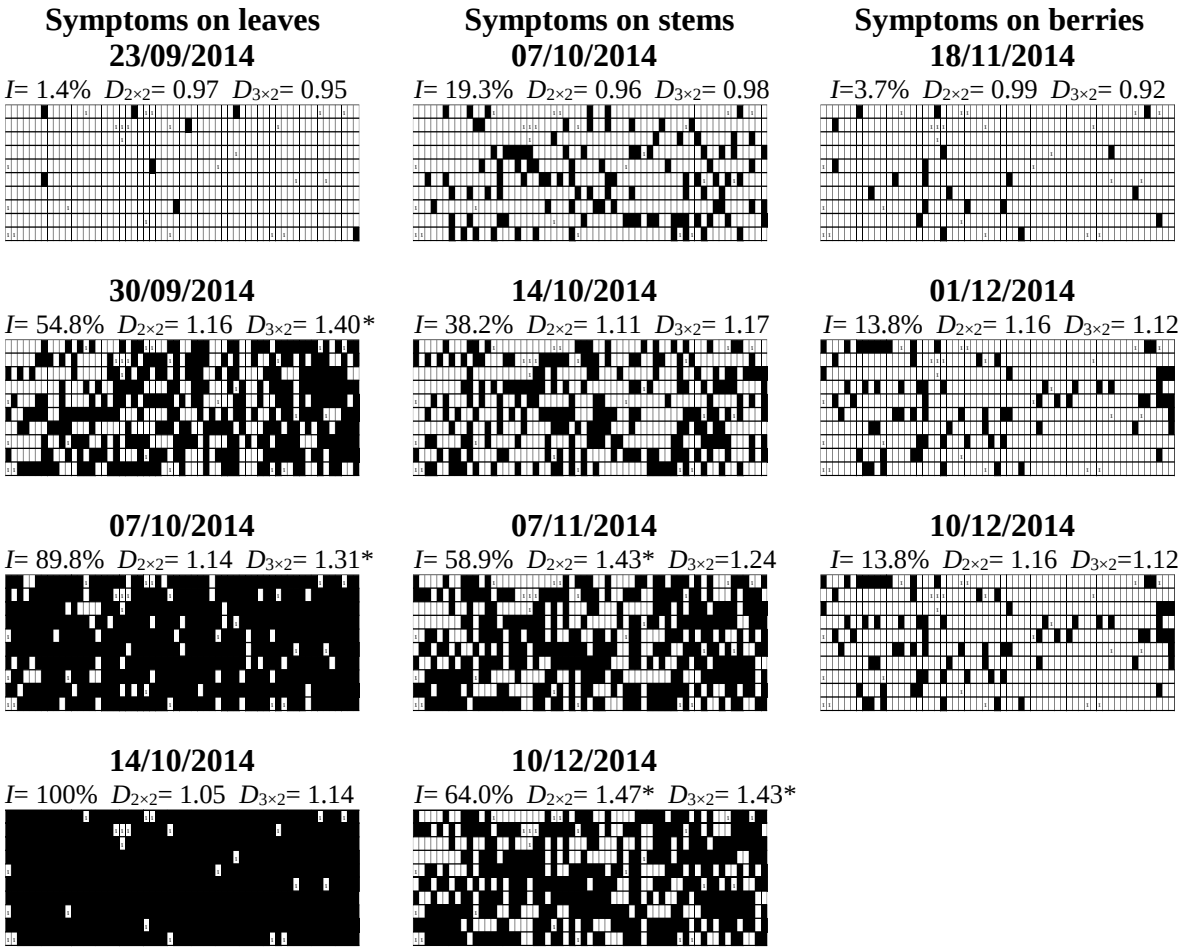

Figure 2 Maps showing the spatial pattern of grapevines with anthracnose symptoms on leaves, stems and berries in a *Vitis labrusca* cv. Niagara Rosada vineyard in Jundiaí, São Paulo State, Brazil, 2014. Black and white quadrants represent symptomatic and asymptomatic grapevines, respectively. Quadrants with 'x' in the centre indicate absence of grapevine. *I* is the incidence of diseased grapevines (percentage). $D_{2\times2}$ and $D_{3\times2}$ are the dispersion indexes for the two quadrat sizes and * indicates the aggregation of diseased grapevines.

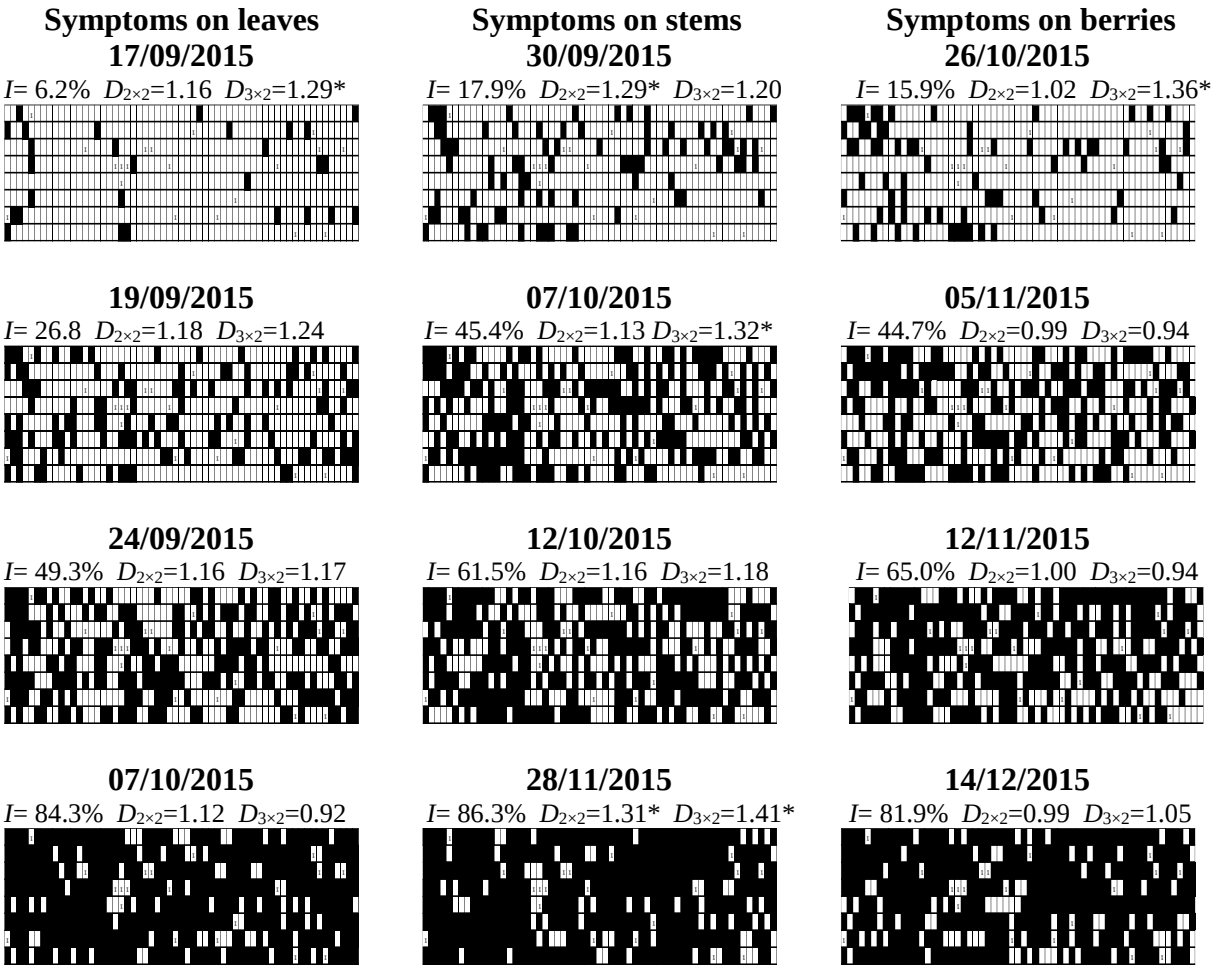

Figure 3 Maps showing the spatial pattern of grapevines with anthracnose symptoms on leaves, stems and berries in a *Vitis labrusca* cv. Niagara Rosada vineyard in Jundiaí, São Paulo State, Brazil, 2015. Black and white quadrants represent symptomatic and asymptomatic grapevines, respectively. Quadrants with 'x' in the centre indicate absence of grapevine. *I* is the incidence of diseased grapevines (percentage). $D_{2\times2}$ and $D_{3\times2}$ are the dispersion indexes for the two quadrat sizes and * indicates the aggregation of diseased grapevines.

The Taylor's power law regressions applied to the pooled data from 2014 and 2015 were significant ($P < 0.05$) for all analyses. For plants with anthracnose symptoms on leaves, aggregation of diseased vines was observed for quadrats 2×2 ($\log(A) > 0$; $b > 1$) (Fig. 4a) and 3×2 ($\log(A) > 0$; $b = 1$) (Fig. 4b). However, for grapevines with symptoms on stems and berries, a random pattern of distribution was observed ($\log(A) = 0$; $b = 1$) (Fig. 4c-f).

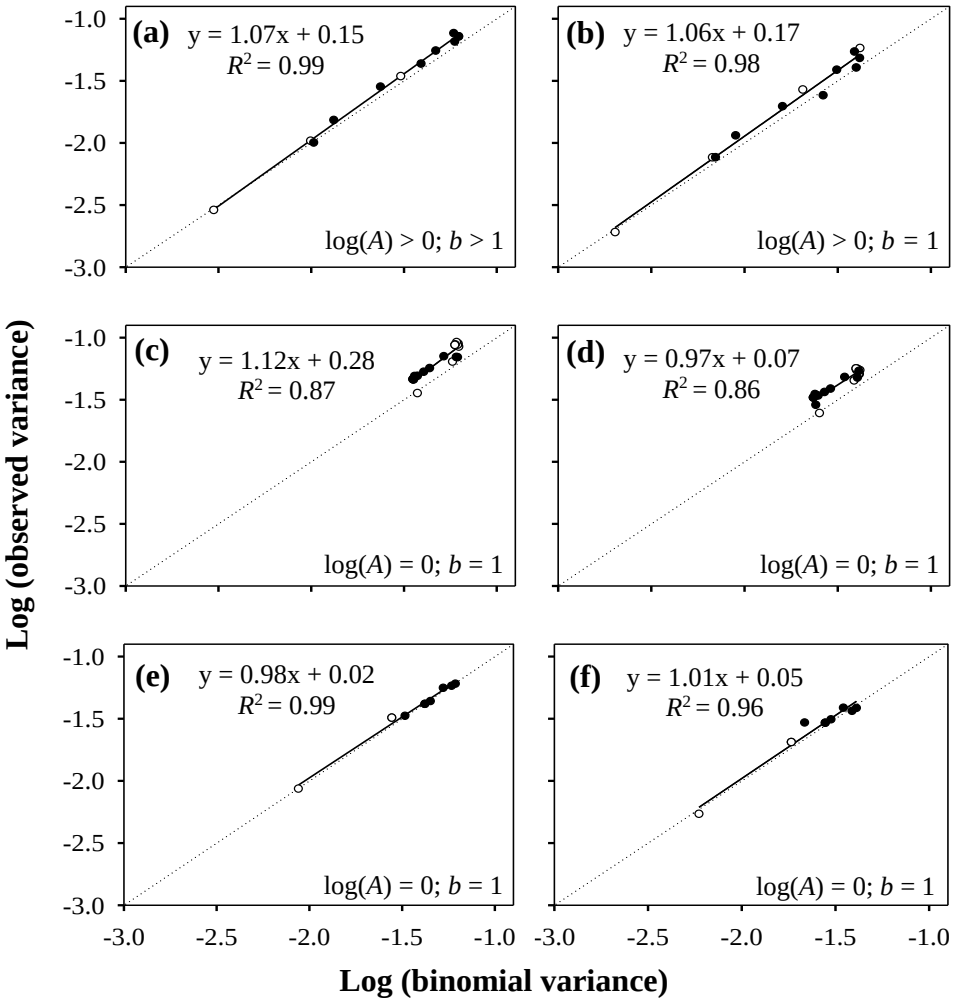

Figure 4 Relationship between the logarithm of the observed variance [log (*V*obs)] and the logarithm of the binomial variance [log (*V*bin)] for incidence of grapevines with anthracnose symptoms on leaves (a, b), stems (c, d) and berries (e, f) using quadrats sizes 2×2 (a, c, e) and 3×2 (b, d, f). The solid line represents the linear regression line fitted to the data collected in a *Vitis labrusca* cv. Niagara Rosada vineyard in Jundiaí, São Paulo State, Brazil. The dashed line represents the binomial line (observed variance = binomial variance). The analyses were carried out with data from 2014 (white circles) and 2015 (black circles) pooled together.

6.4 Discussion

Anthracnose symptoms on 'Niagara Rosada' vines appeared rapidly after bud break, 14 and 10 DAB, respectively in 2014 and 2015. Similarly, in New Zealand's vineyards, conidia from overwintered cane lesions initiate the epidemic soon after bud break in September (Brook, 1973). Although survival of *E. ampelina* has been reported on different vine organs, infected canes are the main source of inoculum in the beginning of each season (Thind, 2015). For instance, in Canada the initial inoculum of grape anthracnose was released

from cane cankers before bud break and continued throughout the spring (Carisse & Lefebvre, 2011). In that study, the mean number of conidia produced per canker in three seasons was 4,428, 14,833 and 18,136 conidia/mm^2.

Incidence of vines with diseased leaves increased rapidly in both seasons, despite the few rainfall events in 2014. Symptoms on stems occurred later than on leaves and the incidence of vines with symptomatic stems approached the asymptote after the beginning of their lignification. The incidence of vines with diseased berries stabilized at 83 DAB, 63 days after anthesis, in 2014 and it had small increments after 82 DAB, 58 days after anthesis, in 2015, due to berry ontogenetic resistance. Berries of *V. vinifera* cv. Palomino became highly resistant about 50 days after anthesis, when soluble solids have risen above 5 to 7% in the juice (Brook, 1973). In 2015, the incidence of vines with diseased stems and berries at the end of the growing season were higher than in 2014 ($P < 0.05$) due to the greater rainfall intensity and distribution. In South Brazil, severe anthracnose epidemics have been observed in years of high rainfall (Barros *et al.*, 2015).

The linear shape of disease severity progress on leaves in both growing seasons can be explained by the low level of disease (on average < 5% disease severity). Under low disease intensity (≤ 5%), monomolecular and linear models can be coincident (Bergamin Filho & Amorim, 2011). This low severity may be related to below-average rainfall during the susceptible period of the organ. During the period favorable to anthracnose infection in leaves, approximately the first 30-40 days after bud break, the rainfall amount was 43 mm in 2014. Although, in 2015 the rainfall events have increased after 45 DAB, the disease severity had tiny increments because the leaves were fully expanded. In a *V. vinifera* cv. Black Hamburgh vineyard, leaves that escaped infection in their first 4 weeks generally remained anthracnose-free (Brook, 1992). Moreover, ontogenic resistance to anthracnose in grape stems and berries were also observed (Brook, 1973); however, the resistance mechanisms are still unknown.

Anthracnose incidence progress of vines with diseased leaves, stems and berries was well described by the monomolecular model. In plant disease epidemiology, the monomolecular model is used to describe monocyclic diseases and the Gompertz and logistic models are used for polycyclic diseases (Madden *et al.*, 2007). However, the monomolecular model also describes the progress of diseases with a variable incubation period as a function of the host phenology, regardless of their behaviour as monocyclic or polycyclic as, for example, diseases on young shoots, young tillers and fully developed fruits (Bergamin Filho

& Amorim, 2002). Grapevine anthracnose is a polycyclic disease (Carisse & Lefebvre, 2011); however, the organ susceptibility is strongly correlated to its phenological stage (Thind, 2015; Amorim *et al.*, 2016). In this context, the circular leaf spot (CLS) incidence progress of persimmon, a polycyclic disease caused by *Mycosphaerella nawae*, in which ontogenic resistance is known, was also represented by the monomolecular growth curve (Vicent *et al.*, 2012). Besides that, other diseases caused by polycyclic pathogens have been represented by monomolecular model (Spósito *et al.*, 2011; Gasparoto *et al.*, 2017).

Estimates of anthracnose progress rates varied among tissues and between growing seasons, ranging from 0.051 to 0.136 per day. Likewise, Vicent *et al.* (2012) found CLS incidence progress rates of 0.085 and 0.117 per day in a persimmon orchard, in Spain. In a study estimating the citrus scab (*Elsinoë fawcettii*) progress, the best fitted-model to explain the disease was Gompertz, which had rates of 0.022 and 0.067 per day (Gottwald, 1995). Barros *et al.* (2015) assessing the anthracnose incidence progress on leaves of different *V. labrusca* and hybrid cultivars and rootstocks combinations in south Brazil, observed that the variation in disease progress was associated with weather conditions, age of the vineyard and inoculum pressure.

The dispersion index and Taylor's power law analyses for both quadrat sizes, in all organs, showed a predominantly random spatial pattern. As the experimental area used was a commercial vineyard formed by 12-year-old vines, the anthracnose inoculum was homogeneously distributed in the area. This uniform distribution of the inoculum may explain the randomness of diseased vines observed in the spatial analyses. Our analyses suggest that the progress of anthracnose incidence and severity over time is governed mainly by the primary inoculum due to age-related resistance of the vine organs; once the pathogen is established in a vineyard, seasonal infection is randomly distributed; and *E. ampelina* survives efficiently between seasons in the vineyard. In this pathosystem, the primary inoculum can be reduced by sanitation measures such as winter treatments and removal of the pruning debris (Thind, 2015). In the last years, many Brazilian grape growers stopped applying winter treatments annually, which has caused epidemics on susceptible cultivars during rainy years. Therefore, anthracnose control measures in Brazilian vineyards should be focused on reduction of the inoculum within the vineyard.

References

Amorim L, Spósito MB, Kuniyuki H, 2016. Doenças da videira. In: Amorim L, Rezende JAM, Bergamin Filho A, Camargo LEA, eds. *Manual de Fitopatologia: doenças das plantas cultivadas*. São Paulo, SP, Brazil: Agronômica Ceres, 745–58.

Balardin RS, Balardin CRR, Chaves LCS, 1994. Efeito de diferentes fungicidas e doses no controle da antracnose da videira (*Elsinoe ampelina*). *Ciência Rural* **24**, 11–4.

Bardin L, Pedro Júnior MJ, Moraes JFL, 2010. Risco climático de ocorrência de doenças fúngicas na videira 'Niagara Rosada' na região do polo turístico do circuito das frutas do estado de São Paulo. *Bragantia* **69**, 1019–26.

Barros LB, Biasi LA, Carisse O, May De Mio LL, 2015. Incidence of grape anthracnose on different *Vitis labrusca* and hybrid cultivars and rootstocks combination under humid subtropical climate. *Australasian Plant Pathology* **44**, 397–403.

Bergamin Filho A, Amorim L, 2002. Doenças com período de incubação variável em função da fenologia do hospedeiro. *Fitopatologia Brasileira* **27**, 561–5.

Bergamin Filho A, Amorim L, 2011. Epidemiologia de doenças de plantas. In: Amorim L, Rezende JAM, Bergamin Filho A, eds. *Manual de Fitopatologia: princípios e conceitos*. São Paulo, SP, Brazil: Agronômica Ceres, 101–18.

Brook PJ, 1973. Epidemiology of grapevine anthracnose, caused by *Elsinoe ampelina*. *New Zealand Journal of Agricultural Research* **16**, 333–42.

Brook PJ, 1992. Epidemiology of grapevine anthracnose and downy mildew in an Auckland, New Zealand vineyard. *New Zealand Journal of Crop and Horticultural Science* **20**, 37–49.

Campbell CL, Madden LV, 1990. *Introduction to plant disease epidemiology*. New York, NY, USA: John Wiley and Sons.

Carisse O, Lefebvre A, 2011. A model to estimate the amount of primary inoculum of *Elsinoë ampelina*. *Plant Disease* **95**, 1167–71.

Carisse O, Morissete-Tomas V, 2013. Epidemiology of grape anthracnose: factors associated with defoliation of grape leaves infected by *Elsinoë ampelina*. *Plant Disease* **97**, 222–30.

Costa TV, Tarsitano MAA, Conceição MAF, 2012. Caracterização social e tecnológica da produção de uvas para mesa em pequenas propriedades rurais da região de Jales-SP. *Revista Brasileira de Fruticultura* **34**, 766–73.

Du Plessis SJ, 1940. *Anthracnose of vines and its control in South Africa*. Stellenbosch, South Africa: Department of Agriculture (Science Bulletin 216), 47 p.

Gasparoto MCG, Lourenço SA, Tanaka FAO *et al.*, 2017. Honeybees can spread *Colletotrichum acutatum* and *C. gloeosporioides* among citrus plants. *Plant Pathology* **66**, 777–82.

Gottwald, 1995. Spatio-temporal analysis and isopath dynamics of citrus scab in nursery plots. *Phytopathology* **85**, 1082–92.

IBGE - Instituto Brasileiro de Geografia e Estatística, 2016. Levantamento sistemático da produção agrícola. [ftp://ftp.ibge.gov.br/Producao_Agricola/Levantamento_Sistematico_da_Producao_Agricola_[mensal]/Fasciculo/lspa_201604.pdf]. Accessed 20 September 2016.

IEA - Instituto de Economia Agrícola, 2016. Estatísticas da produção paulista. [http://ciagri.iea.sp.gov.br/nia1/ subjetiva.aspx?cod_sis=1&idioma=1]. Accessed 03 October 2017.

Keske C, May De Mio LL, Amorim L, 2013. Spatial pattern of brown rot within peach trees related to inoculum of *Monilinia fructicola* in organic orchard. *Journal of Plant Pathology* **95**, 67–73.

Luo W, Pietravalle S, Parnell S *et al.*, 2012. An improved regulatory sampling method for mapping and representing plant disease from a limited number of samples. *Epidemics* **4**, 68–77.

Madden LV, Hughes G, 1995. Plant disease incidence : distributions, heterogeneity, and temporal analysis. *Annual Review of Phytopathology* **33**, 529–64.

Madden LV, Hughes G, van den Bosch F, 2007. *The study of plant disease epidemics*. St Paul, MN, USA: APS Press.

Naves RL, Garrido LR, Sônego OR, Foschesato M, 2006. *Antracnose da videira: sintomatologia, epidemiologia e controle*. Bento Gonçalves, RS, Brazil: Embrapa Uva e Vinho (Circular Técnica 69), 32 p.

Oliveira MDM, Silva PR, Amaro AA, Tecchio MA, 2008. Viabilidade econômica em tratamento antidegrana em uva “Niagara Rosada” no Estado de São Paulo. *Informações Econômicas* **38**, 59–68.

Poolsawat O, Tharapreuksapong A, Wongkaew S, Reisch B, Tantasawat P, 2010. Genetic diversity and pathogenicity analysis of *Sphaceloma ampelinum* causing grape anthracnose in Thailand. *Journal of Phytopathology* **158**, 837–40.

Silva-Junior GJ, Spósito MB, Marin DR, Ribeiro-Junior PJ, Amorim L, 2014. Spatiotemporal characterization of citrus postbloom fruit drop in Brazil and its relationship to pathogen dispersal. *Plant Pathology* **63**, 519–29.

Spósito MB, Amorim L, Bassanezi RB, Bergamin Filho A, Hau B, 2008. Spatial pattern of black spot incidence within citrus trees related to disease severity and pathogen dispersal. *Plant Pathology* **57**, 103–8.

Spósito MB, Amorim L, Bassanezi RB, Yamamoto PT, Felippe MR, Czermainski ABC, 2011. Relative importance of inoculum sources of *Guignardia citricarpa* on the citrus black spot epidemic in Brazil. *Crop Protection* **30**, 1546–52.

StatSoft, 2004. STATISTICA (data analysis software system), version 7. Tulsa, OK, USA: Statsoft, Inc. [http://www.statsoft.com].

Suhag LS, Grover RK, 1972. Overwintering and control of *Elsinoe ampelina*, the cause of grapevine anthracnose. In: Chadha K, Randhowa G, Pal R, eds. *Viticulture in the Tropics*. New Delhi, India: Horticultural Society of India, 294–9.

Thind TS, 2015. Anthracnose. In: Wilcox W, Gubler W, Uyemoto J, eds. *Compendium of grape diseases, disorders, and pests*. St Paul, MN, USA: APS Press, 17–9.

Thind TS, Arora JK, Moham C, Raj P, 2004. Epidemiology of powdery mildew, downy mildew and anthracnose diseases of grapevine. In: Naqvi SAMH, ed. *Diseases of Fruits and Vegetables*. Dordrecht, Netherlands: Kluwer Academic Publishers, 621–38.

Vale FXR, Fernandes Filho EI, Liberato JR, 2003. Quant: a software plant disease severity assessment. In: Close R, Braithwaite M, Havery I, eds. *Proceedings of the 8th International Congress of Plant Pathology, Christchurch, New Zealand*. Sydney, NSW, Australia: Horticulture Australia, 107.

Vicent A, Bassimba DDM, Hinarejos C, Mira JL, 2012. Inoculum and disease dynamics of circular leaf spot of persimmon caused by *Mycosphaerella nawae* under semi-arid conditions. *European Journal of Plant Pathology* **134**, 289–99.